RSC Advances

REVIEW

View Article Online
View Journal | View Issue

Cite this: *RSC Adv.*, 2025, **15**, 15052

Recent advances in the use of N-heterocyclic carbene adducts of N, P, C elements as supporting ligands in organometallic chemistry

Mingdong Zhong * and Minyi Yuan

With the rapid development of N-heterocyclic carbene (NHC) coordination chemistry, the potential of NHCs as strong electron-donating ligands has been fully explored. At the same time, an increasing number of p-block element NHC adducts, due to their possession of lone pairs or polarized carbon-element π-bonds, have gradually become important ligands of significant interest in coordination chemistry. Among these, N-heterocyclic imine (NHI), N-heterocyclic phosphinidene (NHCP) and N-heterocyclic olefin (NHO) adducts, formed by linking the 2-position of the N-heterocycle with nitrogen, phosphorus, and carbon elements, respectively, have been widely applied in both main-group and transition metal chemistry. The efficient stabilization of positive charges by the N-heterocycle allows the exocyclic atoms to accumulate negative charges, thereby significantly enhancing the basicity and nucleophilicity of the exocyclic elements. The improvement in nucleophilicity has facilitated the successful synthesis of numerous complexes with unique element–metal bonds. Additionally, by modifying the *N*-substituents, the kinetic stabilization requirements of highly reactive species can be fulfilled. This review aims to summarize the latest research progress on NHIs, NHCPs, and NHOs in main-group and transition metal compounds. It is important to emphasize that this review focuses on the commonly used five-membered N-heterocyclic carbene adducts, including imidazolin-2-ylidenes, imidazolidin-2-ylidenes, and benzimidazolin-2-ylidenes.

Received 12th April 2025
Accepted 29th April 2025

DOI: 10.1039/d5ra02549d

rsc.li/rsc-advances

1. Introduction

Since the first isolation and structural characterization of N-heterocyclic carbenes (NHCs) by Arduengo in 1991,[1] this field has garnered widespread attention.[2] The cyclic framework and presence of nitrogen atoms in these carbenes confer unexpectedly high stability, enabling them to form strong metal–carbon σ-bonds as ancillary ligands,[3] demonstrating greater bond strength than corresponding phosphine complexes.[4] By linking an exocyclic atom X to the 2-position of the N-heterocycle, the corresponding derivative ligands can be prepared. These adducts often possess polarized C=X bonds[5] or exocyclic atoms carrying lone pairs of electrons, facilitating the transfer of nucleophilicity from the carbene carbon to the exocyclic moiety. The enhanced π-accepting ability of the carbene fragment provides opportunities for constructing unique element–metal bonds. Currently, the widely applied ligand groups mainly include N, P, C element adducts: N-heterocyclic imines (NHIs), N-heterocyclic phosphinidenes (NHCPs) and N-heterocyclic olefins (NHOs). The electron density on the exocyclic atom is directly influenced by the σ-donating and π-accepting properties of the N-heterocyclic carbenes (NHCs). Due to the excellent stabilization of positive charges by the imidazoline ring,[6] the exocyclic C=N, C=P, and C=C double bonds in NHIs, NHCPs and NHOs are significantly polarized, allowing the exocyclic atoms to accumulate negative charges. This significantly enhances their basicity and nucleophilicity. These

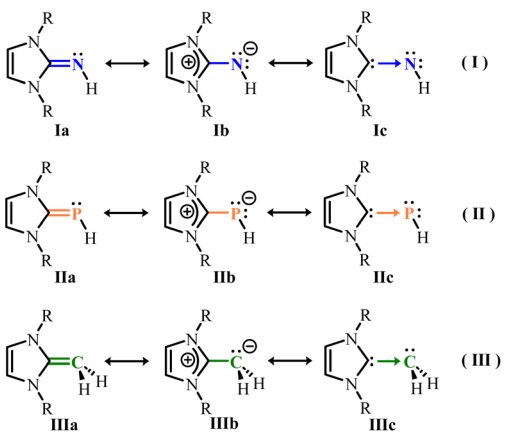

Scheme 1 Canonical resonance structures of neutral N-heterocyclic imines (NHIs), N-heterocyclic phosphinidenes (NHCPs) and N-heterocyclic olefins (NHOs).

Tianjin Key Laboratory of Structure and Performance for Functional Molecules, College of Chemistry, Tianjin Normal University, Tianjin, 300387, China. E-mail: zhongmingdong77@tjnu.edu.cn

ligands are best illustrated by the charge-separated resonance forms shown in Scheme 1.[7]

Nitrogen, as a highly electronegative element, has attracted considerable attention for its prominent role as a strong electron-donating atom in ligand systems. By introducing an exocyclic NH group at the 2-position of the NHC ring, N-heterocyclic imines (NHIs) with significantly enhanced nucleophilicity and basicity have been developed. In the imidazoline ring, the electron-rich π-system reduces the electrophilicity of the imine carbon atom, while the formation of a zwitterionic structure disperses electron density from the heterocycle to the exocyclic nitrogen atom, enhancing its electron-donating ability. In resonance structure **Ib**, the exocyclic nitrogen atom bears a negative charge, while structure **Ic** represents partial N-heterocyclic carbene (NHC) character (Scheme 1(I)). Meanwhile, the resonance form with two negative charges demonstrates the ability to coordinate as a 2σ, 4π electron donor (Scheme 2).[7a,8] Metal complexes formed with NHI ligands typically exhibit short M–N bonds, elongated C–N distances, and large M–N–C angles (160–180°), indicating strong metal–nitrogen interactions and significant metal–2-aza-allyl or metal–imine behavior.[7a] Furthermore, since NHI ligands and the cyclopentadienyl (Cp) group both possess a set of 2-electron frontier orbitals, these two ligand systems can be considered isolobal, with electron-donating capabilities comparable to those of the cyclopentadienyl (Cp) and phosphinimine ($R_3P{=}N$) groups.[9]

N-heterocyclic phosphinidenes (NHCPs) can be regarded as reverse-polarized phosphinidenes.[5,10] This conclusion is supported by ^{31}P-NMR spectroscopic data, which show high electron density on the phosphorus atom, and the degree of polarization of the phosphorus–carbon double bond can serve as an indicator of the π-accepting properties of the corresponding NHC.[11] Resonance structures **IIa** and **IIb** (Scheme 1(II)) each possess one or two lone pairs of electrons on phosphorus available for metal coordination, forming mono- or bidentate complexes. The availability of two lone pairs was demonstrated for the first time by isolating the bis(borane) adduct $[\{(IMes)PPh\}(BH_3)_2]$.[12] The presence of the nitrogen atom adjacent to the P=C double bond leads to the accumulation of π-electron density on the terminally coordinated phosphorus atom, similar to the isolobal N-heterocyclic imines (NHIs) (Scheme 2).

Regarding N-heterocyclic olefins (NHOs), they can be viewed as the coupling product of a terminal methylene unit and an N-heterocyclic carbene (NHC). They are often referred to as deoxy-Breslow intermediates,[13] ylidic olefins,[14] or nitrogen-based N-heterocyclic ketenimines (HKAs).[15] Since 1993, Kuhn and colleagues described the first isolable example of an NHO, NHOs have attracted significant attention in modern chemistry.[16] Due to the tendency of the N-heterocyclic moiety to accommodate positive charges, N-heterocyclic olefins (NHOs) possess an electron-rich double bond. As described by the resonance forms (Scheme 1(III)), the exocyclic C=C bond is highly polarized, with excess electron density concentrated on the exocyclic carbon atom (C_{exo}), rendering it highly nucleophilic and strongly basic. The nucleophilicity of NHOs is significantly stronger than that of commonly used Lewis bases such as DMAP (4-(dimethylamino)pyridine) but weaker than that of their NHC analogs, as verified by kinetic studies of the interaction between different NHOs and electrophiles.[17] Notably, NHOs typically require storage under inert conditions at low temperatures, which is closely related to their strong basicity. The proton affinity (PA) of NHOs lies significantly at the upper end of the superbasic range.[7c,17b,18] The π* orbital of the exocyclic C=C double bond in NHOs overlaps minimally with the d orbitals of metal centers, resulting in little to no backbonding. Therefore, NHOs primarily act as strong σ-donors, capable of transferring significant electron density to the metal center (Scheme 2). Upon coordination, the exocyclic carbon atom (C_{exo}) adopts the expected sp^3 hybridization.

The unique electronic and steric properties of these Lewis base ligands constitute the fundamental principle for stabilizing highly reactive elemental species and organometallic fragments through strong coordination interactions, significantly expanding the research scope of traditionally considered "transient" species. Simultaneously, they serve as highly efficient catalytic ligands widely applied in both metal-based and metal-free homogeneous catalysis systems. The integration of metal–organic frameworks (MOFs) with these ligands also holds promise for establishing novel photoredox-organocatalytic synergistic systems, paving new avenues for developing highly efficient and selective heterogeneous catalysts.[19] By selecting different substituents, the steric bulk of the imidazoline ring can be conveniently modified to meet the specific requirements for the kinetic stabilization of highly reactive species. The common method for obtaining these ligands involves the deprotonation of the corresponding pre-salts using strong bases such as potassium hydride (KH) or organolithium reagents (RLi). However, this method is often limited by the steric hindrance of *N*-substituents. Starting from N-heterocyclic carbenes (NHCs), reacting with appropriate nitrogen, phosphorus, and carbon sources to obtain the desired ligands has proven to be a feasible approach.[8c,18a,20]

In this article, we focus on discussing the coordination chemistry of NHIs, NHOs and NHCPs ligands in recent years. It should be noted that while the contributions of Ghatak,[8d,21] Inoue,[7a] and Naumann,[18a] among others,[8c,20,22–24] who have previously summarized various aspects of NHIs, NHCPs and NHOs chemistry, our work aims to provide a more targeted and updated perspective. Notably, Tamm and colleagues have also provided a review of N-heterocyclic carbene main-group element adducts and their applications in transition metal complexes, which will be partially discussed in this review.[25]

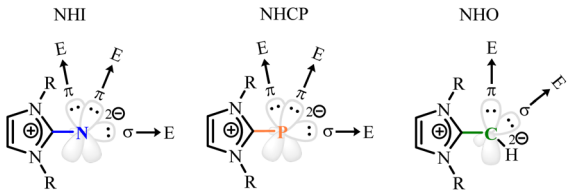

Scheme 2 Donor functions of anionic N-heterocyclic imines (NHIs), N-heterocyclic phosphinidenes (NHCPs) and N-heterocyclic olefins (NHOs).

Importantly, the review will concentrate on NHIs, NHOs, and NHCPs derived from imidazolin-2-ylidenes, imidazolidin-2-ylidenes, and benzimidazolin-2-ylidenes.

2. Mono(N-heterocyclic carbenes) as ligands

2.1. Group 13 element complexes

In 1993, the Kuhn group conducted pioneering work exploring the use of NHOs as ligands to stabilize electron-deficient boron centers.[16] Subsequently, boron complexes of NHCPs and NHIs have also been reported successively.[12,26] Currently, the coordination chemistry of the three ligands related to boron and aluminum has been extensively studied. Notably, in recent years, research has expanded to include the heavier group 13 elements (gallium, indium, thallium), with preliminary studies revealing promising developments in the area.

2.1.1. Boron complexes. To prepare novel borane species, cross-metathesis reactions have been applied multiple times to boron-based compounds. Treating germanium halide ^{R}IPrCH($GeCl_3$) (R = Me(**1a**), H(**1b**); ^{R}IPr = [(^{R}CNDipp)$_2$C])[27] with Li[BH_4] in Et_2O or ^{Me}IPrCH($SiMe_3$) (**2**)[27] mixed with THF·BH_3 in toluene yields the diborane complex [^{R}IPrCH(BH_2)$_2$(μ-H)] (R = Me(**3a**), H(**3b**)) (Scheme 3).[28] The molecular structure of [IPrCH(BH_2)$_2$(μ-H)] (**3b**) shows a sharp B–C–B angle of 72.0(2)°. Interestingly, the exocyclic C–C bond length in **3b** (1.434(2) Å) is shorter than the terminal NHO C–C bond in the noncyclic $B_2H_5^+$ complex [(IPrCH_2)BH_2(μ-H)BH_2(IPrCH_2)]$^+$ (1.467(2) Å) but longer than the terminal C=C double bond (1.332(4) Å) in IPrCH_2. DFT calculations support the explanation that there is no B–B bonding interaction. The structural parameters of the B_2H_5 complexes **3a** and **3b** are similar to those of the diborane [($SPPh_2$)$_2$C(BH_2)$_2$(μ-H)]Li(OEt_2) by Mézailles group reported,[29] which also suggests that the [IPrCH]$^-$ unit acts as a four-electron donor in **3b**. This intramolecular frustrated Lewis pair based on boron holds promise as an effective catalyst for the hydroboration and hydrosilylation of ketone substrates. Surprisingly, it was found that the NHOs themselves, ^{Me}IPrCH_2 and IPrCH_2, are effective organic catalysts for the hydroboration of ketones and aldehydes. For example, the reduction of MesCHO with IPrCH_2 as the organocatalyst achieved a turnover frequency (TOF) of 99 h^{-1}, in contrast to only 0.7 h^{-1} when using IPr under identical conditions. This indicates the great potential of NHOs as organic catalysts in hydroboration and hydrosilylation.

Also, **3a** can also be obtained from (^{Me}IPrCH)$_2$Zn (**4**) with the borane adduct $H_3B{\cdot}SMe_2$.[30] Additionally, mixing **4** with catecholborane (HBcat) in toluene, obtaining the product

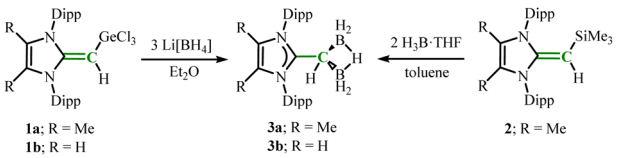

Scheme 3 Synthesis of NHO-stabilized diborane complexes **3a** and **3b**.

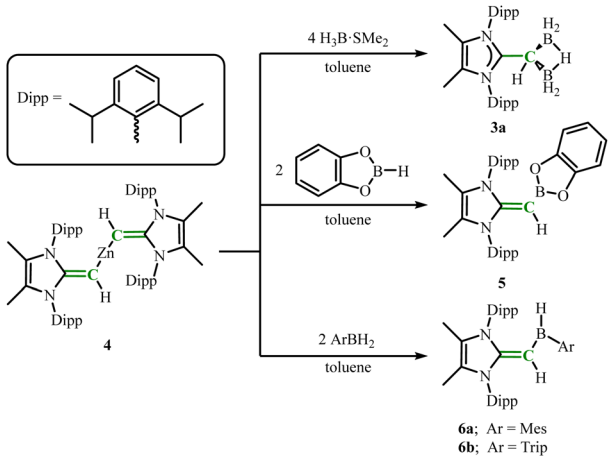

Scheme 4 Synthesis of NHO-stabilized boranes by **4**.

(^{Me}IPrCH)Bcat (**5**) from the soluble fraction (Scheme 4). Subsequently, (**4**) was mixed with $ArBH_2$ to yield (^{Me}IPrCH)B(Ar)H (Ar = Mes(**6a**), Trip(**6b**); Trip = 2,4,6-i$Pr_3C_6H_2$) (Scheme 4). The C–B bonds in products **5–6b** are shorter than those in BPh_3 (average 1.689(6) Å),[31] indicating the presence of some C–B π character. DFT calculations support the interpretation that C–B π interactions exist in **5** and **6b** (WBI_{C-B} = 1.14(**5**), 1.23(**6b**)). Mixing **6a** with trityl triflate [Ph_3C]OTf yielded an unusual triflate salt [(^{Me}IPrCHMes)B(THF)(OTf)H][OTf] (**7**) (Scheme 5) rather than the expected bidentate boronium ion [^{Me}IPrCH–B–Mes]$^+$. The process maybe undergoes 1,2-Mes migration to generate a borane-type radical.

Similarly, [(^{Me}IPrCH)In]$_4$ (**8**) can also be used as transmetalation reagent to yield corresponding boron complexes (**6b**) (Scheme 6).[32] Mixing **4** and HBpin (pin = diphenylmethylidene) in toluene did not yield the expected pinacolborane derivative (^{Me}IPrCH)Bpin, presumably due to the reduced electrophilicity of the boron center in HBpin (relative to HBcat). Notably, compound [(^{Me}IPrCH)Li]$_2$ did not react with HBpin either. However, Rivard and coworkers obtained (^{Me}IPrCH)Bpin (**9**) by mixing **8** with HBpin (Scheme 6). This indicates that **8** has a higher propensity for B–H bond activation/ligand transfer.

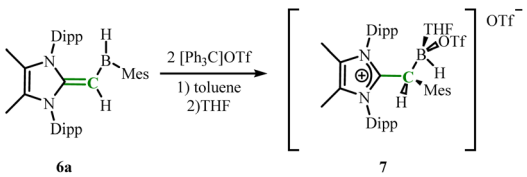

Scheme 5 Reaction of **6a** with [Ph_3C]OTf.

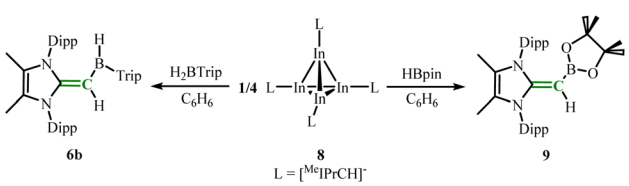

Scheme 6 Synthesis of NHO-stabilized boranes by **8**.

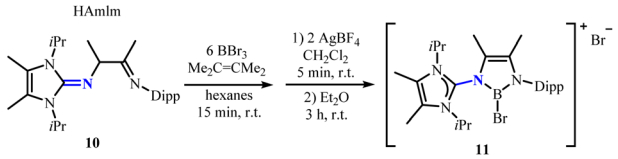

Scheme 7 Preparation of **11** by HAmIm **10**.

In 2020, Frank and coworkers isolated a complete series of Lewis acid-free neutral chalcogenoboranes with B=X structures (X = O, S, Se, Te) by using novel ligand systems (**10**, HAmIm).[33] The corresponding oxoboranes and telluroboranes were reported for the first time in a non-Lewis acid form. Adding hexane solution of **10** to BBr_3 solution in the same solvent and then decomposing it with $AgBF_4$ can obtain the suitable precursor **11** for preparing B=X species (Scheme 7). Subsequently, the precursor **11** reacted with an equimolar amount of water in the presence of triethylamine to yield the ionic hydroxyborane **12**. Deprotonation with KHMDS in the presence of 2,2,2-cryptand isolated oxoborane **13** (Scheme 8). The precursor **11** further converted with lithium chalcogenides Li_2X in 1,2-dimethoxyethane to obtain the other B=X species (X = S, Se, Te), with the thioborane (**14**) and selenoborane (**15**) requiring treatment with the complexing agent 12-crown-4 to remove the byproduct LiBr (Scheme 8). The B=O bond length in **13** (1.353(9) Å) is very short, which may result from the absence of oxygen-coordinating Lewis acids strengthens the B=O double bond character. The Wiberg bond indices of compounds **13–16** are 1.86, 1.75, 1.69 and 1.69, respectively, indicating that the novel series of chalcogenoboranes exhibit significant double bond character. Meanwhile, the decrease in WBI values indicates a weakening of π–π interactions between the boron atom and the heavier chalcogen atoms. At the same time, the chemical behavior of the B=O bond in oxoboranes is similar to the classical carbonyl reactivity of C=O bonds.

To isolate borasilene, Rivard group reacted dichloroborane **17** (ref. 34) with potassium hypersilanide ($KSi(SiMe_3)_3$) to obtain the precursor $(Me_3Si)_3SiB(Cl)NHI$ **18**. Treatment of **18** with KO*t*Bu is postulated to form the elusive borasilene **INT(19)**. Further isolation of the N-heterocyclic carbene (NHC)-stabilized borasilene adduct **20** was achieved (Scheme 9).[35] The B–Si bond in **20** exhibits zwitterionic character, with the positive charge localized at the trigonal-planar boron atom and the negative charge at the silicon atom, which marks the apex of a trigonal

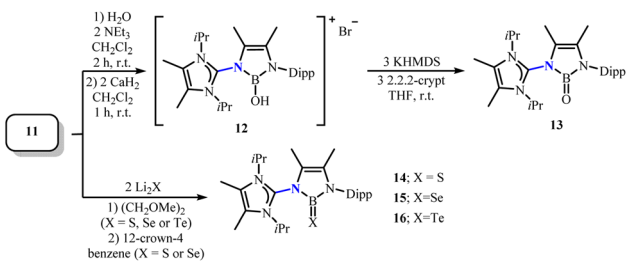

Scheme 8 Synthesis of a series of neutral chalcogenoboranes with B=X structures **13–16**.

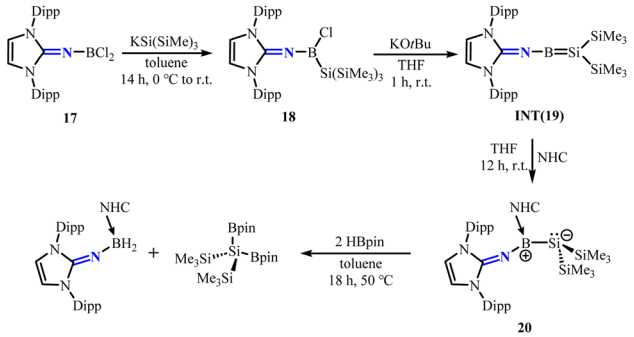

Scheme 9 Synthesis of borasilene **20** and its reaction with HBpin. NHC = 1,3,4,5-tetramethylimidazol-2-ylidene.

pyramid. The conversion of **20** with pinacolborane (HBpin) results in the cleavage of the B–Si bond, yielding (NHI) BH_2(NHC) and $(Me_3Si)_2Si(Bpin)_2$, consistent with the polarized nature of the B–Si bond in **20.**

Using a similar ligand support approach, the separation of alkyl borane **21** supported by N-heterocyclic imine (NHI) and NHC ligands is achieved through dehydrohalogenation/NHC coordination (Scheme 10).[36] The effective weakening of the B–C bond strength in **21** by σ- and π-electron donors allows for the synthesis of novel organoboron compounds through

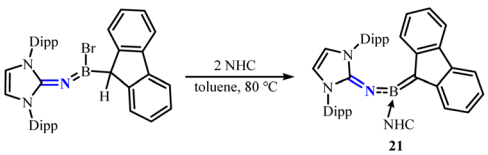

Scheme 10 Synthesis of alkyl borane **21**.

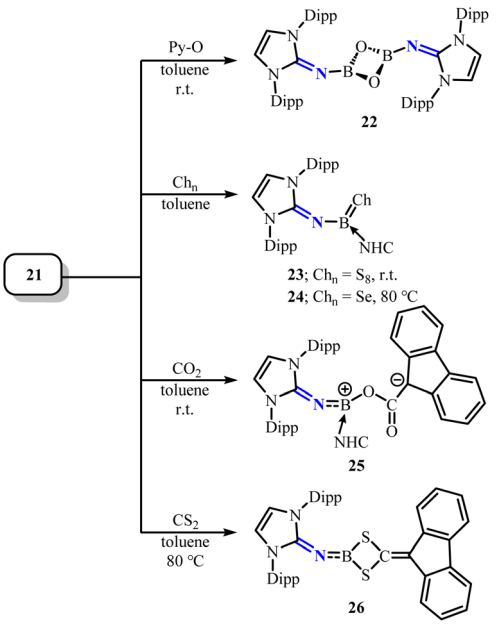

Scheme 11 Reactions of **21** with pyridine-*N*-oxide, sulfur, selenium, CO_2 and CS_2. NHC = 1,3-diisopropyl-4,5-dimethylimidazol-2-ylidene.

unconventional transformations. Compound **21** reacts with pyridine-*N*-oxide, sulfur, and selenium to form 1,3-dioxa-2,4-diboracyclobutane **22**, thioxoborane **23**, and selenoborane **24**, respectively (Scheme 11). Additionally, the reaction of **21** with CO_2 and CS_2 yields borenium/fluorenide **25** and dithiaboretane **26** (Scheme 11). Notably, **25** rapidly converts into transient oxoborane and imidazolium enolate under heating conditions. These reactions demonstrated the oxidative functionalization, insertion, and boron-Wittig reactions of alkyl boranes.

2.1.2. Aluminium complexes. The use of N-heterocyclic imine-based ligands has enabled the synthesis of a variety of aluminum hydrides. Utilizing a previously established strategy,[37] the reaction of $\{IMesNAlH_2\}_2$ (**27**)[38] with Me_3SiOTf yielded the novel dimeric aluminum hydride $\{IMesNAl(H)OTf\}_2$ (**28**) (Scheme 12).[39] Unlike the bulkier analogue $\{IDippNAl(H)OTf\}_2$, where the triflate substituents adopt a *cis* configuration, the triflate groups in **28** are arranged in a *trans* configuration on the central four-membered Al_2N_2 ring. Moreover, N-heterocyclic imine-supported aluminum hydride compounds can serve as catalysts for the hydroboration of pinacolborane, CO_2 reduction, and amine–borane dehydrocoupling, demonstrating broad catalytic applications.[40] By modifying the substituents and stoichiometry, the conversion of (benzo)imidazolin-2-imine ligands with $AlMe_3$ enables the preparation of a series of mononuclear, binuclear, and trinuclear structural aluminum complexes **29–35** (Scheme 13).[41] These complexes are capable of effectively catalyzing the ring-opening polymerization of ε-caprolactone, yielding polycaprolactones. Among them, mononuclear complex **29c** achieved near-quantitative monomer conversion (>99%) within 1 hour, while its dinuclear analogue **31b** yielded 44% poly(ε-caprolactone) under identical conditions. Both catalysts showed significantly higher activity than $AlMe_3$ reference (21% yield). Moreover, the reaction of [(SIDipp)NH] with $AlH_3{\cdot}NMe_2Et$ allows for the isolation of the dimeric aluminum dihydride $\{\mu\text{-}LAlH_2\}_2$ (**36**) (Scheme 14), which can undergo substitution reactions with various small molecules.[42]

In 2019, three novel NHO–trialkylaluminum complexes (**37a–38**) were reported.[43] At room temperature, combining $^{Me}IPrCH_2$ with one equivalent of AlR_3 in toluene yielded the monoadducts $^{Me}IPrCH_2{\cdot}AlR_3$ (R = Me(**37a**), Et(**37b**)) (Scheme 15). XRD analysis of **37a** showed that the C_{NHO}–Al bond length of 2.1198(13) Å is longer than the coordinating N_{NHI}–Al interaction in the NHI·$AlMe_3$ complex by Masuda group reported (1.9648(19) Å).[44] This observation follows the general rule that the ligand–element bond in N-heterocyclic imine (NHI) adducts is shorter than that in NHO–element bonds. Combining $^{Me}IPr{=}CH{-}CH{=}CH_2$ with $AlMe_3$ yielded $^{Me}IPr{=}CH{-}CH{=}CH_2{\cdot}AlMe_3$ (**38**) (Scheme 15) coordinated through the terminal exocyclic carbon atom rather than the hoped-for product coordinated to the proximal exocyclic carbon, which may be due to the large steric hindrance near the heterocycle and the more Lewis basic terminal coordination site. Interestingly, it was found that $^{Me}IPrCH_2{\cdot}AlMe_3$ (**37a**) exhibited FLP-type behavior in THF,

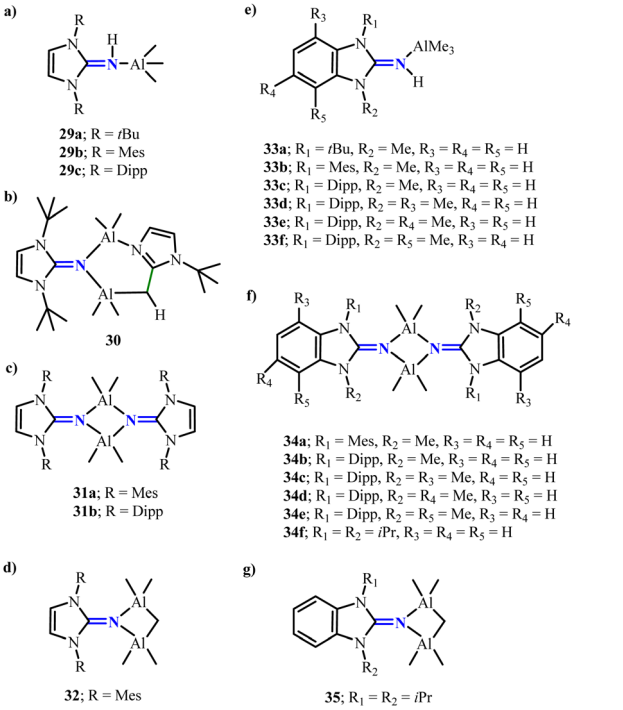

Scheme 13 Synthesis of a series of mononuclear, binuclear, and trinuclear structural aluminum complexes **29–35**.

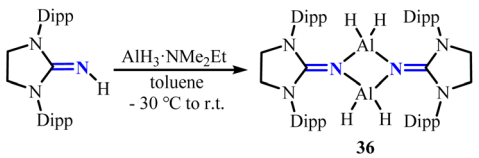

Scheme 14 Synthesis of NHI-stabilized dimeric aluminum hydride $\{\mu\text{-}LAlH_2\}_2$ (**36**).

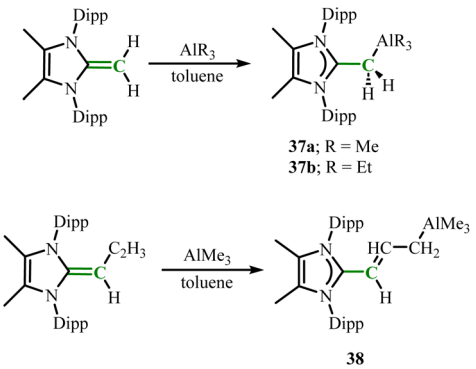

Scheme 15 Synthesis of NHO-stabilized trialkylaluminum complexes **37–38**.

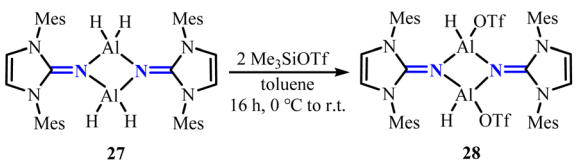

Scheme 12 Synthesis of NHI-stabilized dimeric aluminum hydride $\{IMesNAl(H)OTf\}_2$ (**28**).

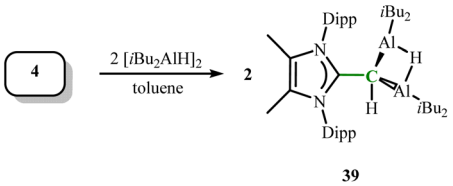

Scheme 16 Synthesis of NHO-stabilized dialane complexes **39**.

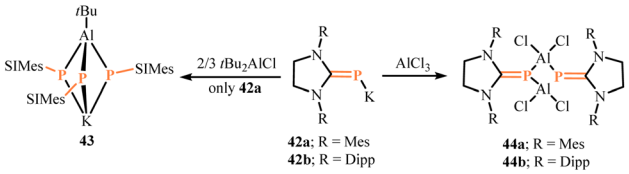

Scheme 18 Synthesis of NHCP-stabilized aluminum complexes **43** and **44** by the precursor **42**.

leading to the polymerization of several Michael-type monomers under mild conditions.

Combining **4** with diisobutylaluminum hydride (DIBAL–H, $[iBu_2AlH]_2$) *via* transmetallation yields the dialane product $[^{Me}IPrCH–(AliBu_2)_2(\mu\text{-}H)]$ (**39**) (Scheme 16).[30] The adjacent C_{NHO}–Al bonds in **39** (2.0513(17) and 2.0328(15) Å) are shorter than the C_{NHO}–Al bond length in **37a**. The bridging Al–H bond lengths in **39** are obtained as 1.662(18) and 1.753(18) Å, similar to the average bridging Al–H bond length in α-AlH_3 (1.715 Å).[45]

Similarly, the monoaluminum complexes [{(IDipp)PH}$AlMe_3$] and [{(IMes)PH}$AlMe_3$] (R = Dipp(**40a**), Me(**40b**)) were synthesized by the transformation of (IDipp)PH and (IMes)PH with $AlMe_3$, respectively (Scheme 17).[46] However, (^{Me}IMes)PH reacted with $AlMe_3$ (two equivalents) to yield the dialuminum complex [{(^{Me}IMes)PH}$(AlMe_3)_2$] (**41**) (Scheme 17). The P–Al–C angles in **40a** ranged from 89.02(5)° to 116.77(5)°; the Al–P–C angle in **40a** was 124.98(4)°, indicating that the Al atom is in a distorted tetrahedral environment. The P–C bond lengths of **40a–41** were slightly longer than their corresponding reactants, and even more so in the bis(trimethylaluminum) complex **41**, which is a result of the coordination of the $AlMe_3$ groups. These structural features suggest that the P–Al interactions in complexes **40a–41** enhance the polarization of the carbon–phosphorus double bond towards the P atom. Interestingly, it was found that the monoaluminum complexes **40a** and **40b** could initiate the ring-opening polymerization of racemic lactide, yielding poly(racemic lactide) with high *meso* selectivity, whereas the dialuminum complex **41** produced an almost atactic polymer.

Hänisch group reported the synthesis of novel alane complexes utilizing the precursor (SIMes)PK (**42a**).[47] The potassium salt **42a** was prepared through the deprotonation of the saturated N-heterocyclic carbene-stabilized phosphinidene SIMesPH with benzyl potassium. Interestingly, converting **42a** with tBu_2AlCl yielded the novel cage compound $[K(SIMesP)_3\text{-}AltBu]$ (**43**) (Scheme 18). The three phosphorus atoms in **43** are not in a planar environment, with their angles summing to 306.6(3)°. The K–P distance (375.0(1) pm) is longer than other reported potassium counterion-containing anionic Al–P compounds, such as $K[Al_4(PPh_2)_7PPh]$ (318.2(1) pm).[48] The K–C distances are 359.6(1) pm (K–C_{ipso}) and 311.2(1) pm (K–C_{ortho}), suggesting that the potassium atom in **43** interacts with the aromatic system of the methylphenyl substituents. The structure of compound **43** can be inferred as an ion pair consisting of an aluminate anion and a potassium cation coordinated by an aryl group.

Subsequently, the same group reacted $AlCl_3$ with identical precursors (SIMes)PK (**42a**) and (SIDipp)PK (**42b**) in a saturated toluene solution to obtain the cyclic dimers $[(NHC)PAlCl_2]_2$ (NHC = SIMes(**44a**), SIDipp(**44b**)) (Scheme 18).[49] The structures of compounds **44a** and **44b** were characterized. Compound **44a** formed a butterfly-shaped Al_2P_2 ring (internal angles: 83.9(1)–86.5(1)°) with the NHC ligands in a *cis* orientation; whereas compound **44b** formed an almost planar square Al_2P_2 ring (internal angles: 86.8(1)–93.2(1)°) with the NHC ligands in a *trans* orientation.

2.1.3. Gallium, indium and thallium complexes. Treatment of (SIDipp)PK (**42b**) with one equivalent and two equivalents of $GatBu_2Cl$ yielded the mixed bridging system [(SIMes)$P(GatBu_2)_2Cl$] (**45**) and the four-membered ring compound $[SIMesPGatBu_2]_2$ (**46**), respectively (Scheme 19).[47] XRD analysis showed that **46** has an almost planar coordination environment, with the angles on the phosphorus atoms sum to 355.6(2)°. The Ga–P bond lengths in **45** (239.34(4) and 240.84(4) pm) are shorter than those in **46** (246.21(7)–248.12(7) pm), indicating that the steric hindrance in the structure of **45** is less

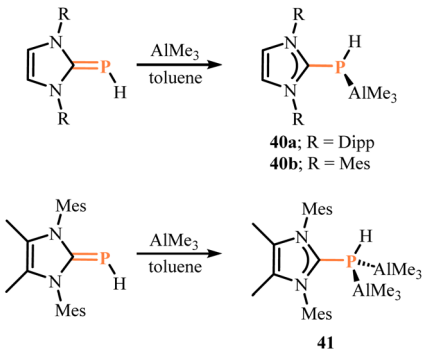

Scheme 17 Synthesis of NHCP-stabilized monoaluminum complexes **40a** and **40b** and dialuminum complex **41**.

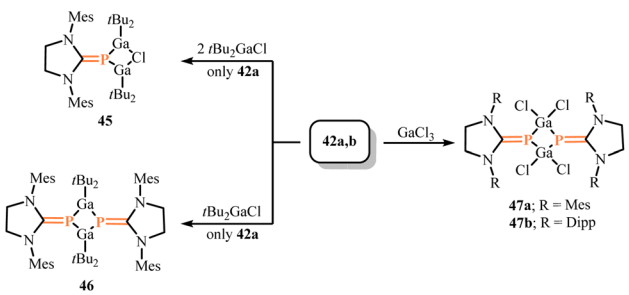

Scheme 19 Synthesis of NHCP-stabilized gallium complexes **45–47**.

than that in **46**. Similarly, mixing the precursors **42a** and **42b** with $GaCl_3$ in a 1 : 1 ratio yielded the dimers $[(NHC)PGaCl_2]_2$ (NHC = SIMes(**47a**), SIDipp(**47b**)) (Scheme 19).[49] Similar to **44a** and **44b**, the shape of the central Ga_2P_2 ring (butterfly-shaped or nearly planar square) depends on the steric hindrance of the NHC ligands.

In 2021, the first five-membered ring triel(I) carbene analogues E(AmIm) (E = Ga, In, Tl; AmIm = aminoimidazolin-2-imine) were reported.[50] The potassium salt of HAmIm **48** was prepared *via* benzyl potassium and reacted with GaCp* to obtain **49** (Scheme 20). In(I) or Tl(I) species **50** and **51** were obtained by conversion of the lithium salt of HAmIm **48** with InCp or $TlBF_4$, respectively (Scheme 20). In compounds **49–51**, the imidazolin-2-imine part and the phenyl part are arranged vertically, with the exocyclic N–C bond distance increased compared to **48**, indicating a weakening of the double bond character. The pentagonal ring structures of compounds **49–51** all belong to planar geometry. Furthermore, the bond angles between N–E–N decreased from 79.67(7)° to 70.41(5)°, consistent with the regular increase of longer E–N bonds in the heavier triel.

N-Heterocyclic imine-based bis-gallium(I) carbene analog **52** can be synthesized through the reaction of (IDipp)NLi, *t*BuOK, and Cp*Ga (Scheme 21).[51] Compound **52** features a four-membered Ga_2N_2 ring structure, with the HOMO primarily dominated by non-bonding lone pairs of gallium atoms. Moreover, compound **52** demonstrates excellent nucleophilicity and potential as an imino-group transfer reagent, as evidenced by its addition reactions with MeOTf, diphenyl disulfide, and 9,10-phenanthrenequinone, as well as its reactions with ECl_2 (E = Ge or Sn) to form chlorogermylene dimers and chlorostannylene dimers.

Mixing $[(^{Me}IPr{=}CH)Li]_2$ (**53**) with CpIn in toluene can isolate $[(^{Me}IPr{=}CH)In]_4$ (**8**) (Scheme 22).[32] The In–In–In angles in **8** [59.112(13) to 61.104(13)°] are close to the tetrahedral arrangement. The C=C bonds in the $[^{Me}IPr{=}CH]$ ligands of **8** (average 1.345(5) Å) are similar in length to those in free $^{Me}IPr{=}CH_2$ (1.3489(18) Å),[52] revealing that the C–C double bond character is

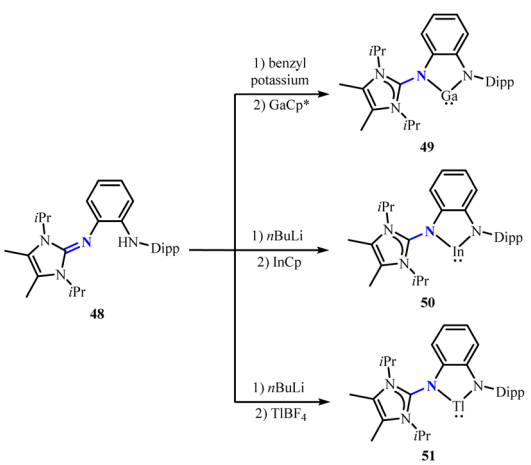

Scheme 20 Synthesis of five-membered ring triel(I) carbene analogues **49–51**.

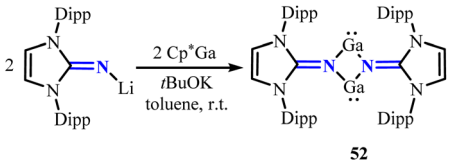

Scheme 21 Synthesis of NHI-stabilized gallium complex **52**.

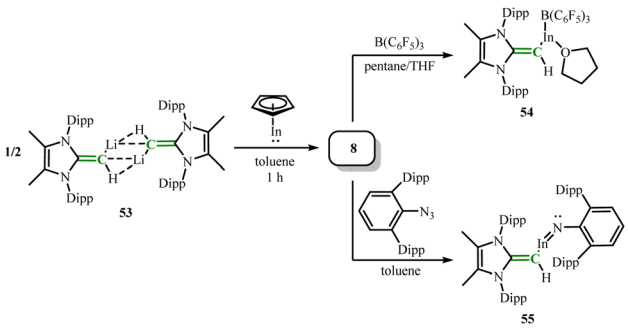

Scheme 22 Synthesis of NHO-stabilized indium complex **8** and its reactions with $B(C_6F_5)_3$ and $ArDippN_3$.

retained. Combining **8** with $B(C_6F_5)_3$ yielded $(^{Me}IPr{=}CH)In(THF)\cdot B(C_6F_5)_3$ (**54**) (Scheme 22), indicating that **8** can serve as a feasible source of monomeric RIn: units. The In(I) centers in **8** can also activate the B–H bonds in boranes, facilitating rapid H/NHO ligand exchange on boron (see above). To further expand the neutral indium imine species, treatment of **8** with the sterically hindered diphenyl azide $ArDippN_3$ (ref. 53) to form indium imine $(^{Me}IPr{=}CH)In{-}NArDipp$ (**55**) (Scheme 22). AIM analysis showed that the delocalization index δ(In, N) for the InN unit in **55** is 1.13, which is notably lower than the δ(In, N) values for HNInH (1.73) and $PhNIn(HC{=}C(NHCH)_2)$ (1.39), indicating weak In–N π-bonding. Also, NBO analysis indicated that there is only one σ-bonding orbital in **55** which may result from the In–N bonding in **55** is highly polarized/weak π-bonding.

2.2. Group 14 element complexes

The trimethylsilyl adducts of NHIs, NHCPs and NHOs have been widely demonstrated to be highly efficient synthons, useful for preparing a variety of ligands and serving as transmetalation reagents for the synthesis of main-group element and transition metal complexes.[7b,27,54] In recent years, these ligands have also proven to be highly effective in stabilizing group 14 elements, particularly achieving significant progress in the synthesis of low-coordinate group 14 alkenes, showcasing their exceptional ability to stabilize low-coordinate species.

2.2.1. Silicon complexes. To obtain novel silaalkenes, Rivard and coworkers designed to prepare stable acyclic silaalkenes (R_2Si:) through the steric effects of the vinyl N-heterocyclic olefin ligands and the electron-donating ability of the hypersilyl group $[Si(SiMe_3)_3]$.[55] By conversion of $^{Me}IPrCH_2$ with $SiBr_4$ to obtain the precursor $(^{Me}IPrCH)SiBr_3$ (**56**). Further, reacting **56** with hypersilyl potassium $[K(THF)_2][Si(SiMe_3)_3]$

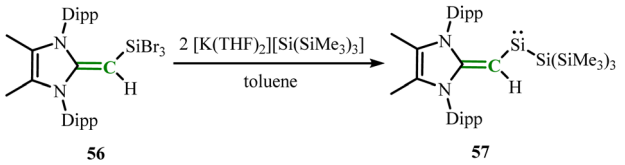

Scheme 23 Synthesis of NHO-stabilized acyclic silaalkenes **57**.

yielded the first bicoordinated acyclic silaalkene stabilized by a carbene ligand, (^{Me}IPrCH)Si{Si(SiMe$_3$)$_3$} (**57**) (Scheme 23). The ^{29}Si NMR spectrum shows a signal at 432.9 ppm, within the range of known bicoordinated acyclic silylkenes.[56] Additionally, the vinyl C–C bond in **57** (1.406(3) Å) is longer compared to that in the free NHO ^{Me}IPrCH$_2$ (1.3489(18) Å),[52] presumably due to the transfer of partial π-electron density from the vinyl group to silicon. The C–Si–Si angle of 101.59(7) is consistent with the high s-character of the silicon lone pair, further validating the formation of the silaalkene. Surprisingly, compound **57** also exhibited high reactivity towards small molecules, capable of activating strong homonuclear and heteronuclear bonds such as B–H, P–P and C–H at room temperature.

In 2021, the same group reported the synthesis of the first bicoordinated acyclic silaalkene without heteroatom donor binding.[57] By treatment of [K(THF)$_2$][Si(SiMe$_3$)$_3$] and SiBr$_4$ with ^{Me}IPr obtaining the degradation-resistant Si(II) precursor ^{Me}IPr·SiBr$_2$ (**58**). Further mixing **58** with [(^{Me}IPr=CH)Li]$_2$ (**53**) in toluene yielded the target product divinylsilylene (^{Me}IPr=CH)$_2$Si: (**59**) (Scheme 24). The C–Si–C bond angle in **59** (100.58(8)°) is in line with the mixed s/p character of the Si lone pair, which validates the formation of the silylene. The ^{29}Si NMR chemical shift (272 ppm) is in the highly shielded region compared to **59** (433 ppm). Notably, the initial half-wave potential $E_{1/2}$ of compound **59** is −1.35 V, making it a potential strong reductant. Combining **59** with an equimolar amount of [Pd$_3$(dba)$_2$] (dba = dibenzylideneacetone) yielded (^{Me}IPr=CH)$_2$Si(dba) (**60**) (Scheme 24), indicating that the Si(II) center in **59** has both electrophilic and nucleophilic properties.

In recent years, the isolation of multiple silicon seven-membered rings formed through the intramolecular insertion of acyclic silylenes into aromatic C=C bonds has been reported.[56c,58–60] Treating IPrNSiBr$_3$(**61**)[61] with reagents bearing different silyl ligands yields the corresponding silylenes (**62**)

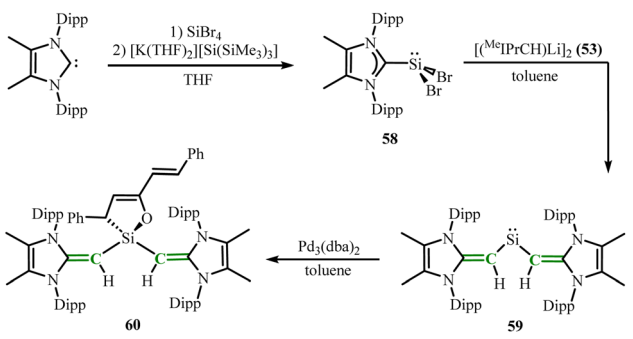

Scheme 24 Synthesis of bicoordinated acyclic silaalkenes **59** and its reaction with [Pd$_3$(dba)$_2$].

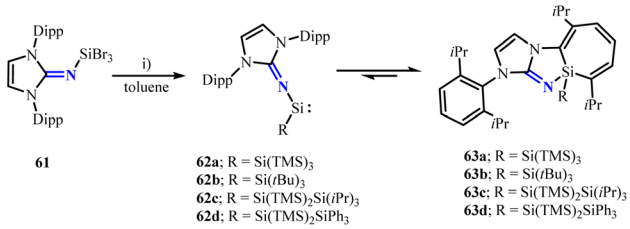

Scheme 25 Synthesis of silylenes **62**/silepins **63**. (i) For **62a**: KSiTMS$_3$; for **62b**: [Na·(THF)$_2$]Si*t*Bu$_3$; for **62c**: KSi(TMS)$_2$Si(iPr)$_3$; for **62d**: KSi(TMS)$_2$SiPh$_3$.

(Scheme 25). These silylenes are stabilized by NHI as a π-donor and silyl groups as σ-donors, and they can reversibly transform into silepins (**63**), showing the facile interconversion between Si(II) and Si(IV) (Scheme 25). Among these, the modification of different silyl ligands significantly influences the σ-donating and π-accepting abilities of the silylenes. Such silepins have been proven to function as "masked" silylenes for small molecule activation, exhibiting superior catalytic potential.

Furthermore, exposing **63a** and **63b** to an atmosphere of N$_2$O led to the isolation of the first acyclic, neutral, three-coordinate silanones **64** (Scheme 26).[58] In **64b**, hyperconjugation exists between the Si–C σ-bond of the silyl group to the π*-bonding orbital of Si=O moiety. Concurrently, the Si=O π-bond in **64b** mixes with the nonbonding orbital of the exocyclic nitrogen atom, consistent with the shorter Si–N distance (1.646(3) Å), demonstrating the electron-donating effects of the NHI ligand and the silyl group. Silanones **64** converted with CO$_2$ and methanol to yield the corresponding silicon carbonate complexes **65** and silanol **66**, respectively (Scheme 27). Notably, **64a** can undergo a 1,3-silyl migration in THF-d_8 to generate the

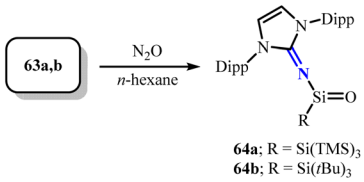

Scheme 26 Synthesis of silanones **64**.

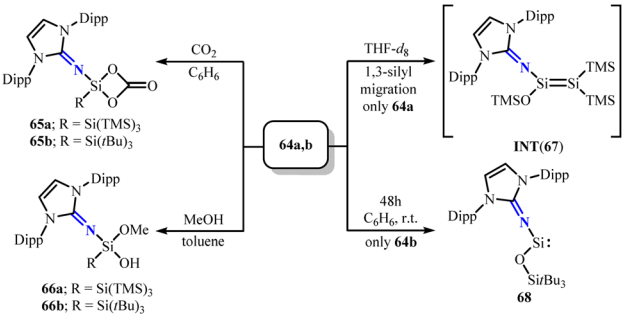

Scheme 27 Reaction of silanones **64** with CO$_2$ and MeOH, isomerization pathway of silanone **64a** to **INT(67)** and selective transformation of silanone **64b** to **68**.

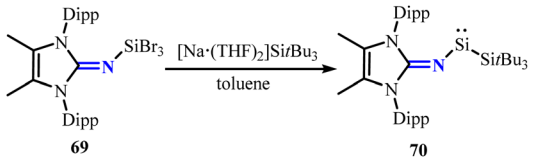

Scheme 28 Synthesis of silylenes **70**.

intermediary disilene **INT(67)** (Scheme 27), which is subsequently trapped by reacting with ethylene and IMe_4. It is worth mentioning that the application of the Wittig reaction to silanone **64b** was reported in 2019, contributing to the extension of the synthetic methods for heavier alkenes.[62] Interestingly, **64b** undergoes thermal rearrangement in C_6D_6 or THF-d_8 solution to form *N*,*O*-silylene **68** (Scheme 27). Compound **68** demonstrates diversified oxidation reactions, successfully activating small molecules such as P_4, NH_3, CO_2 and N_2O.[63]

Using the same strategy, the methylated backbone N-heterocyclic iminosilicon tribromide **69** was converted with the silanide complex $[Na\cdot(THF)_2]Si\textit{t}Bu_3$ to yield silylene **70** (Scheme 28).[64] Unlike the above silylenes **62**, the silylene center in compound **70** did not insert into the aromatic C–C bonds of the Dipp substituent to form a silepin structure, which can be a result of the steric hindrance of the methylated backbone. Silylene **70** can react with benzene and its derivatives or N-heteroarenes, inserting into aromatic C–C and C–N bonds to form corresponding seven-membered rings. Moreover, silylene **70** had been proven to activate various small molecules and undergo metathesis type process with aryl isocyanides, demonstrating higher reactivity compared to the silylenes **62**.[65,66]

Similarly, the NHCP-stabilized silylene–phosphinidene **72** was prepared by treatment of $KSiTMS_2SiTol_3$ (Tol = *p*-Tolyl) with IDippPSiBr$_3$ (**71**) in toluene (Scheme 29).[67] The ^{29}Si NMR chemical shift (455.0 ppm, $^1J^{Si-P}$ = 187.5 Hz) and ^{31}P NMR chemical shifts (269.4 ppm) are in the significantly downfield, which may due to the polarization of the P–Si bond. The angles Si–Si–P (97.99(3)°) and Si–P–C (101.43(6)°) showed a bent geometry in **72**, indicating the presence of lone pairs on both silicon and phosphorus. Additionally, DFT calculations support the multiple bond character between Si and P exist in **72** (WBI = 1.47; MBO = 1.53). Therefore, compound **72** can be inferred as a rare NHC-stabilized phosphosilaalkyne. Similar to the reactivity of silylenes,[65,68] the silicon center in **72** allows for oxidative addition to various unsaturated small molecules such as CO_2, ethylene and acetylene, and coordination with iron tetracarbonyl to yield relevant compound **73–76** (Scheme 30), showing a highly nucleophilic silicon center. Further investigation into the mechanism of ammonia activation by

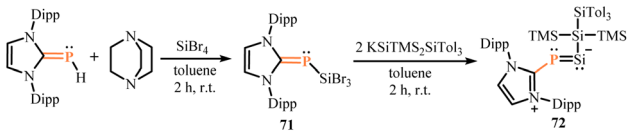

Scheme 29 Synthesis of NHCP-stabilized silylene–phosphinidene **72**.

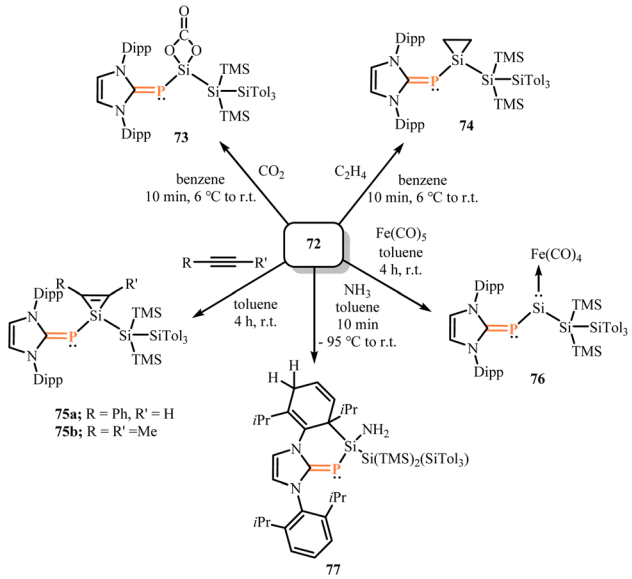

Scheme 30 Reactions of **72** with small molecules and coordination with iron tetracarbonyl.

compound **72**. Unlike known tetrahedral center ammonia activation, after forming the silylene–ammonia adduct, further conversion to a Meisenheimer-type complex followed by deprotonation of ammonia to yield **77** (Scheme 30).[69] This series of reactions led to intermolecular 1,5-hydroamination with dearylation on the NHC flank. Notably, compound **72** can isomerize to the corresponding phosphasilenylidene **78**, similar to the isomerization rearrangement from nitriles to isonitriles. Compound **78** can also *via* conversion with acetylene and coordinate with iron tetracarbonyl to yield corresponding compound **79** and **80**, exhibiting similar reactivity to **72** (Scheme 31).

Mo group successfully isolated an N-heterocyclic imino-stabilized silylene [LSi(NHI)] (**81**) (L = PhC(N*t*Bu)$_2$) with strong σ-donor property and significant steric hindrance through reacting [LSiCl] with [NHILi] (Scheme 32).[70] Notably, utilizing silylene **81** can isolate rare disilicon(0) complex **82** and ditin(0) complex **83** (Scheme 33).[70,71] The complexes **82** and **83** can be further transformed into a series of unique silicon and tin complexes, demonstrating the remarkable potential of silylene **81** in stabilizing low-valent element complexes.

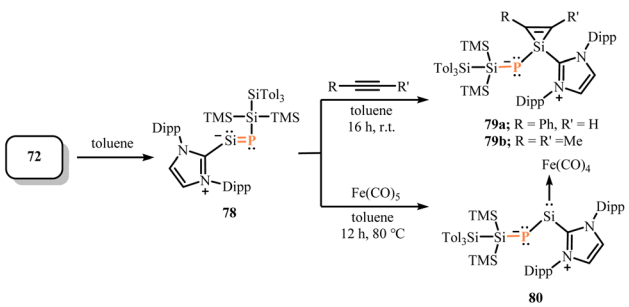

Scheme 31 Isomerization of **72** to **78** and its reaction with acetylene and iron tetracarbonyl.

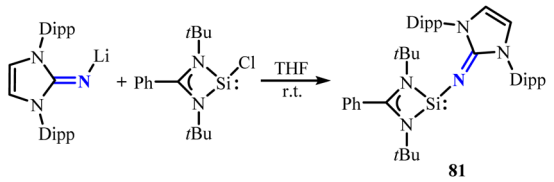

Scheme 32 Synthesis of silylenes **81**.

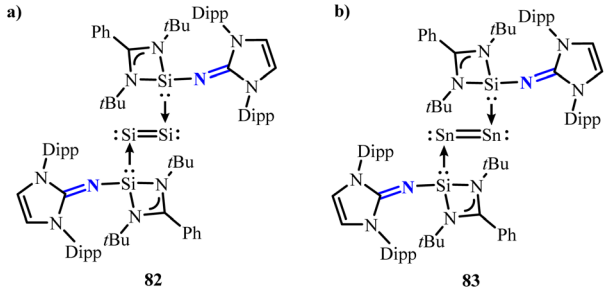

Scheme 33 Disilicon(0) complex **82** and ditin(0) complex **83**.

Recently, the synthesis of a silyl radical **86** stabilized by an NHI ligand and two silyl substituents has been reported (Scheme 34).[72] The synthesis of silyl radical **86** can be achieved intentionally through the reaction of the conversion of I*t*BuNSiBr$_3$ (**84**) with three equivalents of NaSi*t*Bu$_2$Me or one equivalent of NaSi*t*Bu$_2$Me with imino(silyl)disilene (**85**). The central silicon atom of compound **86** resides in a slightly pyramidalized geometry, with a bond angle sum of 353.51°, slightly less than that reported for several other silyl radicals (close to 360°).[73] Moreover, the Mulliken spin population of 0.922 at the central silicon atom, further confirming the formation of a silicon-centered radical.

2.2.2. Germanium, tin and lead complexes. In 2019, the synthesis of NHCPs stabilized group 14 heavier tetrelenes **87a–87c** *via* salt elimination reactions were reported.[74] Using the deprotonated compound (SIDipp)PK (**42b**) as a precursor, they reacted it with (SIMes)MX$_2$ (0.5 equivalents, M = Ge, Sn, Pb; X = Cl or Br) in toluene to obtain single crystals of [(SIDipp)P]$_2$M(M = Ge(**87a**), Sn(**87a**), Pb(**87c**)) (Scheme 35), which were deep purple crystals. The deep color of compounds **87a–87c** initially revealed π–π interactions. The ^{31}P NMR spectra (145.2 ppm, **87a**; 121.4 ppm, **87b**; 116.8 ppm, **87c**) showed upfield shifts compared to other corresponding phosphinimine complexes, indicating multiple bond character between phosphorus and group 14 atoms. The P–M–P angles in compounds **87a–87c** were 87.4(1)°, 85.8(1)°, and 84.6(1)°, respectively, which were lower than those in other known corresponding compounds

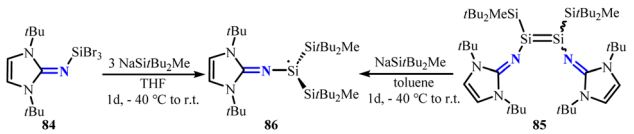

Scheme 34 Synthesis of silyl radical **86**.

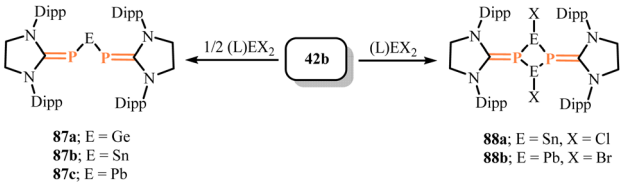

Scheme 35 Synthesis of NHCP-stabilized heavier tetrelenes **87** and **88**, L = SIMes.

([(Dipp)$_2$P]$_2$Ge (107.40(4)°),[75a] [(Dipp)$_2$P]$_2$Sn (106.20(3)°),[72] and [{(Tripp)(*t*Bu)(F)Si}(iPr$_3$Si)P]$_2$Pb (97.88(4)°)[75b]), which could attributed to steric hindrance from large substituents. Additionally, conversion of **42b** with (SIMes)MX$_2$ (M = Ge, Sn, Pb; X = Cl or Br) (one equivalent) only successfully isolated [(SIDippP)SnCl]$_2$ (**88a**) and [(SIDippP)PbBr]$_2$ (**88b**) (Scheme 35). Both compounds **88a** and **88b** did not show π–π interactions, demonstrating the significant ability of bis(phosphinimine) coordination to stabilize group 14 atoms. Recently, the isolation of NHCP–silyl-substituted stannylene (IDipp)PSn(SiTMS$_2$SiTol$_3$) along with NHCP–silyl- and aryl-substituted plumbylenes (IDipp)PPb(SiTMS$_2$SiTol$_3$) and (IDipp)PPb(^{Mes}Ter) (^{Mes}Ter = 2,6-Mes$_2$C$_6$H$_3$) has opened new avenues for developing mono-NHCP plumbylene systems featuring Pb–P partial multiple bond character with aryl/silyl substituents.[76]

Gudat group reported the reaction of imidazolium phosphinides with organotin chlorides.[77] Conversion of imidazolium phosphinides **89a,b** with organotin chlorides Me$_3$SnCl and Ph$_3$SnCl in the presence of tertiary amines did not yield the expected substitution reactions but instead produced tin-based (oligo)phosphides and imidazolium salts without phosphorus, along with some intractable solids. Treatment of imidazolium phosphinides with diorganotin dichlorides produced Lewis adducts **90a,b** and **91a,b** (Scheme 36), which underwent base-induced dechlorination reactions in the presence of excess base and electrophilic reagents to generate cationic imidazolium bis(stannyl)phosphides chloride complexes **92a,b** and **93a,b** (Scheme 36). These studies showed that product selectivity was influenced by the electrophilicity of the Lewis acids and can clearly distinguish the following three different species: (a) weak electrophiles: for example, R$_3$SnCl, which will form unstable Lewis adducts; (b) moderate strength electrophiles: such as R$_2$SnCl$_2$, which can form stable Lewis adducts; (c) strong electrophiles: for example, PCl$_3$, which can produce Lewis pairs with sufficient PH acidity and transfer protons to the auxiliary base.

Utilizing the strong electron-donating properties of N-heterocyclic imine ligands and reacting the trimethylsilyl

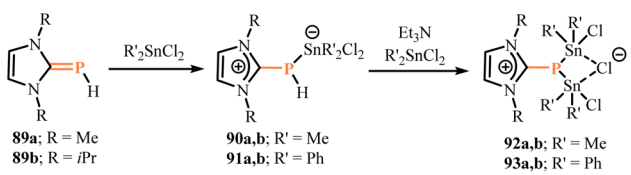

Scheme 36 Reaction of NHCP **89** with diorganotin dichlorides.

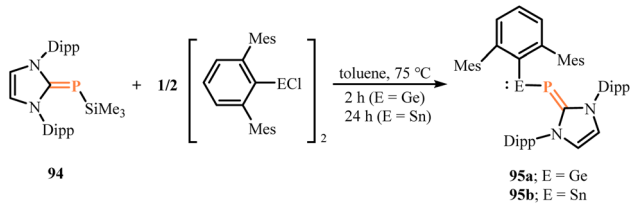

Scheme 37 Synthesis of NHCP-stabilized germanium and tin complex **95a** and **95b**.

phosphinidene complex (IDipp)PSiMe$_3$ (**94**) with the germylene and stannylene chloride dimers [^{Mes}TerECl]$_2$ to isolate the ^{Mes}TerEP(IDipp) (E = Ge(**95a**), Sn(**95b**)) (Scheme 37).[78] The group 14 metals exhibit sharp bond angles (89.56(5)° at Ge, 86.69(6)° at Sn), similar to those in (amino)tetrylenes (^{Mes}Ter)(NHDipp) Ge: (88.6(2)°)[79a] and (^{Mes}TerNH)$_2$E: (88.6(2)° at Ge, 87.07(8)° at Sn).[79b] The E–P bond distances in **95a** and **95b** (2.2364(6) Å and 2.4562(7) Å) suggest the presence of multiple bond character in the E–P bonds. The complex formed by the reaction of compound **95b** with tris(pentafluorophenyl)borane (BCF) features a very short Sn–P bond, revealing a unique "push–pull" zwitterionic structure. Notably, compound **95b** exhibited high catalytic activity in the hydroboration of aldehydes and ketones. As exemplified by acetophenone reduction, complete and selective conversion is achieved within 30 minutes using only 0.05 mol% catalyst loading, highlighting its significant potential for practical synthetic applications.

The transmetallation reagent (^{Me}IPrCH)$_2$Zn (**4**) can also be applied to group 14 halides. Mixing **4** with one equivalent of GeCl$_2$ dioxane formed the germylene–zinc chloride adduct (^{Me}IPrCH)$_2$Ge·ZnCl$_2$ (**96**) (Scheme 38).[30] In compound **96**, the germanium and zinc centers adopt a trigonal planar geometry, which is a rare Ge–Zn bonded species involving a tricoordinated germanium center. When **4** was reacted with two equivalents of ECl$_2$ dioxane (E = Ge, Sn), it formed the halogen-bridged products, the binuclear propeller-shaped cations [(^{Me}IPrCHE)$_2$(μ-Cl)]$_2$[Zn$_2$Cl$_6$] (E = Ge(**97a**), Sn(**97b**)) (Scheme 38). Compounds **97a** and **97b** both contain a C$_2$E$_2$Cl propeller-shaped core structure, which is a significant feature of their cationic components.

Rivard group first used N-heterocyclic olefin ligands to isolate divinylgermylene in 2017.[27] Subsequently, the same group in 2021 synthesized a series of N-heterocyclic olefin stabilized group 14 heavier tetrelenes (^{Me}IPrCH)$_2$E: (E = Ge(**98a**), Sn(**98b**), Pb(**98c**)) by deprotonating vinyl lithium

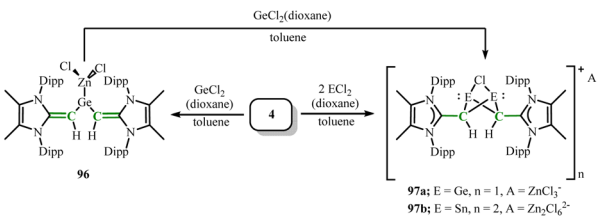

Scheme 38 Reaction of the transmetallation reagent **4** with ECl$_2$ dioxane (E = Ge, Sn).

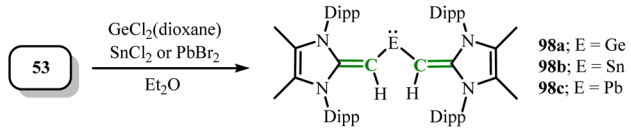

Scheme 39 Synthesis of NHO-stabilized disilylenes heavier tetrelenes **98a**, **98b** and **98c**.

reagents (^{Me}IPr=CH)Li (**53**) with Cl$_2$Ge·dioxane, SnCl$_2$, and PbBr$_2$ in Et$_2$O (Scheme 39).[57] The C–Sn–C bond angle in compound **98b** [90.83(14)°] validated the existence of the Sn lone pair. The C–Pb–C bond angle in compound **98c** (88.6(2)°) was sharper than that in the first known diarylplumbylene (94.5(1)°),[80] showing its structural uniqueness and differences.

Inoue group reported the synthesis of the dimeric cyclopentadienyl(imino)stannylene [(η1-Cp)SnNIPr]$_2$ (**99**) through the conversion of (IDipp)NLi with Cp$_2$Sn.[81] The central Sn$_2$N$_2$ ring of stannylene **99** adopts a nearly planar structure. Unlike similar stannylenes ([(η^3-Cp)SnNC(NMe)$_2$]$_2$),[82] compound **99** did not exhibit an equilibrium between *cis* and *trans* Cp isomers

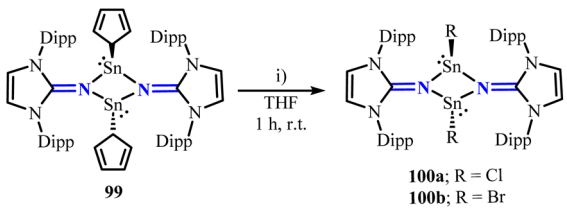

Scheme 40 Synthesis of halogenated compounds **100a** and **100b**. (i) For **100a**: CH$_2$Cl$_2$; for **100b**: BrCH$_2$CH$_2$Br.

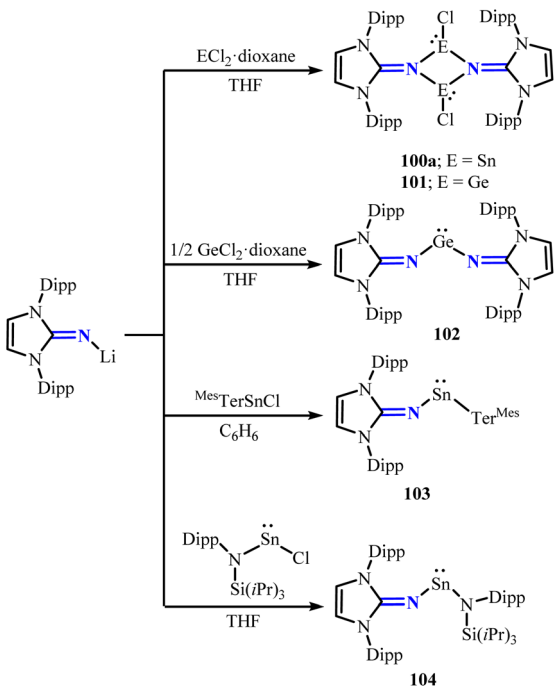

Scheme 41 Synthesis of tetrelenes **100a**, **101–104**. ^{Mes}Ter = 2,6-Mes$_2$C$_6$H$_3$.

in solution. Moreover, stannylene **99** can undergo substitution reactions with CH_2Cl_2 or $BrCH_2CH_2Br$ to yield the corresponding halogenated compounds $[ClSnNIPr]_2$ (**100a**) and $[BrSnNIPr]_2$ (**100b**) (Scheme 40). In contrast to the fluxional behavior of the Cp ligands in stannylene **99**, the halogen groups in compounds **100a** and **100b** adopt a *trans* configuration relative to the Sn_2N_2 ring.

Subsequently, the same group achieved various N-heterocyclic imine stabilized group 14 heavier tetrelenes (**100a**, **101–104**) through reacting (IDipp)NLi with corresponding chloride (Scheme 41).[83–86] Similar to **100a**, the Ge–Cl bonds in compound **101** adopt a *trans* configuration relative to the Ge_2N_2 ring. Furthermore, conversion of compounds **100a** and **101** with $Na_2Fe(CO)_4$ yielded $Fe(CO)_4$-bridged tin and germanium complexes **105a** and **105b**. Notably, a reversible formation exists between the monocoordinated and bridged species (**105a** and **105b**) and their corresponding monocoordinated counterparts (**106a** and **106b**) (Scheme 42).[83] Interestingly, compound **100a** can convert with $M[Fe(CO)_2(\eta5\text{-}C_5H_5)]$ (M = Li, K) to form the Li/Sn/Fe trimetallic complex **107**. The electrophilicity of complex **107** is demonstrated by its reaction with LiI, affording the iodo-substituted tin complex **108** (Scheme 43).[83] The $^{119}Sn\{^1H\}$ NMR spectrum of **108** (61.6 ppm) shows a significant upfield shift compared to that of **107** (314.0 ppm), which can be attributed to the higher electron-donating ability of the iodide ligand.

By treatment of the bis(imino)germylene **102** (ref. 61) with gaseous N_2O, a rare three-coordinate germanone $[IPrN]_2Ge{=}O$ (**109**) was isolated (Scheme 44),[84] with the germanium center situated in a trigonal planar environment. Germanone **109** exhibits shorter Ge–N bonds (1.7819(12) Å and 1.7825(12) Å) and longer exocyclic N–C bonds (1.2872(18) Å and 1.2914(18) Å), compared to that in germylene **102** (Ge–N: 1.8194(15) Å; N–C: 1.273(2) Å), demonstrating partial metalimide character. In addition, germanone **109** displays rich reactivity toward small molecules, highlighting its polarized $Ge^{\delta+}$–$O^{\delta-}$ reactivity and the ability to mimic of nucleophilic transition-metal oxides. Regarding the heteroleptic stannylene **103**, it has been demonstrated to effectively activate and catalytically reduce CO_2 through ligand assistance.[85]

Recently, the synthesis of novel N-heterocyclic imine stabilized group 14 heavier tetrelenes has been reported.[87] Through a ligand exchange reaction, Inoue group successfully synthesized an isostructural amino stannylene compound (TMS_2-N)(I*t*BuN)Sn: (**110**) by treatment of (I*t*BuN)H with stannylene $(TMS_2N)_2Sn$ (Scheme 45).[88] Additionally, when reacting ECl_2·dioxane (E = Ge, Sn) with two equivalents of lithiated ligand

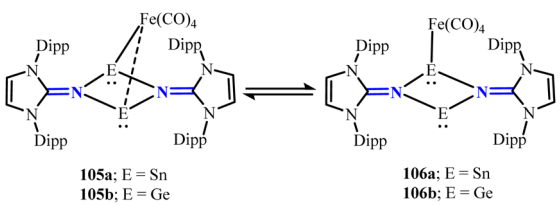

Scheme 42 Exchange between **105a** and **105b** to **106a** and **106b**.

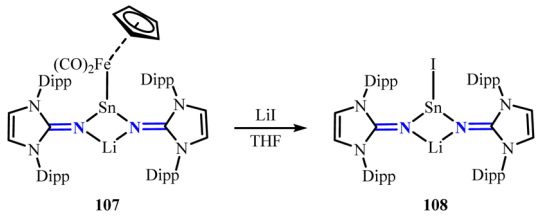

Scheme 43 Reaction of the Li/Sn/Fe trimetallic complex **107** with LiI.

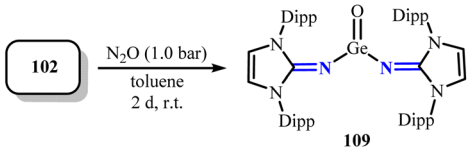

Scheme 44 Synthesis of germanone **109**.

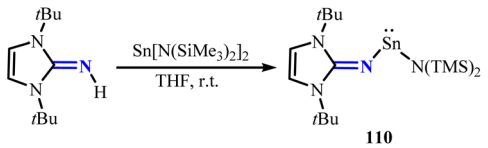

Scheme 45 Synthesis of NHI-stabilized stannylene **110**.

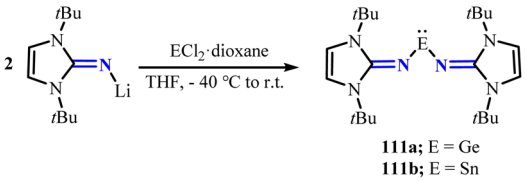

Scheme 46 Synthesis of NHI-stabilized homostructural tetrelenes **111a** and **111b**.

(I*t*BuN)Li, obtaining homostructural tetrelenes $(ItBuN)_2E$: (E = Ge(**111a**), Sn(**111b**)) (Scheme 46). Compound **111a**, in toluene-d_8 solvent, reaches a dynamic equilibrium between monomer and dimer forms with temperature changes, tending to exist as a monomer at room temperature. Compound **111b**, whether in solution or in the solid state, stably exists as a monomeric molecular structure without showing changes in aggregation state. Notably, **111a** and **111b** exhibit high selectivity in the conversion reactions with N_2O or CO_2, which expanding the application scope of homostructural tetrelenes in chemical synthesis, and providing new perspectives and tools for studying small molecule activation mechanisms.

2.3. Group 15 element complexes

Among the pnictogen elements, the combination of NHIs, NHCPs and NHOs ligands with nitrogen facilitates the creation of novel ligand systems, expanding the field of sterically hindered ligands and providing more possibilities for applications in organometallic chemistry and catalytic chemistry.[7a] For

phosphorus, the three ligands have demonstrated even broader utility, with significant developments in stabilizing phosphinyl radicals and constructing new ligand systems.[7a,22–23]

2.3.1. Nitrogen complexes. Rivard group isolated compound NHO (IPrCH)NMe_2 (**112**) by reacting Eschenmoser's salt $[H_2C{=}NMe_2]I$[89] with two equivalents of the carbene ^{Dip}IPr.[90] Notably, research found that the amine donor attached to this neutral N-heterocyclic olefin primarily coordinates with AuCl (**113**) through the exocyclic olefin part rather than the terminal N-based center (Scheme 47).

N-heterocyclic olefins react with N_2O in acetonitrile, where the N–O bond breaks to form NHO dimers (**114a–114c**) connected by azo-bridge (Scheme 48).[91] These dimers, as emerging superelectron donors, exhibit significant characteristics, with their first oxidation potential ($E_{1/2} = -1.34$) indicating the strong reducing ability. Additionally, these dimers can undergo selective single-electron or double-electron oxidation processes, respectively converting into stable radical cations or di-cationic forms of imidazolium salts. Surprisingly, finding the formation of diazene (**115a–115d**) from the treatment of NHOs with N_2O (Scheme 48),[92] where the nature of the solvent is a key factor in product selectivity. Like azo compounds, compounds **115a–115d** are easily decomposed under ultraviolet light but exhibit significant thermal stability. N-heterocyclic diazenes possess high charge density, showing strong ylide characteristics. Notably, N-heterocyclic diazenes can serve as strong C-donor ligands, combining with transition metal and main group metal complexes to separate diazene complexes **116–119** without releasing dinitrogen (Scheme 49).[92] Additionally, N-heterocyclic diazene can undergo (2 + 3) cycloaddition reactions with CS_2, dimethyl acetylenedicarboxylate, *N*-phenylmaleimide, and tetracyanoethylene (TCNE) to yield compound **120–123** (Scheme 49);[92] in methanol, it undergoes head-to-tail dimerization through a (3 + 3) cycloaddition reaction to produce strongly reducing quinone-type tetrazines (**124a–124c**) (Scheme 49),[93] demonstrating rich reactivity and broad application prospects. Furthermore, neutral group 14 diazoolefin

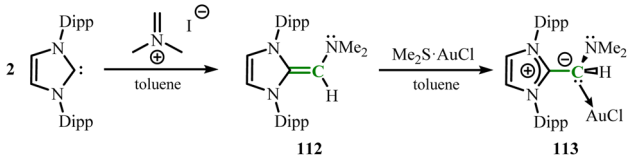

Scheme 47 Synthesis of (IPr=CH)NMe_2 (**112**) and its reaction with AuCl.

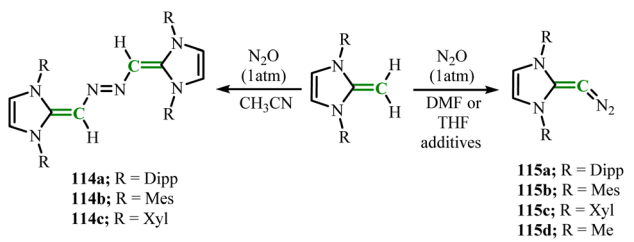

Scheme 48 Reaction of NHOs with N_2O.

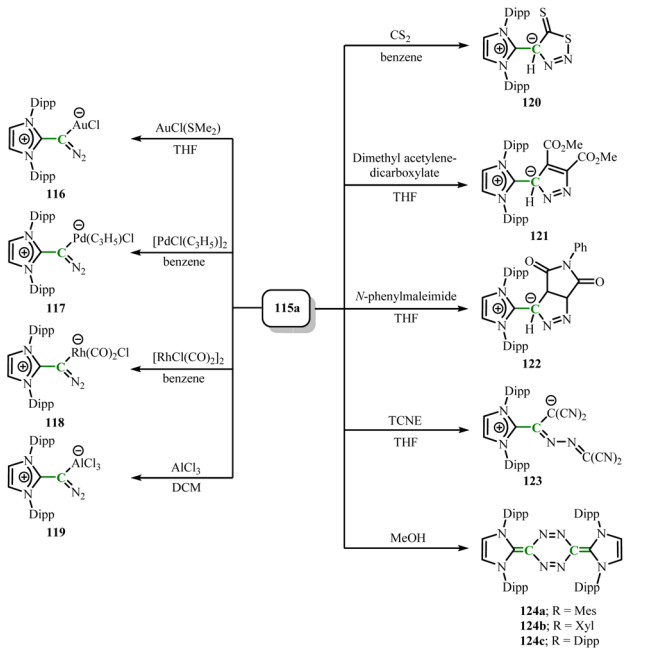

Scheme 49 Reaction of N-heterocyclic diazene **115a**.

complexes **125** (M = Ge(**125a**), Sn(**125b**)) can be isolated starting from **115a** (Scheme 50). Interestingly, the reaction of **125a** with potassium hypersilanide ($KSiTMS_3$) yields the cyclic bis-vinyl germylene **126**, which features an aromatic five-membered ring structure.[94]

Similarly, Hansmann group recently prepared novel benzimidazole-derived diazoalkene **127** through an NHC/N_2 ligand exchange reaction.[95] Compound **127** can react with DAC, releasing N_2 and generating a new polarized carbodicarbene **128** (Scheme 51). This metal-free N_2/DAC exchange strategy enables the free carbodicarbene ligand to react with any chosen metal. By conversion with (dms)AuCl or $[RhCl(CO)_2]_2$, the corresponding metal complexes **129** and **130** were generated (Scheme 51), respectively, validating the effectiveness of this approach.

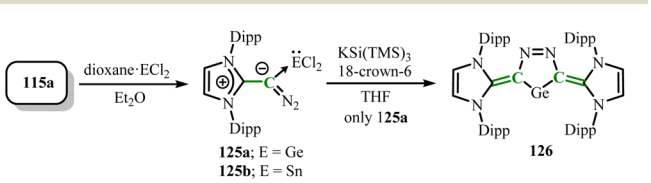

Scheme 50 Synthesis of neutral group 14 diazoolefin complexes **125** and cyclic bis-vinyl germylene **126**.

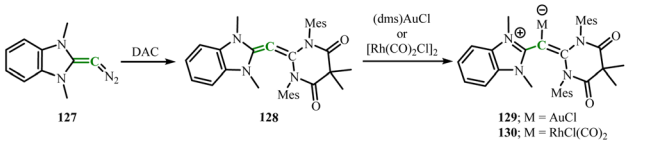

Scheme 51 Reaction of benzimidazole-derived diazoalkene **127** with DAC and coordination reaction of **128** with metal.

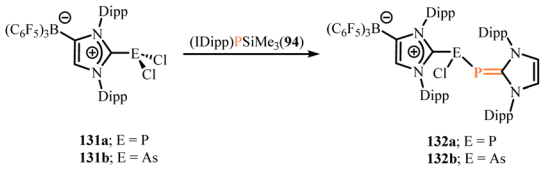

Scheme 52 Synthesis of the monochlorides (WCA–IDipp)E(Cl)P(IDipp) **132a** and **132b**.

2.3.2. Phosphorus complexes. In 2019, a new method to synthesize heteroleptic bis(NHC) complexes diphosphines and diarsines was reported.[96] By treatment of the anionic N-heterocyclic carbenes **131a** and **131b** with (IDipp)$PSiMe_3$(**73**), obtaining the monochlorides (WCA–IDipp)E(Cl)P(IDipp) (E = P(**132a**), As(**132b**)) (Scheme 52). Subsequently, dechlorination with $GaCl_3$ yielded the mono-cationic diphosphine and diarsine species [(WCA–IDipp)EP(IDipp)][$GaCl_4$] (E = P(**133a**), As(**133b**)) (Scheme 53). Conversion of compounds **132a** and **132b** with 1,4-bis(trimethylsilyl)-1,4-dihydropyrazine yielded the neutral radical species **134a** and **134b** (Scheme 53). The X-band EPR spectrum of compound **134a** exhibited a broad doublet of doublets (g = 2.0087), accompanied by two distinct hyperfine coupling constants of $A(^{31}P1)$ = 53.5 G and $A(^{31}P2)$ = 35.9 G. In contrast, the spectrum of compound **134b** showed a broad multiplet (g = 2.0249), with hyperfine coupling constants $A(^{75}As1)$ = 26.8 G and $A(^{31}P2)$ = 33.9 G, revealing a high degree of asymmetry in the spin density distribution in **134a** and **134b**. This method provides the possibility to prepare various other types of hetero-diatomic species.

Similarly, Weigand group reduced (^{Cl}ImDipp)PP(Dipp)[OTf] (**135**[OTf]) or (^{Cl}ImDipp)PP(Cl)(Dipp) (**136**) with cobaltocene ($CoCp_2$) to yield novel mixed-substituted neutral diphosphinyl radical (**137**).[97] The X-band EPR spectrum of **137** showed a hyperfine doublet signal generated by the interaction of the unpaired electron with two inequivalent phosphorus nuclei ($A(^{31}P1)$ = 15.1 G and $A(^{31}P2)$ = 70.5 G, g = 2.0095). This EPR data is similar to **134a**, revealing that the spin density is mainly concentrated on the two phosphorus atoms. Interestingly, **137** reacts with P_4 to yield P_8 compound **138** (Scheme 54). Additionally, this process can also be achieved by adding P_4 after the formation of **136**. The P_4 core of compound **138** is configured in a butterfly shape, with the P_2 units arranged in an *exo*, *exo*-configuration on either side, and the Dipp substituents on the phosphorus atoms pointing in opposite directions.

By abstracting chloride ions from the corresponding phosphoryl chlorides, two oxophosphonium ions [**139**]$^+$ and [**140**]$^+$, stabilized by bulky imidazolin-2-imine and imidazolin-2-olefin

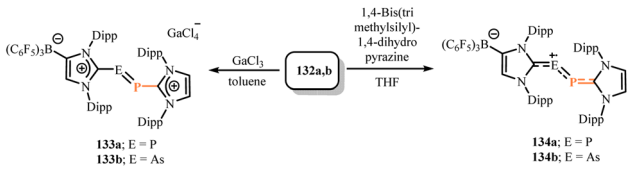

Scheme 53 Synthesis of the mono-cationic and neutral heteroleptic diphosphine and diarsine **133** and **134**.

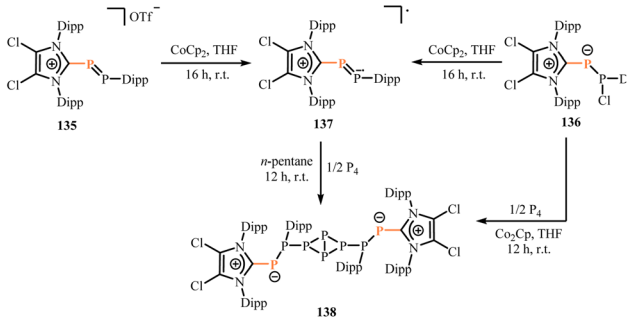

Scheme 54 Synthesis of the neutral diphosphinyl radical **137** and its reaction with P_4.

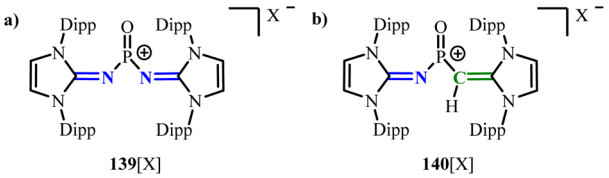

Scheme 55 NHI, NHO-stabilized oxophosphonium salts **139**[X] and **140**[X]. [X] = $[OTf]^-$ or $[BAr^F]^-$.

substituents on phosphorus, can be prepared (Scheme 55).[98] Due to the differing donor capabilities of N-heterocyclic olefins and N-heterocyclic imines, the electrophilicity of the phosphorus center can be effectively modulated, with [**139**]$^+$ exhibiting significantly stronger Lewis acidity compared to [**140**]$^+$.

Dielmann group reported rare Lewis base-free phosphonium dication salts **141** and **142** (Scheme 56),[99] in which the phosphonium dications adopt a trigonal planar geometry, and the electron-deficient phosphorus centers maintain a suitable distance from the anions. In 2023, the same group further isolated the first terminal methylene phosphonium ions **143** and **144** (Scheme 56),[100] which can serve as suitable precursors for generating mono-substituted phosphine carbenes.

Interestingly, the generation of electron-rich phosphines with photo-switchable electronic properties is achieved by utilizing the NHI substituents linked to dithienylethene (DTE).[101] This is accomplished through the deprotonation of imidazolium salt **145** using *n*-butyllithium, followed by

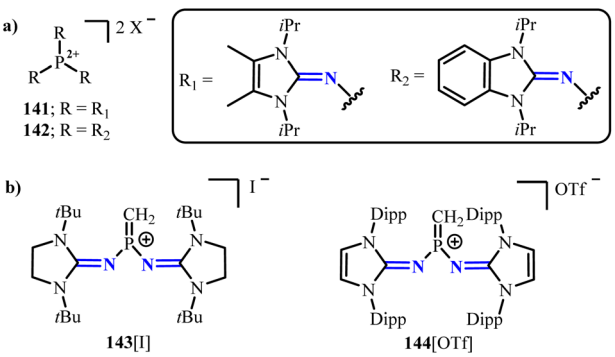

Scheme 56 NHI-stabilized phosphonium salts **141–144**. For **141**: [X] = $[B(C_6F_5)_4]^-$ or $[BAr^F]^-$; for **142**: [X] = $[B(C_6F_5)_4]^-$.

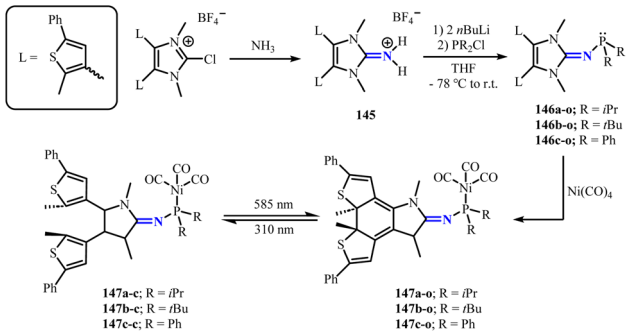

Scheme 57 Synthesis of NHI-stabilized electron-rich phosphines **146** and its interconversion under different light conditions. The linkage of NHOs with a *P*-substituted indenyl heterocycle.

a reaction with the corresponding chlorophosphine to yield photo-switchable electron-rich phosphines PS–IAPs (R = iPr(**146a–o**), *t*Bu(**146b–o**), Ph(**146c–o**)) with varying donor capabilities (Scheme 57), where the notation o indicates the open-ring form of the DTE unit and c indicates the close-ring form of the DTE unit. Through measuring the TEP values of the corresponding nickel complexes [(PS–IAP)Ni(CO)$_3$] (R = iPr(**147a**), *t*Bu(**147b**), Ph(**147c**)), showing that under UV and visible light irradiation, the photochromic DTE unit undergoes a reversible photocyclization reaction, thereby changing the electron-donating ability of the phosphine.

In 2024, a series of P(III) and P(V) bis(azido)phosphines and bis(azido)phosphine chalcogenides were reported (**148–150**) (Scheme 58).[102] These bis(azido)phosphines can undergo chemoselective Staudinger reactions with tertiary or secondary phosphines, generating modular mono(azido) *P*-chiral phosphines (**151–153**) (Scheme 59), demonstrating the stabilizing effect of NHI ligands on storable bis(azido)phosphines.

Very recently, a open-shell singlet diphospha-indenylide system featuring imidazole-based N-heterocyclic olefin with terminal CH$_2$ donor groups has been reported (Scheme 60).[103] The imidazolyl group can undergo thermal rotation around the central C–C bond connecting it to the phosphorus-substituted indenyl ring, thereby modulating the charge separation and diradical character. For compounds **154a–154c**, the LUMO is predominantly localized on the indenyl ring, whereas in compound **154d**, the LUMO is mainly situated on the NHO moiety. This localization makes the perylene segment in **154d** more susceptible to reduction, leading to the formation of a magnesium salt byproduct containing a radical anion during the synthesis of **154d**.

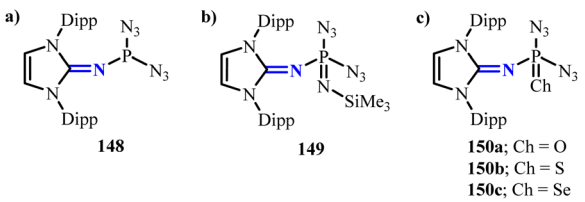

Scheme 58 Synthesis of P(III) and P(V) bis(azido)phosphines and bis(azido)phosphine chalcogenides **148–150**.

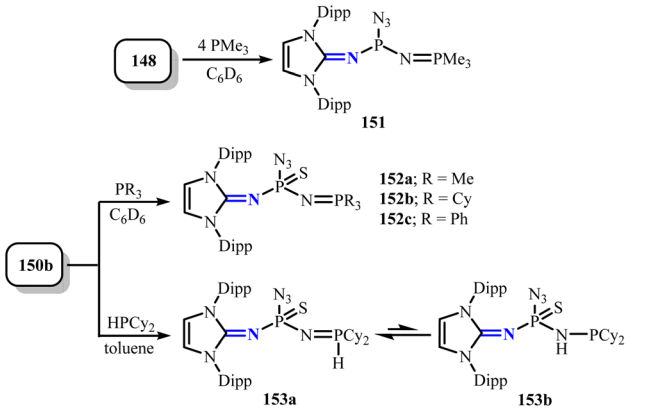

Scheme 59 Synthesis of mono(azido) *P*-chiral phosphines **151–153**.

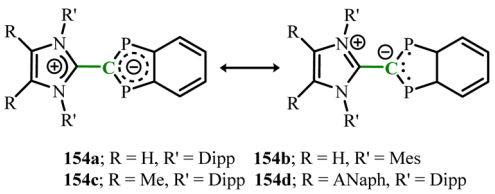

Scheme 60 Synthesis of the linkage of NHOs with a *P*-substituted indenyl heterocycles **154a–154d**.

In recent years, similar to N elements, the combination of NHC ligands with P-based donors to prepare novel large-bulky phosphine ligands has attracted increasing attention. In early research reports, Beller group revealed that imidazolium-alkylphosphines (**155**) can generate highly active catalysts under the synergistic effect of Pd(II) sources and bases, promoting the hydroxylation of aryl halides, and applied to the construction of C–N bonds in Buchwald–Hartwig coupling and C–C bonds in Sonogashira coupling, fully demonstrating the great potential of such ligands.[104]

Rivard group isolated the target product (IPrCH)PR$_2$ (R = iPr(**156a**); Ph(**156b**)) by mixing IPr=CH$_2$ with ClPR$_2$ in THF (Scheme 61).[100] The C(sp^2)–P bond in **156a** (1.780(3) to 1.788(2) Å) are shorter compared to the C(olefin)–P bond in *cis*-Ph$_2$P–CH=CH–PPh$_2$ (1.817(3) and 1.825(3) Å),[105] which may be due to the increased C(π) → P–C(σ*) hyperconjugation effect. The donor capabilities of the new phosphines NHOPs **156a** and **156b** were verified through coordination of the terminal P atoms with Lewis acids BH$_3$ and Me$_2$S·AuCl (Scheme 62).

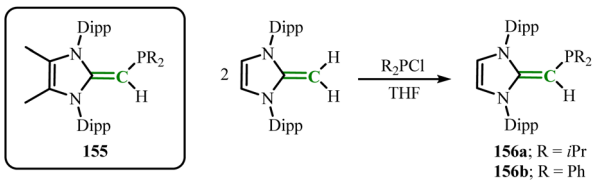

Scheme 61 Synthesis of (IPrCH)PR$_2$ (R = iPr(**156a**); Ph(**156b**)) and imidazolium-alkylphosphines **155**.

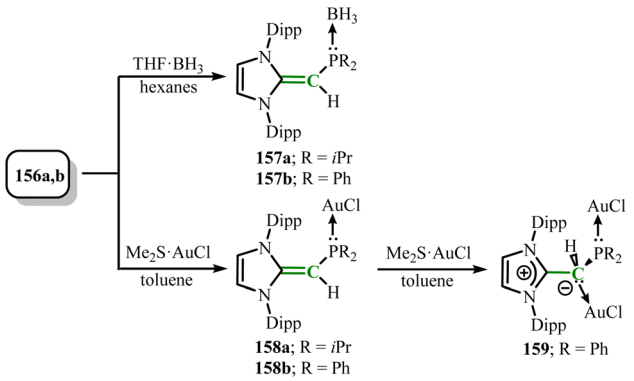

Scheme 62 Reaction of **156a** and **156b** with BH_3, $Me_2S{\cdot}AuCl$.

Subsequently, the same group further expanded their research on the coordination chemistry of N-heterocyclic olefin phosphine ligands.[106] By mixing **156b** with [AuCl(SMe$_2$)] in toluene, isolating the target bis(gold(I)) chloride adduct [(IPrCH)PPh$_2$(AuCl)$_2$] (**159**) (Scheme 62), which confirmed that the P and C donor sites in **156a,b** can be simultaneously utilized. In compound **159**, the length of the exocyclic C–C bond (1.477(14) Å) is significantly longer than the corresponding C–C bond in compound **158b** (1.381(4) Å), indicating a weakening of the double bond character in compound **159**. Additionally, the AuCl units in compound **159** are arranged in a *trans* configuration, and no significant Au···Au interactions were observed.

Recently, corresponding ruthenium complexes using N-heterocyclic olefin–phosphine ligands (NHOP) were synthesized.[107] By treatment of the N-heterocyclic olefin with PPh$_2$Cl, followed by reaction with [Ru(*p*-cymene)Cl$_2$]$_2$ yielded the half-sandwich ruthenium complexes [{(**160a**/**160b**)}Ru(*p*-cymene)Cl$_2$]I (**161**) (Scheme 63). Notably, **161b** can be obtained directly from *N*-benzyl benzamide derivatives and internal alkynes in a one-pot two-step sequence to yield cyclized and olefinated isoquinolinones, showing great potential as catalysts for C–H and N–H functionalization reactions.

To further expand phosphine carbene complexes, a series of monodentate or bidentate phosphine ligands modified with N-heterocyclic imine groups have be synthesized recently (Scheme 64).[108] These ligands exhibit strong electron-donating capabilities, even surpassing those of alkyl phosphines and classical NHC ligands. Moreover, Dielmann group has reported the synthesis and characterization of a novel class of NHI-substituted phosphino(silyl)carbenes.[109] Conversion of the phosphonium chloride salts **167a,b** (ref. 110) with lithium-(trimethylsilyl)diazomethane, obtaining compound **168a,b**. Further, **168a,b** were formed into room temperature stable

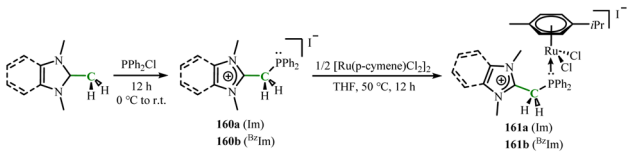

Scheme 63 Synthesis of NHOP **160a** and **160b** and its ruthenium complexes **161a** and **161b**.

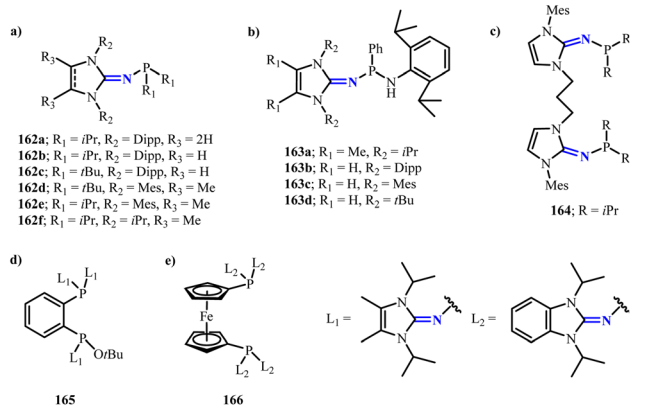

Scheme 64 Phosphine carbene complexes bearing N-heterocyclic imine group **162–166**.

carbenes **169a,b** by irradiation with 365 nm ultraviolet light or sunlight in *n*-hexane solution (Scheme 65). Notably, compared to other phosphine carbenes,[111] **169a** (132°) and **169b** (135°) exhibited significantly smaller carbene bond angles, which would be beneficial for them to coordinate with transition metals. Access to the complex **170** is granted by conversion of **169a** with AuCl(tht) (tht = tetrahydrothiophene), while complex **171** can be similarly obtained by reacting **169b** with CuO*t*Bu (Scheme 65). These results demonstrate the significant function of such phosphine carbenes in stabilizing transition metals.

2.4. Transition element complexes

Over the past two decades, the coordination chemistry of NHIs, NHCPs and NHOs ligands has experienced extensive development, encompassing nearly all transition metals. The following section will briefly document the latest advancements in the chemistry of transition metals and rare earth metals featuring the NHIs, NHCPs and NHOs as supporting ligands in recent years.

Conversion of the tris(aminobenzyl) rare earth complexes RE(CH$_2$C$_6$H$_4$NMe$_2$-*o*)$_3$ with imidazolin-2-imines at room

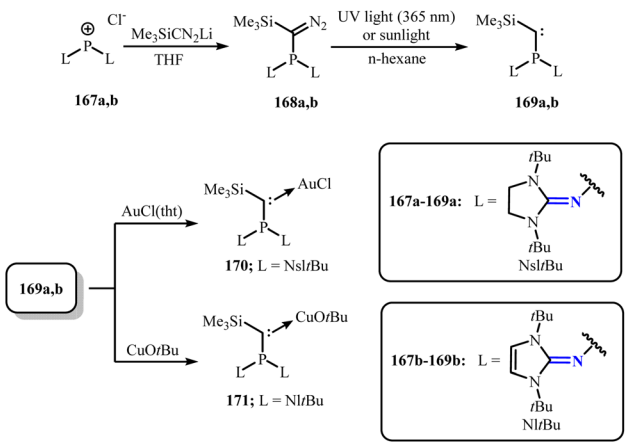

Scheme 65 Synthesis of phosphino(silyl)carbenes **169a** and **169b** and its reaction with AuCl(tht) (tht = tetrahydrothiophene) and CuO*t*Bu.

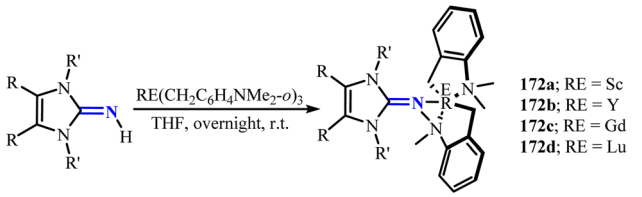

Scheme 66 Synthesis of NHI-stabilized rare earth alkyl complexes **172a–172d**.

temperature can obtain a series of imidazolin-2-imine-based rare earth alkyl complexes **172a–172d** (Scheme 66).[112] DFT calculations support the existence of a significant strong interaction between the N atom of the NHI and the scandium(III) ion in **172a** ($WBI_{Sc-N} = 1.36$). Further MBO decomposition analysis found that the formation of the Sc–N bond benefited from the contributions of one σ orbital and two π orbitals, revealing the ability of the N atom to act as a 2σ, 4π-electron donor.

Recently, a series of tetravalent cerium(IV) complexes **173–175** using imidazolin-2-iminato ligands as auxiliary ligands were reported (Scheme 67).[113] Studies have shown that the 5d orbitals play a crucial role in the bonding process, and the strong electron-donating properties of the imidazolin-2-iminato ligands significantly enhance the energy-level matching between the Ce(IV) 5d orbitals and the alkyl, aryl and alkynyl groups. This discovery further validates the broad application potential of imidazolin-2-iminato ligands in rare-earth metal complexes.

Xu and coworkers reported the combination of unsaturated N-heterocyclic olefins or N-heterocyclic carbenes with rare earth aryloxide complexes and their synergistic reactivity. By combining the unsaturated NHC(I*t*Bu) with rare earth aryloxide complexes $RE(OAr)_3$, obtaining unusually bound NHC complexes (RE = La(**176a**), Sm(**176b**), Y(**176c**)) (Scheme 68),[114] and no expected product was obtained for the complex of the smallest atom, Sc. Although the reaction of NHO (4,5-dimethyl-2-isopropyl imidazole) with rare earth aryloxide complexes did not yield the corresponding metal–NHO adducts, studies showed that the Lewis acid–base pairs formed by the combination of $RE(OAr)_3$ with NHO and RE/aNHC could achieve synergistic H_2 activation (**177**) (Scheme 68). Interestingly, the Lewis acid–base pair formed by La/NHO could convert with (trimethylsilyl)diazomethane to generate isocyanide trimethylsilyl lanthanum amine complex (**178**) (Scheme 68). At the

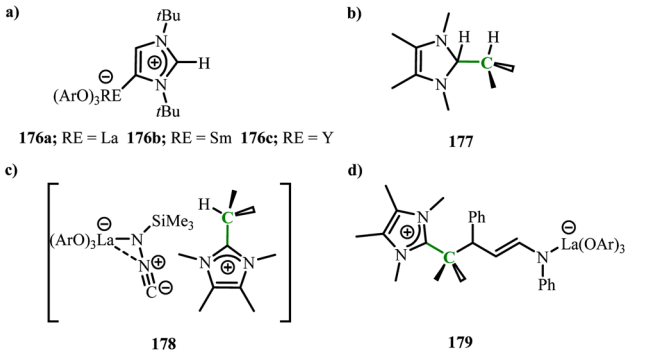

Scheme 68 Unusually NHC-stabilized rare earth aryloxide complexes **176a–176c**, NHO with activated hydrogen **177**, isocyanide trimethylsilyl lanthanum amine complexes **178** and La/C 1,4-addition products **179**.

same time, it could also *via* conversion with α, β-conjugated imines to produce La/C 1,4-addition products (**179**) (Scheme 68).

A series of mono- and bis-benzimidazolin-2-imino titanium complexes (**181–182**) were prepared by treatment of *N*-silylated benzimidazolin-2-imine ligands (**180**) with $TiCl_4$ (Scheme 69).[115] The structures of **181a**, **181c** and **182a** were characterized, showing distorted tetrahedral geometries. The C–N(C=N)–Ti bond angles were nearly linear (171.7(2)°, **181a**; 175.93(17)°, **181c**; 170.1(3)° and 167.5(3)°, **182a**). Additionally, the C=N and N(C=N)–Ti bond distances and cone angles were smaller than those of other analogues,[116] indicating stronger electron-donating ability and larger coordination space. These complexes demonstrate promising catalytic performance in both ethylene homopolymerization and α-olefin copolymerization, producing polymers with narrow molecular weight distributions (PDI = 1.2–2.8) while maintaining good polymerization activity even under elevated temperatures (90 °C).

To further prepare titanium(IV) complexes formed by the combination of asymmetric imidazolin-2-imine ligands, reacting the silylated imines **183a** and **183b** with titanium chloride precursors, removing Me_3SiCl, obtaining a series of mono- and bis(imidazolin-2-imino) titanium complexes **184–186** (Scheme 70).[117] Similar to **181a** and **181c**, **184a** and **184b** showed distorted tetrahedral geometries. The Ti–N–C angle in **184a** was 162.58(5)°, significantly deviating from linearity, which may due to the different steric hindrance of the methylphenyl and adamantyl substituents. The titanium complexes **184–186** all had short Ti–N distances and large Ti–N–C angles (162°–173°), revealing that these systems can effectively provide electrons to

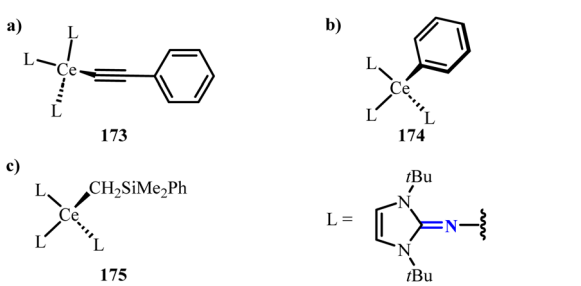

Scheme 67 Synthesis of NHI-stabilized cerium complexes **173–175**.

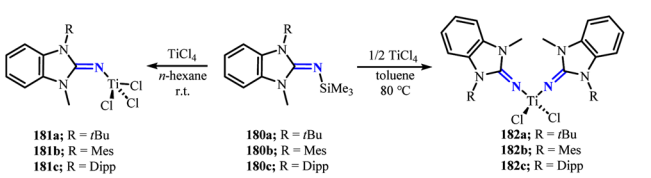

Scheme 69 Synthesis of NHI(**180**)-stabilized titanium complexes **181** and **182**.

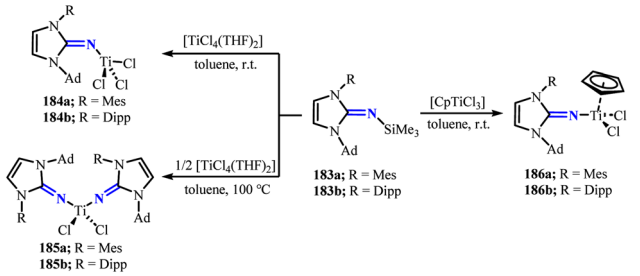

Scheme 70 Synthesis of NHI(**183**)-stabilized titanium complexes **184–186**.

form stable chemical bonds with the central metal ions as ligands.

In 2022, Beckhaus group obtained the deprotonated product **188** by reacting the bistitanium complex (**187**) with $ImMe_4{=}CH_2$ (Scheme 71).[118] The corresponding anionic N-heterocyclic olefin unit ($ImMe_4{=}CH^-$) added to the Ti center in the reaction without the formation of by-products. The structure of complex **188** showed a trigonal pyramidal geometry around the central titanium atom. DFT calculations indicated that the HOMO contains a polarized titanium–carbon π bond, which is distributed over the Ti–C–C motif. This polarized titanium–carbon π bond indicates the presence of delocalized π bonding along the Ti–C–C axis. The Wiberg bond indices for exocyclic C–C and Ti–C ($WBI_{C-C} = 1.49$, $WBI_{Ti-C} = 1.02$) further indicate the partial π bond character along the Ti–C–C axis.

Subsequently, novel NHO–transition metal complexes ($^{Me}IPrCH)_2ECl_2$ (E = Ti(**189a**), Zr(**189b**), Hf(**189c**)) were reported (Scheme 72),[119] which were prepared by the salt exchange reaction of ($^{Me}IPrCH)Li$ with group 4 tetrachlorides. DFT calculations found that the most red-shifted HOMO to LUMO transition in **189a** was calculated to be 550 nm, close to the experimental value of 520 nm, involving the overlap of the ligand C=C π and metal Ti(d) orbitals. This calculation result validated the deep color characteristics of the complex **189a**. It is speculated that the NHO–metal interaction is stronger in its heavier homologues, leading to blue shifts in absorption and downfield shifts in the ^1H NMR C=CH resonances. Interestingly, mixing **189b** with excess sodium metal yielded the rare arene-masked zirconium complex ($^{Me}IPrCH)_2Zr$ (**190**) (Scheme 72).[119]

Mono-(imidazolin-2-iminato) hafnium(IV) complexes **191–194** (R = iPr(**191**), *t*Bu(**192**), Mes(**193**), Dipp(**194**)) can be prepared by reacting imidazolin-2-imines with hafnium tetrabenzyl complex ($HfBn_4$) (Scheme 73).[120] Among these, complex

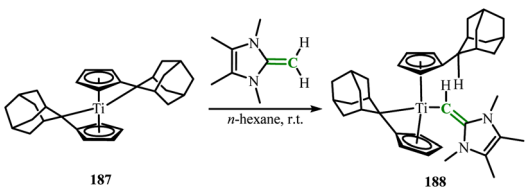

Scheme 71 Synthesis of NHO-stabilized titanium complexes **188**.

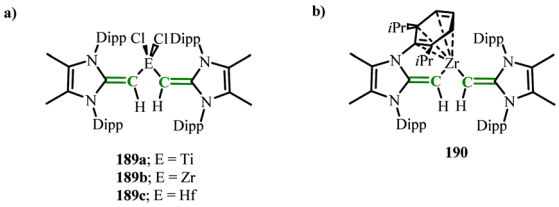

Scheme 72 ($^{Me}IPr{=}CH)_2ECl_2$ (E = Ti(**189a**), Zr(**189b**), Hf(**189c**)) and arene-masked zirconium complex **190**.

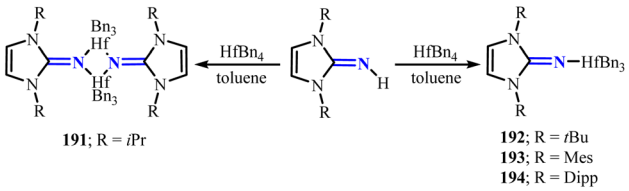

Scheme 73 Synthesis of NHI-stabilized hafnium complexes **191–194**.

191 adopts a dimeric structure, which can be attributed to the smaller steric hindrance around the Hf center. Furthermore, by reacting with different equivalents of iPrOH and BnOH, triisopropoxide complex **195** and dimeric complexes **196–198** can be obtained (Scheme 74). Notably, these hafnium complexes effectively catalyze the block copolymerization of ε-caprolactone with *rac*-lactide. Particularly, complexes **195** and **197** exhibit outstanding performance with TOF of $140 \times 10^5\ h^{-1}$ and $130 \times 10^5\ h^{-1}$, respectively, highlighting their significant potential for oxygen-containing substrate transformations.

The rare half-sandwich imidazolin-2-imine iron and cobalt complexes were reported (Scheme 75).[121] The $Cp'_{cent} - Fe$ distance of the "pogo stick" structure iron complex [Cp′Fe(-NImDipp)] (**199a**) is 1.90 Å, which was comparable to the values of related Fe(II) high-spin species (1.88–2.05 Å) and consistent

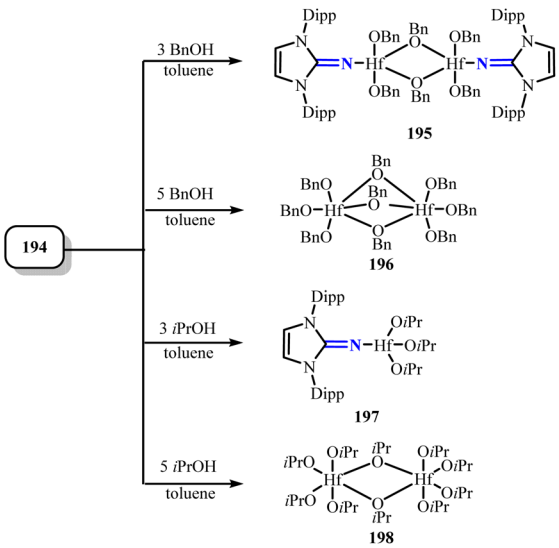

Scheme 74 Reactions of **194** with different equivalents of iPrOH and BnOH.

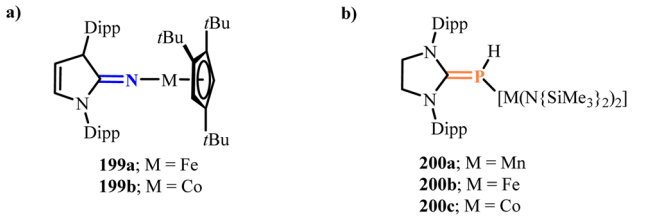

Scheme 75 Half-sandwich imidazolin-2-imine iron and cobalt complexes **199a** and **199b** and NHCP-stabilized 3d metal(II) complexes **200a**, **200b** and **200c**.

with the high-spin system of $4e^-$.[122] The high-spin state of the Fe center was initially revealed, which was further confirmed by intermediate paramagnetic relaxation in the Fe Mössbauer spectrum. Similar cobalt complex (**199b**) represent a rare single-legged piano stool species. The spin state of the cobalt center in **199b** exhibited temperature-dependent spin crossover. These half-sandwich imidazolin-2-imine metal complexes all showed short M–N bond lengths, which can be attributed to the multiple bond character induced by the strong 2σ, 4π electron-donating effect of the imidazolin-2-imine ligand.

In 2021, the first open-shell, tricoordinated 3d metal(II) phosphinimine adduct complexes $[M\{PH(SIDipp)\}\{N(SiMe_3)_2\}_2]$ (M = Mn(**200a**), Fe(**200b**), Co(**200c**)) were reported,[123] which were prepared by treatment of $[M\{N(SiMe_3)_2\}_2]$ (M = Mn–Co) with [(SIDipp)PH] (Scheme 75). The M–P distances in the complexes (2.6033(10) Å (**200a**), 2.5185(6) Å (**200b**), and 2.4572(8) Å (**200c**)) were significantly longer than those in other similar adducts such as $[(NHC)P(H)Fe(CO)_4]$ (1.828(3) Å).[124] Additionally, these complexes showed a Y-shaped geometry with M–P–C angles (about 135°) larger than those in [(NHC)PH] or [(NHC)PPh] type ligands (about 110°),[124–126] indicating weaker σ and π electron-donating interactions between the metal and the phosphinimine, which may due to steric repulsion between the Dipp groups of the NHC framework and the silylamine ligands.

Lin group reported a series of three-coordinate terminal halide complexes of first-row transition metals **201** supported by imidazolin-2-iminato ligand.[127] Furthermore, salt elimination reactions between these halide complexes and methyl transfer reagents ($LiCH_3$ and CH_3MgCl) yielded methyl complexes **202** and **203**, adopting bridging (Cr) and terminal (M = Mn, Fe, Co) coordination modes, respectively (Scheme 76).

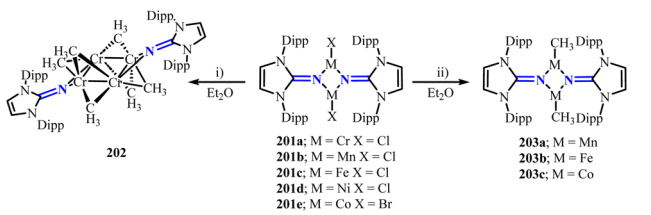

Scheme 76 Synthesis of NHI-stabilized methyl complexes of transition metals **202** and **203**. (i) For Cr: 3 equivalents CH_3Li in DME. (ii) For Mn, Fe: 2 equivalents CH_3MgCl in THF; for Co: 3 equivalents CH_3Li in DME.

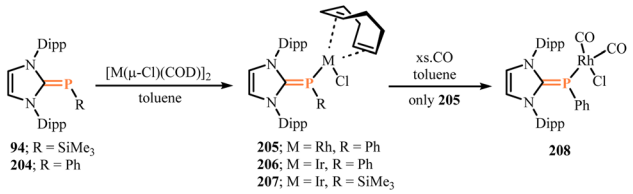

Scheme 77 Synthesis of NHCP-stabilized rhodium and iridium complexes **205–208**.

Antiferromagnetic coupling was observed between the metal ions in these methyl complexes. Moreover, **201d** and **202** demonstrated competent catalytic activity in Kumada cross-coupling reactions.

The conversion of (IDipp)PPh (**204**) with the dimer $[M(\mu\text{-}Cl)(COD)]_2$ (M = Rh, Ir, COD = 1,5-cyclooctadiene) led to the isolation of the corresponding complexes **205** and **206** (Scheme 77). Following a similar approach, $(IDipp)PSiMe_3$ (**94**) reacted with the dimer $[Ir(\mu\text{-}Cl)(COD)]_2$ to yield $[Ir(COD)Cl\{(IDipp)PSiMe_3\}]$ (**207**) (Scheme 77). Furthermore, exposing complex **205** to CO gas resulted in the formation of the rhodium–carbonyl complex **208** (Scheme 77).[126] The $P–C_{carbene}$ bond lengths in **205–207** (1.817(3) to 1.828(3) Å) are significantly longer than those in (IDipp)PPh (**149**) (1.7658(10) Å) and $(IDipp)PSiMe_3$ (**94**) (1.7800(13) Å), indicating single-bond character. Notably, the phosphorus atoms in **205–207** exhibit a trigonal pyramidal coordination geometry, consistent with the presence of a lone pair on the central phosphorus atom, suggesting potential for further coordination.

Tamm group reported the synthesis of iridium(I) catalysts with phosphine-imidazolin-2-imine ligands.[128] Combining the novel bidentate *P*,*N* ligand (**209**) with $[Ir(COD)Cl]_2$ (COD = 1,5-cyclooctadiene). Then, adding sodium tetrakis[3,5-bis(trifluoromethyl)phenyl]borate, $NaBAr^F$ and lithium tetrakis(nonafluoro-*tert*-butoxy)aluminate, $Li[Al\{OC(CF_3)_3\}_4]$, respectively, to obtain complexes **210a** and **210b** (Scheme 78). Placing complex **210b** in a dihydrogen atmosphere to obtain the diiridium tetrahydride (**211b**) (Scheme 78). **211b** formed an Ir_2H_4 core with two bridging and two *trans*-oriented terminal hydrogen atoms, featuring the rare structural characteristic of terminal hydride ligands with empty coordination sites on the opposite side. Notably, **211a** and **211b** showed similar catalytic performance, exhibiting significant performance for aromatic substrates. In particular, these two catalysts could efficiently perform *ortho*-selective deuteration and tritium labeling of

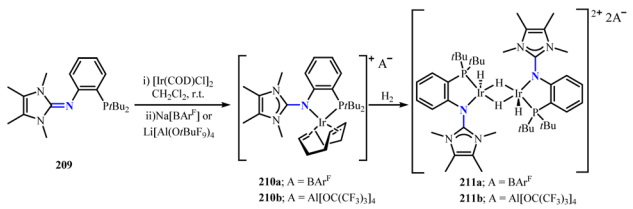

Scheme 78 Synthesis of NHI-stabilized iridium complexes **210** and **211**.

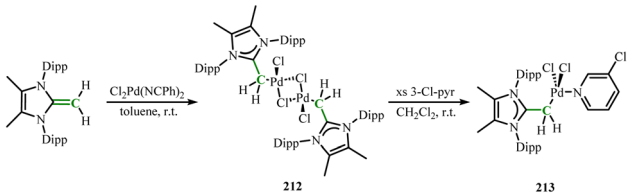

Scheme 79 Synthesis of NHO-stabilized palladium complexes **212** and **213**.

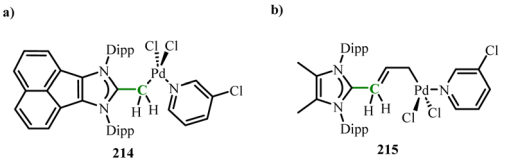

Scheme 80 NHO-stabilized palladium complexes **214** and **215**.

phenylacetic acid esters and amides, which are of significant pharmacological importance.

In 2019, a series of structurally different Pd(II)–NHO complexes was reported.[129] By combining ^{Me}IPrCH$_2$ with *trans*-[Cl$_2$Pd(NCPh)$_2$] in toluene, obtaining the dimer [(^{Me}IPrCH$_2$)PdCl(*m*-Cl)]$_2$ (**212**). Adding 3-chloropyridine to **212** further yielded [(^{Me}IPrCH$_2$)PdCl$_2$(3-Cl–pyr)] (**213**) (Scheme 79). The exocyclic C–C distance in **212** (1.453(3) Å) was longer than the C=C bond in the free NHO ligand (1.3489(18) Å),[52] indicating π electron transfer to the C–Pd bond. Subsequently, using different NHO ligands to obtain complexes **214**, and **215** through the same procedure (Scheme 80). Notably, using NaO*t*Bu as a base and combining the framework-methylated NHO with [Pd(cinnamyl)Cl]$_2$, obtaining the system with the highest catalytic activity in promoting C–N bond formation between hindered arylamines and aryl halide substrates.

Recently, novel linear-coordinated copper(I) complexes were reported, and further synthesis of challenging copper complexes with the AlCp* ligand was achieved.[130] Reacting [(CF$_3$SO$_3$Cu)$_2$(C$_6$H$_6$)] with 1,3-bis(2,6-diisopropylphenyl)-2-(trimethylsilylimino)imidazoline (DippImTMS) and 1,3-bis(2,6-diisopropylphenyl)imidazolin-2-imine (DippImH) to obtain [Cu(DippImSiMe$_3$)(OTf)] (**216**) and [Cu(DippImH)$_2$][OTf] (**217**), respectively (Scheme 81). The Cu–N bond lengths (1.884 Å (**216**), 1.842 Å (**217**)) showed shorter distances, revealing strong interactions between copper and the NHI ligand. Both compounds **216** and **217** showed a linear coordination environment centered on copper, with N–Cu–O (174.93° (**216**), 179.83° (**217**)). Conversion of the air-stable compound **217** with NaBAr^F in dichloromethane yielded [Cu(DippImH)$_2$][BAr^F] (**218**). Further, conversion of [Cu(DippImH)$_2$][BAr^F] (**218**) with AlCp* (four equivalents) to obtain the rare homonuclear CuAl$_4$ cationic complex [Cu(AlCp*)$_4$][BAr^F] (**219**) (Scheme 81). Compound **219** has equidistant Cu–Al bonds (2.266 Å) and exhibits a nearly perfect tetrahedral geometry. The molecular structure is similar to [Ni(AlCp*)$_4$], but the average Al–Cp* center distance (1.858 Å) is shorter than that in [Ni(AlCp*)$_4$] (1.933 Å). This contration may result from the enhanced electrophilicity of the cationic copper center compared to its neutral nickel analogue, attributable to its positive charge and distinct electronic configuration. Interestingly, upon isolating the mixed products from the reaction of imidazolin-2-imine acid with copper(I) chloride, the triangular cluster compound [Cu$_3$(DippIm)$_2$Cl] (**220**) was obtained (Scheme 81). In compound **220**, the three copper atoms showed a triangular configuration, with Cu–Cu distances (2.470–2.522 Å) all within the effective range of copper affinity interactions (below 2.8 Å).

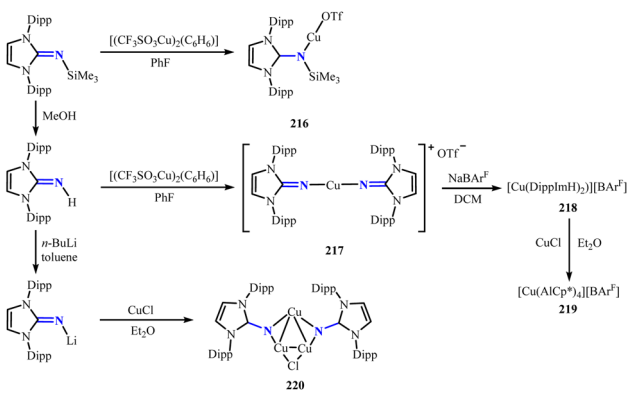

Scheme 81 Synthesis of NHI-stabilized copper complexes **216–220**.

Tamm group obtained monometallic complexes [{(IMes)PH}MCl] (M = Cu(**221a**), M = Ag(**221b**)) and [{(IDipp)PH}MCl] (M = Cu(**222a**), M = Ag(**222b**)) *via* conversion of (NHC)PH derivatives (IMes)PH and (IDipp)PH with copper(I) or silver(I) chlorides (one equivalents) (Scheme 82).[131] The molecular structure of **221a** showed a trimer form, with each molecule having a six-membered Cu$_3$P$_3$ ring, and **222a** formed a dinuclear silver complex [{(IMes)PH}(AgCl)$_2$] at low temperature. This can be attributed to the smaller steric hindrance of (IMes)PH, which tends to form multinuclear structures, while the larger steric hindrance of (IDipp)PH allows the formation of stable mononuclear complexes. It is noteworthy that the reaction of (IMes)PH and (IDipp)PH with two equivalents of copper(I) chloride led to the isolation of copper complexes **223a** and **223b**, which contain phosphonium ion [(NHC)PH$_2$]$^+$ as a byproduct (Scheme 82). **223b** contains two linear and two triangular planar copper sites, forming a Cu$_2$(μ_2-Cl)$_2$ core, with a nearly planar four-membered Cu$_2$Cl$_2$ ring, and a folding angle between the CuCl$_2$ planes of 3.93(5)°.

Under different reaction conditions, the reaction of (benzo)imidazolin-2-imine ligands with ZnEt$_2$ can yield corresponding dimeric or trimeric zinc complexes (**224–226**) (Scheme 83).[41]

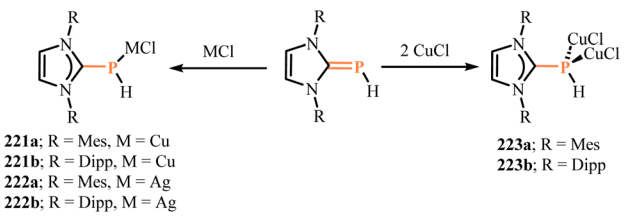

Scheme 82 Synthesis of NHCP-stabilized copper and silver complexes **221–223**.

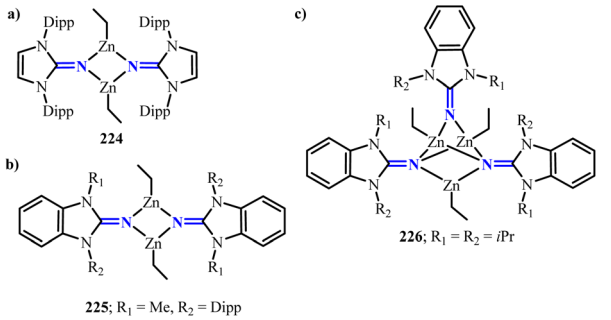

Scheme 83 Synthesis of NHI-stabilized zinc complexes **224–226**.

Due to the smaller steric hindrance of *N*,*N*′-diisopropylbenzimidazolin-2-imine, a trinuclear complex is formed after the reaction, in which two ligands bridge three zinc atoms and another ligand bridges two zinc atoms. Additionally, when the metal alkyl precursor is replaced with Mg(*n*-Bu)$_2$, a dimeric magnesium complex similar to **224** can be obtained.

Conversion of actinide complexes **227a** and **227b**, as well as metallocenes **228a** and **228b**, with equimolar neutral imidazolin-2-imine ligands ImRNH to obtain mono(imidazolin-2-imine) actinide(IV) complexes [(Im^{Ad,R}N)An{N(SiMe$_3$)$_2$}$_3$] (R = Mes) (**229a–230b**) and (**231a–232b**) in high yield (Scheme 84).[132] The An–N–C angles (175.9(3)°, **229a**; 162.7(6)°, **229b**; 178.5(3)°, **230a**; 162.0(3)°, **230b**) showed nearly linear configurations, while the An–N$_{imido}$ bond lengths (2.177(3) Å, **229a**; 2.191(7) Å, **229b**; 2.119(4), **230a**; 2.123(5) Å, **230b**; 2.195(3) Å, **231a**; 2.218(10) Å, **231b**; 2.117(3) Å, **232a**; 2.258(11) Å, **232b**) were all shorter, indicating high double bond character between the An–N$_{imido}$ bonds. Studies revealed that these complexes all exhibited catalytic activity in the transfer hydrogenation of aldehydes, ketones, and 2-propanol. Notably, the thorium complexes exhibit significantly superior catalytic performance compared to the uranium complexes. Case studies show that with 1 mol% catalyst loading and within 5 hours of reaction time, thorium complex **229b** achieves a high conversion rate of 75%, while structurally similar uranium complex **230b** yields only 33% conversion under identical conditions, clearly demonstrating the activity gradient between thorium complexes (moderate-to-high efficiency) and uranium complexes (low-to-moderate efficiency).

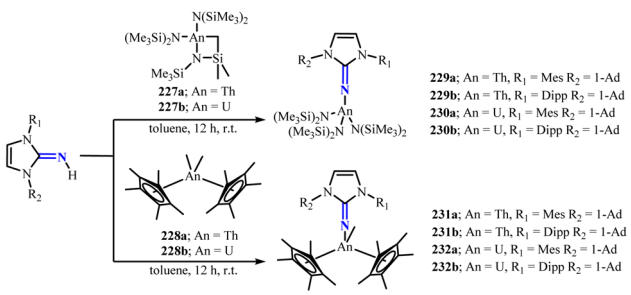

Scheme 84 Synthesis of NHI-stabilized actinide complexes **229–232**.

3. Bis(N-heterocyclic carbenes) as ligands

3.1. Bis(NHIs) as ligands

Bis(imidazolin-2-imine) ligands often serve as highly effective electron-donating ligands that coordinate with main group elements and transition metals. When the bridging unit contains additional functional groups, a tridentate or multidentate ligand system is formed. The effective charge delocalization of the guanidine CN$_3$ unit enhances the basicity and nucleophilicity within the system, enabling it to effectively stabilize positive charges. These biguanide ligands can be regarded as superbases. Primary bis-NHIs ligands (**233–241**) shown in Scheme 85, the related synthesis methods and researchs have been reviewed elsewhere.[25,133] These guanidine ligands have broad applications as superbases "proton sponges" and in metal coordination.[134]

The stabilization of electron-deficient three-coordinate boron dicationic species was achieved through the use of a strongly electron-donating system with ligand **233b**. The reaction of **233b** with phenyl dibromoborane led to the isolation of a mononuclear boron(III) dicationic salt **242**. Further, conversion of **233b** with (B(Cl)NMe$_2$)$_2$ followed by the addition of SbCl$_5$ resulted in the isolation of a dinuclear, three-coordinate diboron(II) dication **244**. Both boron centers exhibited a trigonal planar coordination environment. The hydrogen transfer reactions of **242a** with LiBH$_4$ to form the boronium cation **243** and of **244** with LiAlH$_4$ to form the dialuminum hydride cation **245** validated the Lewis acidity of the boron centers in **242** and **244** (Scheme 86).[135]

The isolation of chlorotetrylium ylidenes stabilized by bis-NHIs ligands **246**, **247a** and **247b**, which was achieved through the conversion of ligand **233b** with ECl$_2$ (E = Si, Ge, Sn) (Scheme 87).[136,137] The reactivity of the lone pair electrons of the siliconylidene **246** was validated through coordination with heavier chalcogens and group 11 metals (Scheme 88). Notably, a zwitterionic heterobimetallic siliconylidene complex **250**,

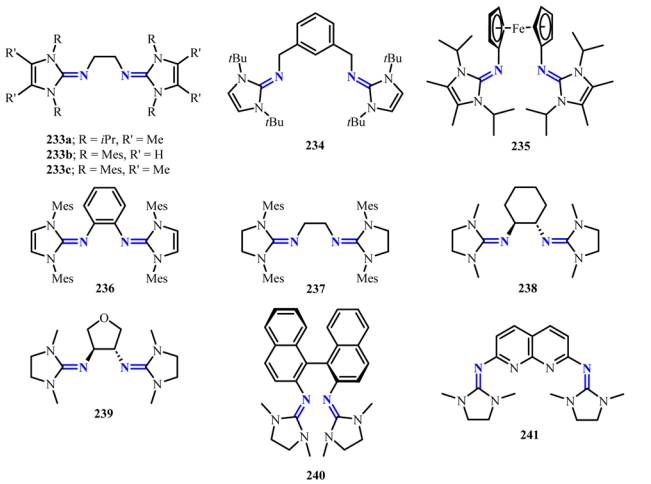

Scheme 85 Primary bis(NHIs) ligands **233–241**.

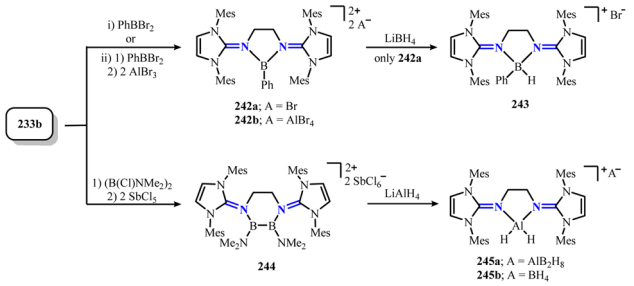

Scheme 86 Synthesis of bis(NHI)-stabilized borane **242** and **244** and its reaction with metal hydrides.

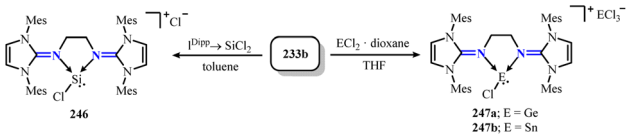

Scheme 87 Synthesis of bis(NHI)-stabilized tetryliumylidenes **246**–**247**.

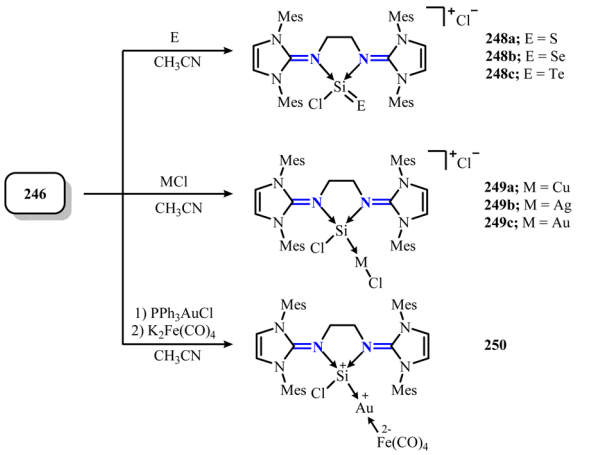

Scheme 88 Reaction of **246** with heavier chalcogens, group 11 metals and coordinate with PPh_3AuCl and $K_2Fe(CO)_4$.

which is overall neutral, was isolated *via* a double anion exchange reaction between siliconylidene **246** and PPh_3AuCl and $K_2Fe(CO)_4$ (Scheme 88). Complex **250** exhibits an almost linear Si–Au–Fe structure (173.65(3)°), with a short distance between the gold atom and the *meso*-methyl ligand, indicating rare weak interactions. The Au d(*xz*) and d(*yz*) orbitals exhibit significant π-backbonding capability of the siliconylidene ligand, and there is a coordination interaction between the silicon lone pair and the gold atom.[136]

Scheme 89 Reaction of **247a** with metal hydrides.

Scheme 90 Reaction of **247b** with metal hydrides.

Further treatment of **247a** and **247b** with TMSOTf resulted in the isolation of the trifluoromethanesulfonates **247a**[OTf] and **247b**[OTf]. In **247b**[$SnCl_3$], tin center is in a trigonal pyramidal coordination environment, with nearly perpendicular Cl–Sn–N bonds (93.42° and 89.23°), confirming the formation of the tin(II) cation **247a**$^+$. Both **247a**[OTf] and **247b**[OTf] exhibit similar ^{1}H NMR spectra and bonding situations, with only the germylidene cationic unit and stannylidene cationic unit observed. Additionally, the outer ring N–C bonds are slightly elongated, and the inner ring N–C bonds are slightly shortened, indicating electron transfer from the ligand to the metal center. Studies have shown that the electron-rich **247a**[OTf] and **247b**[OTf] also exhibit a tendency to undergo metal transfer reactions. In the case of treatment with $LiAlH_4$, metal transfer products were generated. However, the conversion with the weaker reducing agent $NaBH_4$ exhibited different results. The reaction of **247b**[OTf] with $NaBH_4$ yielded the expected metal transfer product, while the reaction of **247a**[OTf] with $NaBH_4$ yielded a push–pull stabilized hydridogermylidene complex (Schemes 89 and 90).[137]

Subsequently, Inoue group further explored the application of bis-NHI ligands **233c**, **236** and **237** in stabilizing tetryliumylidenes.[138] Stannyliumylidenes (**255a**[A], **256a**[A], **257a**[A]) and germyliumylidenes (**255b**[A], **256b**[A], **257b**[A]) (A = ECl_3^-, OTf^-) (Scheme 91) were obtained *via* the same reaction pathway as described above. Due to the lack of an extended conjugated π-system and the more rigid *o*-phenylene geometry in **257a**$^+$, the ^{119}Sn NMR chemical shifts of **257a**$^+$ showed resonances at higher fields (−232.53 ppm, **255a**$^+$; −154.49 ppm, **256a**$^+$ and −261.25 ppm, **257a**$^+$). However, the corresponding strategy for silyliumylidenes could only be prepared as **257c**[Cl], which can be attributed to the greater steric demands of bis-NHI ligands **233c** or **236**. Interestingly, **255c**[$SnCl_3$] was successfully prepared through transmetalation of **255a**[$SnCl_3$] (Scheme 91). The transmetalation of the synthesized stannyliumylidenes with $LiAlH_4$ yielded the corresponding aluminum complexes.

The bis-NHI ligand **233b** reacting with $AuCl(SMe_2)$ to obtain the dinuclear gold(I) complex 1,2-(IMesN–AuCl)$_2$–C_2H_4 (**258**) was reported (Scheme 92).[139] The N–Au–Cl angles were 176.71(7) and 178.45(7)°, respectively, showing a linear coordination

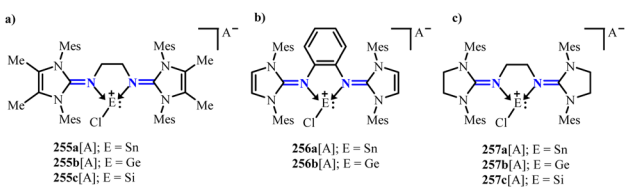

Scheme 91 Synthesis of bis(NHI)-stabilized tetryliumylidenes **255**–**257**, A = ECl_3^-, OTf^-.

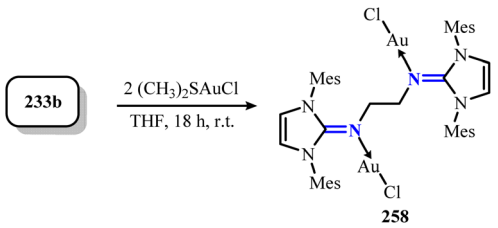

Scheme 92 Synthesis of bis(NHI)-stabilized gold complex **258**.

environment around the Au centers, with the coordinating nitrogen atoms in the *trans* position. Compound **258** mainly exhibited gold–arene interactions (Au···C (2.946(2) Å and 2.999(2) Å)), and no interactions were observed between the two Au center atoms. Additionally, the high stability of complex **258** in aqueous solution was verified, with its ^{1}H NMR spectrum showing no significant decay recorded within 24 hours. Notably, complex **258** exhibited high selectivity and significant antiproliferative activity against A549 lung carcinoma cells, which may provide a new effective means for cancer treatment.

As early as 2010, a series of Mn–Zn complexes using bis-NHIs ligand **233a** were published.[140] Using the same strategy, a series of complexes [{fc(NIm)$_2$}MCl$_2$] (M = Mn, Fe, Co, Ni, Cu, Zn, Pd) (**259a–259g**) (Scheme 93) were obtained vis conversion of bis-NHIs ligand **235** with MCl$_2$ salts.[141,142] Both the zinc and palladium complexes (**259f** and **259g**) were confirmed to be diamagnetic. Due to insufficient quantities, NMR analysis of the copper complex has not yet been performed. Similar to the values established in ethylene-bridged bis(imidazolin-2-imine) zinc(II) complexes, the ^{1}H NMR spectrum of the zinc complex **259f** shows a septet at 5.53 ppm and a doublet at 1.48 ppm. Notably, the palladium complex **259g** exists in a slightly distorted square planar environment. The ^{1}H NMR spectrum reveals a mixture of two diamagnetic species, with one set of signals showing a small chemical shift difference ($\Delta\delta$ = 0.13 ppm) between the ferrocene α- and β-protons, indicating the formation of a Fe–metal bond, demonstrating the ability of the ferrocene moiety in the ligand to act as a strong donor in metal–metal bonding.[143] Except for the palladium complex **259f**, all other complexes exhibit a slightly distorted tetrahedral geometry. Additionally, the reaction of ligand **235** with Cu(I) salts yielded dimeric (CuCl, CuBr) or polymeric (CuI) structures (**260a**, **260b** and **261**) (Scheme 93).

3.2. Bis(NHCPs) as ligands

NHC-stabilized phosphinidenes, as inversely polarized phosphoalkenes, each phosphorus atom hold two lone pairs of electrons. This allows the corresponding chelating bis-phosphinidene ligands to possess multiple binding sites, potentially forming chelate complexes accommodating more metal centers. In recent years, this class of ligands has been preliminarily explored. Currently, there are two main synthetic routes for chelating bis-phosphinidene ligands: (1) reducing bis-phosphine precursors with N-heterocyclic carbenes (NHCs);[144,145] (2) starting from bis(NHC)s with triphosphiranes, which can conveniently yield the corresponding chelating bis-phosphinidenes.[146,147] Using these strategies, chelating

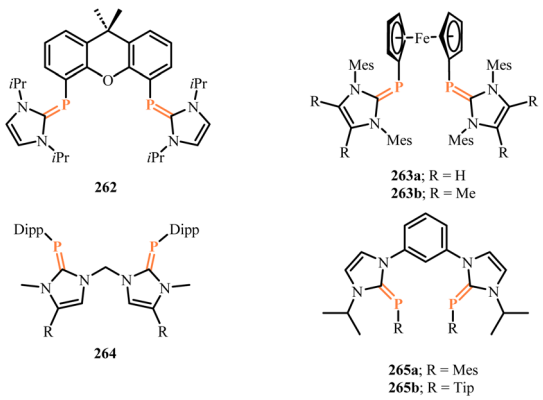

Scheme 94 Primary bis(NHCPs) ligands **262–265**.

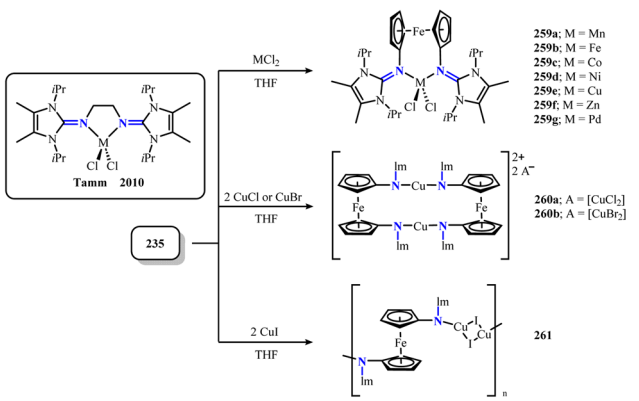

Scheme 93 Synthesis of bis(NHI)-stabilized manganese, iron, cobalt, nickel, copper zinc and palladium complexes **259–261**.

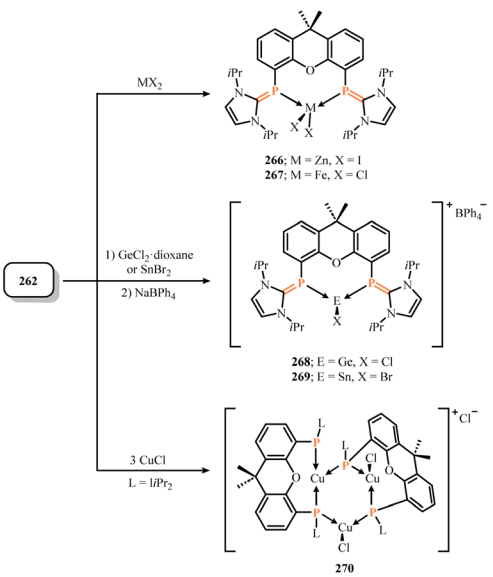

Scheme 95 Synthesis of bis(NHCP)-stabilized germanium, tin, iron, copper and zinc complexes **266–270**.

bis(NHCP)s (**262–265**) (Scheme 94) have been synthesized and utilized as ligands to form multiple metal complexes.

The coordination chemistry of compound **262** was probed through the addition of Fe, Zn, Ge, Sn, and Cu halides.[144] In reactions with ZnI_2, $FeCl_2$, $GeCl_2$, and $SnBr_2$, corresponding cationic complexes (**266–269**) containing tetravalent elements were obtained (Scheme 95). Among these, the Ge and Sn complexes tended to form ion-separated pairs, manifesting as germylenes and stannylenes salts. However, due to the excessive binding angles on the opposite side of the phosphinimine ligand, no expected bimetallic species were obtained when more EX_2 halides (E = Fe, Zn, Ge, Sn) were added. When compound **262** reacted with CuCl, a cationic Cu_3P_3 cyclic complex (**270**) was obtained (Scheme 95), where three P centers bridged two Cu centers, forming a six-membered ring structure, revealing the ability of **262** as a tetradentate chelating ligand. Similarly to compound **262**, **263** yielded corresponding stannylenes salts (**271–272**) upon reaction with SnX_2 complexes (X = Cl, Br, I, OTf) (Scheme 96),[145] where the Sn(II) cation exhibited a trigonal pyramidal coordination environment. Interestingly, stannylene salt **271b** was demonstrated to be capable of transferring the $[SnCl]^+$ unit from a bis-NHCP system to a bis-NHI system in a THF-d8 solution. Additionally, compound **263a** was shown to be capable of stabilizing Si(IV) dications, with the isolated SiH_2 dications **275** and **276** exhibiting high Lewis acidity and thermal stability (Scheme 96).[148]

In 2023, Hering-Junghans group employed strategy (2) to synthesize novel bis(NHC)-bridged bis(NHCP) ligands **264** and **265**.[146,147] Starting from **264**, further synthesizing the complexes **277** and **278** (Scheme 97). The Fe(II) center in **277** showed a distorted tetrahedral coordination environment, with only one pair of lone pairs on each P atom participating in coordination in the complex. One of the C–H bonds of the bridging N–CH_2–N part in **277** and **278** face towards the metal atom (CH···Fe 2.5408(5) Å, H···Rh 2.6094(5) Å, C···Rh 3.4885(47) Å),

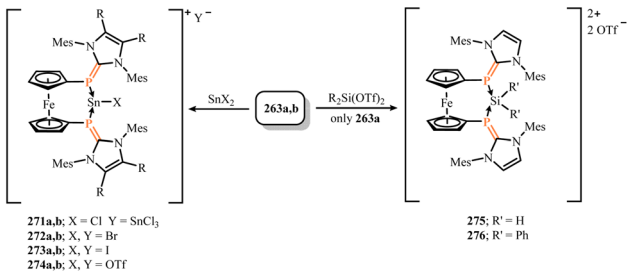

Scheme 96 Synthesis of bis(NHCP)-stabilized silicon and tin complexes **271–276**.

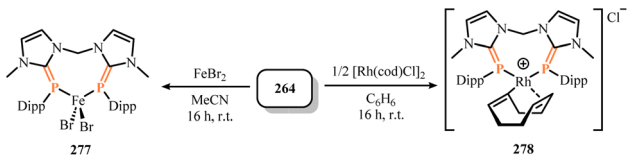

Scheme 97 Synthesis of bis(NHCP)-stabilized iron and rhodium complexes **277** and **278**.

Scheme 98 Synthesis of bis(NHCP)-stabilized gallium and germanium complexes **279** and **280**.

indicating the presence of weak interactions. Subsequently, the coordination chemistry of ligand **265** with GaI_3 and $GeCl_2$(-dioxane) has been reported (Scheme 98). In **265a**, the two MesP units are *trans*-arranged on either side of the benzene bridge. Interestingly, the MesP in **279** units are *cis*-arranged on the same side of the benzene plane, indicating the flexibility of the ligand framework. The Ga–I bond in **279** is coplanar with the central benzene group, and the Ga···C distance is short (3.127(4) Å), suggesting an aromatic ring interaction between the Ga atom and the central benzene bridge. Compounds **280a** and **280b** both showed three resonances for the benzene bridge in the ^{1}H NMR spectra, indicating C_s symmetry in solution. The angles around the germanium atoms are 267.661(17)° (**280a**) and 264.55(3)° (**280b**), indicative of the trigonal coordination geometry for germanium. No interactions with the trichlorogermanate anion in **280a** indicate the presence of charge-separated ion pairs. The charge transfer from the ligands to the germanium atoms in the germaniumium subunits **280a** (−1.054 e$^-$) and **280b** (−1.082 e$^-$) is significant, showing strong polarization of the P–Ge bonds.

3.3. Bis(NHOs) as ligands

Although bis(N-heterocyclic imidazoliums) (NHIs) and bis(N-heterocyclic carbenes) (NHCPs) have been extensively developed as multidentate ligands, complexes supported by bis(NHOs) remain relatively rare. Two bridging methods for bis(NHOs) (**281** and **282**) (Scheme 99) have been reported to date.

In 2017, the first bis(NHOs) ligand (**281**) were reported.[149] Treatment of **281** with phosphorus trichloride yielded the isophosphindolium chloride derivatives (**283a** and **283b**) (Scheme 100). Both **283a** and **283b** featured a nearly planar PC_4 five-membered ring with delocalized π-electrons, demonstrating aromaticity. The HOMO orbital of **283a** and **283b** were primarily

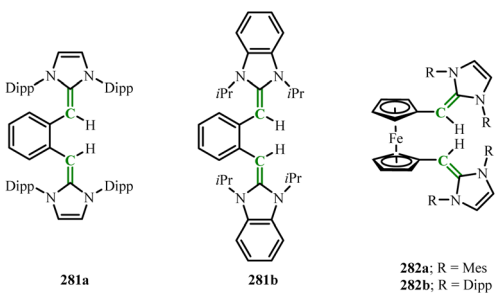

Scheme 99 Primary bis(NHOs) ligands **281–282**.

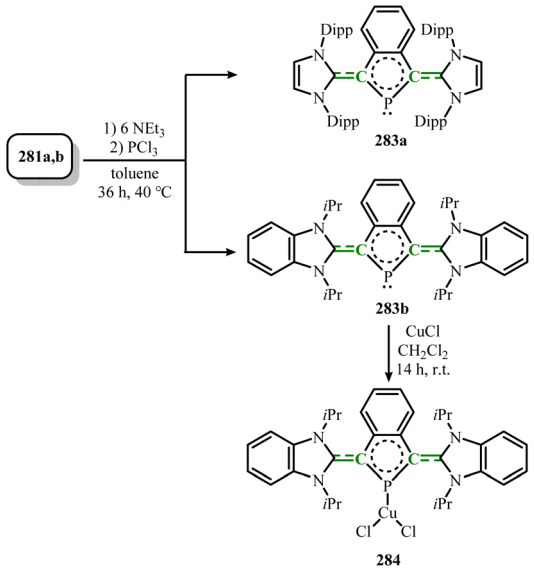

Scheme 100 Synthesis of isophosphindolium chloride derivatives **283a** and **283b** and its reaction with CuCl.

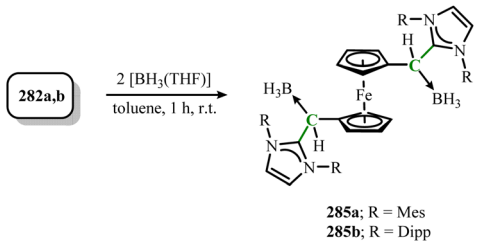

Scheme 101 Reaction of bis(NHO) **282a** and **282b** with BH_3.

located on the C–P–C moiety, indicating the nucleophilicity of the P atom. Further, the reaction of **283b** with metal complexes was studied. The conversion with CuCl produced the copper phosphonium complex (**284**) (Scheme 100) where the P atom coordinated to the Cu center, demonstrating the potential application of **283** as a ligand. In the ferrocenyl-bridged bis(NHOs) ligand (**282**) the cyclopentadienyl rings were in an anti-staggered conformation, and the N atoms were in a trigonal planar environment. Conversion of **282** with [BH_3(THF)] led to the isolation of **285a** and **285b** (Scheme 101),[150] verifying their ability to act as bidentate ligands. The terminal C atoms of the exocyclic double bonds in **282** coordinated to the Lewis acid (BH_3), changing from a three-coordinate to a four-coordinate state, resulting in the formation of *rac*- and *meso*-diastereomers.

4. Organocatalytic reactions enabled by N-heterocyclic carbenes

After the first study on N-heterocyclic carbenes (NHCs) organopolymerization was reported in 2010,[151] this field has rapidly developed. In 2015, Dove group disclosed the preparation of poly(propylene oxide) (PPO) using N-heterocyclic olefins (NHOs) as organocatalysts.[152] The nucleophile and base properties of

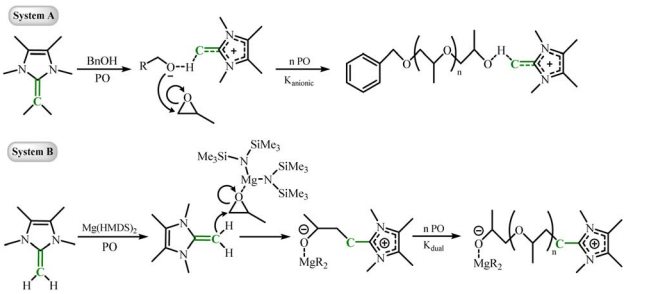

Scheme 102 PO copolymerization using NHO organocatalysis (system A) and dual catalysis (system B). For system A: toluene-d_8, 72 h, 50 °C; for system B: toluene-d_8, 4 h, −36/−20/0 °C.

NHOs was crucial to success in catalytic instance. Recently, the copolymerization of ethylene oxide (EO) and propylene oxide (PO) was successfully achieved through a dual catalytic system based on NHO organocatalysis and Mg(II) co-catalysis. The copolymerization behavior of PO using NHO organocatalysis (system A) and dual catalysis (system B) was compared through *in situ* ^{1}H NMR measurements (Scheme 102). For system A, the reactivity ratios were determined to be $r_{EO} = 3.4$ and $r_{PO} = 0.30$; whereas for system B, the reactivity ratios were $r_{EO} = 7.9$ and $r_{PO} = 0.13$. This difference can be attributed to the presence of $Mg(HMDS)_2$, which leads to zwitterionic propagation within the Lewis acid–base pair, further activating the epoxide mechanism.[153]

In 2023, after achieving the chiral amidation and trifluoromethyl thiolation of β-ketoesters,[154] Dong group further developed the application of NHO organocatalysts in the α-functionalization of β-keto esters, achieving asymmetric formal coupling of β-ketoesters with quinones (Scheme 103).[155] Under the optimized conditions (−78 °C, NHO* loading as low as 1 mol%), the reaction efficiently produced the desired asymmetric synthesis products with high yields (up to 96%) and high enantioselectivity (up to 99% ee), as well as high regioselectivity (up to 19 : 1 rr). Research revealed that the outer olefin moiety of the NHO organocatalyst significantly influenced the enantioselectivity of the reaction. Additionally, ketoesters with larger sterically hindered ester groups and naphthoquinones with electron-withdrawing groups exhibited higher enantioselectivity as substrates.

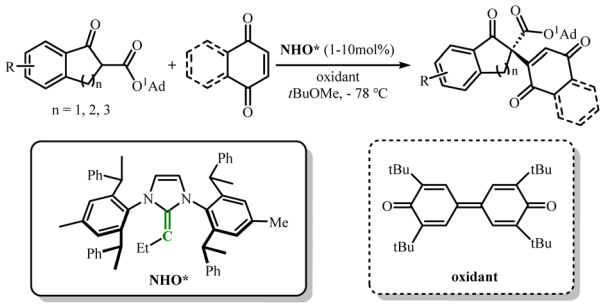

Scheme 103 Asymmetric formal coupling of β-ketoesters with quinones achieved by NHOs.

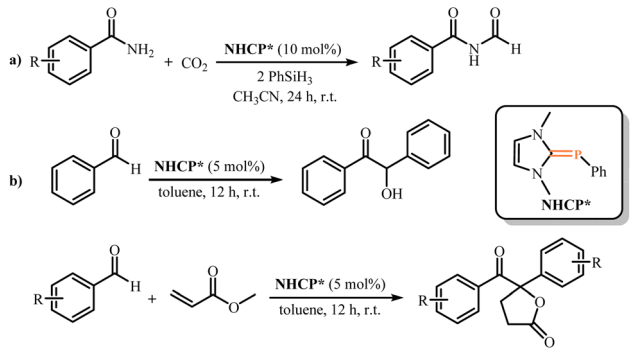

Scheme 104 (a) CO_2 activation achieved by NHCP; (b) activation of aldehydes and methyl acrylates to synthesize γ-butyrolactone catalyzed by NHCP.

Mandal group have demonstrated a novel method for the activation of CO_2 (Scheme 104).[156] Using NHCPs as organocatalysts. This method employs NHCPs as organiccatalysts in 10 mol%, using acetonitrile as the solvent, and successfully activates CO_2 in the presence of silane, achieving the highest yield of formylated products (82%). The authors inferred through DFT calculations and intrinsic bond orbital analysis that the activation of CO_2 occurs *via* a weakly bonded phosphinidene–silane intermediate. Notably, the phosphorus in NHCPs exhibits strong nucleophilicity, and the interaction between the phosphorus and silane plays a crucial role in the activation of CO_2.

Recently, the same group further expanded the application of NHCPs as metal-free organic catalysts for the activation of aldehydes and methyl acrylates to synthesize the corresponding γ-butyrolactones with exceptional yields up to 94%.[157] The study demonstrated that the catalytic process involved a P(I)/P(III) redox cycle, forming benzoin, which successfully. Produced the target product, avoiding the harsh conditions required when using transition metals as catalysts.

Rare-earth organometallic complexes supported by imidazolin-2-iminato ligands demonstrate unique selectivity in C–H bond activation, with the smallest ionic radius Sc(III) complexes exhibiting optimal catalytic versatility. These complexes efficiently catalyze C–H alkylation reactions of anisoles, pyridines, and tertiary amines with olefins, showing remarkable preference for benzylic $C(sp^3)$–H bond activation over *ortho*-aromatic $C(sp^2)$–H bonds.[112,158,159] Notably, Dong's group recently developed cationic imidazolin-2-iminato scandium alkyl catalysts (**286–291**) (Scheme 105) that enable highly selective hydroallylation of styrene derivatives with internal/terminal alkenes, as well as alkene dimerization, achieving exceptional yields up to 99%.[160] Mechanistic studies reveal that the imidazolin-2-imine ligand plays a decisive role in modulating catalytic activity, further confirming the distinctive advantages of this ligand system in catalytic applications.

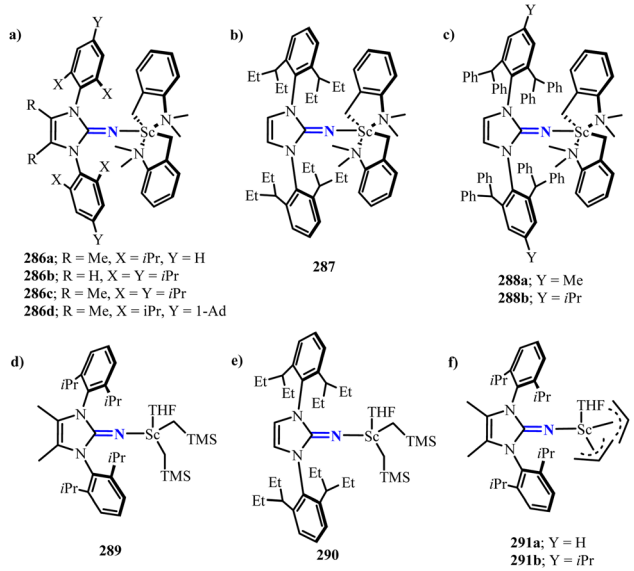

Scheme 105 Cationic imidazolin-2-iminato scandium alkyl catalysts **286–291**.

5. Conclusions and perspectives

This review systematically summarizes the recent advances in organometallic complexes supported by N-heterocyclic imines (NHIs), N-heterocyclic phosphinidenes (NHCPs) and N-heterocyclic olefins (NHOs). The combination of N-heterocyclic carbenes (NHCs) with X (X = N, P and C) offers significant potential for isolating metal-centered compounds with novel coordination environments. These ligands, through effective delocalization of cationic charge density within the five-membered ring system, act as strong electron donors, transferring substantial electron density to the metal center, thereby significantly enhancing the stability of the metal center. Additionally, these ligands exhibit broad tunability, allowing for the customization of backbone, ring size, and *N*-substituents to meet the stabilization needs of different elements.

Beyond their diverse interactions with metals, these ligands also demonstrate immense potential in the field of catalysis. Among them, NHOs have been proven to be highly efficient catalysts, widely applied in various organic synthesis reactions. However, research on NHIs and NHCPs remains in the preliminary exploration stage, with future prospects for further expanding their applications. Furthermore, future studies should prioritize computational modeling investigations of these ligand effects to provide theoretical guidance for designing novel complexes and high-efficiency catalysts.

Data availability

No primary research results, software or code have been included and no new data were generated or analysed as part of this review.

Conflicts of interest

There are no conflicts to declare.

Acknowledgements

This work was supported by the National Natural Science Foundation of China (No. 22201210).

Notes and references

1 (*a*) A. J. Arduengo III, R. L. Harlow and M. Kline, A Stable Crystalline Carbene, *J. Am. Chem. Soc.*, 1991, **113**, 361–363; (*b*) A. J. Arduengo III, H. V. R. Dias, R. L. Harlow and M. Kline, Electronic Stabilization of Nucleophilic Carbenes, *J. Am. Chem. Soc.*, 1992, **114**, 5530–5534.

2 (*a*) P. Bellotti, M. Koy, M. N. Hopkinson and F. Glorius, Recent Advances in the Chemistry and Applications of N-Heterocyclic Carbenes, *Nat. Rev. Chem*, 2021, **5**, 711–725; (*b*) D. Munz, Pushing Electrons-Which Carbene Ligand for Which Application?, *Organometallics*, 2018, **37**, 275–289; (*c*) F. E. Hahn, Introduction: Carbene Chemistry, *Chem. Rev.*, 2018, **118**, 9455–9456.

3 R. Jazzar, M. Soleilhavoup and G. Bertrand, Cyclic (Alkyl)- and (Aryl)-(amino)carbene Coinage Metal Complexes and Their Applications, *Chem. Rev.*, 2020, **120**, 4141–4168.

4 G. C. Fortman and S. P. Nolan, N-Heterocyclic Carbene (NHC) Ligands and Palladium in Homogeneous Cross-Coupling Catalysis: a Perfect Union, *Chem. Soc. Rev.*, 2011, **40**, 5151–5169.

5 G. Frison and A. Sevin, Theoretical Study of the Bonding between Aminocarbene and Main Group Elements, *J. Chem. Soc., Perkin Trans. 2*, 2002, **113**, 1692–1697.

6 (*a*) M. Majumdar, V. Huch, I. Bejan, A. Meltzer and D. Scheschkewitz, Reversible, Complete Cleavage of Si=Si Double Bonds by Isocyanide Insertion, *Angew. Chem., Int. Ed.*, 2013, **52**, 3516–3520; (*b*) A. G. Trambitas, J. Yang, D. Melcher, C. G Daniliuc, P. G. Jones, Z. Xie and M. Tamm, Synthesis and Structure of Rare-Earth-Metal Dicarbollide Complexes with an Imidazolin-2-Iminato Ligand Featuring very Short Metal-Nitrogen Bonds, *Organometallics*, 2011, **30**, 1122–1129.

7 (*a*) T. Ochiai, D. Franz and S. Inoue, Applications of N-Heterocyclic Imines in Main Group Chemistry, *Chem. Soc. Rev.*, 2016, **45**, 6327–6344; (*b*) A. Doddi, D. Bockfeld, T. Bannenberg, P. G. Jones and M. Tamm, N-Heterocyclic Carbene-Phosphinidyne Transition Metal Complexes, *Angew. Chem., Int. Ed.*, 2014, **53**, 13568–13572; *Angew. Chem.*, 2014, **126**, 13786–13790; (*c*) R. Schuldt, J. Kästner and S. Naumann, Proton Affinities of N-Heterocyclic Olefins and Their Implications for Organocatalyst Design, *J. Org. Chem.*, 2019, **84**, 2209–2218.

8 (*a*) N. Kuhn, M. Göhner, M. Grathwohl, J. Wiethoff, G. Frenking and Y. Chen, 2-Iminoimidazolines - Strong Nitrogen Bases als Ligands in Inorganic Chemistry, *Z. Anorg. Allg. Chem.*, 2003, **629**, 793–802; (*b*) A. G. Trambitas, T. K. Panda and M. Tamm, Rare Earth Metal Complexes Supported by Ancillary Imidazolin-2-Iminato Ligands, *Z. Anorg. Allg. Chem.*, 2010, **636**, 2156–2171; (*c*) Y. Wu and M. Tamm, Transition Metal Complexes Supported by Highly Basic Imidazolin-2-Iminato and Imidazolin-2-Imine N-Donor Ligands, *Coord. Chem. Rev.*, 2014, **260**, 116–138; (*d*) P. Raja, S. Revathi and T. Ghatak, Recent Advances of Imidazolin-2-Iminato in Transition Metal Chemistry, *Eng. Sci.*, 2020, **12**, 23–37.

9 (*a*) K. Dehnicke and A. Greiner, Unusual Complex Chemistry of Rare-Earth Elements: Large Ionic Radii - Small Coordination Numbers, *Angew. Chem., Int. Ed.*, 2003, **42**, 1340–1354; (*b*) A. Diefenbach and F. M. Bickelhaupt, Coordination Behaviour of the Isolobal Phosphoraneiminato and Cyclopentadienyl Ligands in $TiCl_3(NPH_3)$, $TiCl_3Cp$, $ReO_3(NPH_3)$ und ReO_3Cp, *Z. Anorg. Allg. Chem.*, 1999, **625**, 892–900.

10 (*a*) L. Weber, Phosphaalkenes with Inverse Electron Density, *Eur. J. Inorg. Chem.*, 2000, **2000**, 2425–2441; (*b*) P. Rosa, C. Gouverd, G. Bernardinelli, T. Berclaz and M. Geoffroy, Phosphaalkenes with Inverse Electron Density: Electrochemistry, Electron Paramagnetic Resonance Spectra, and Density Functional Theory Calculations of Aminophosphaalkene Derivatives, *J. Phys. Chem. A*, 2003, **107**, 4883–4892.

11 (*a*) O. Back, M. Henry-Ellinger, C. D. Martin and G. Bertrand, ^{31}P NMR Chemical Shifts of Carbene-Phosphinidene Adducts as An Indicator of the π-Accepting Properties of Carbenes, *Angew. Chem., Int. Ed.*, 2013, **52**, 2939–2943; *Angew. Chem.*, 2013, **125**, 3011–3015; (*b*) S. Dutta, B. Maity, D. Thirumalai and D. Koley, Computational Investigation of Carbene-Phosphinidenes: Correlation between ^{31}P Chemical Shifts and Bonding Features to Estimate the π-Backdonation of Carbenes, *Inorg. Chem.*, 2018, **57**, 3993–4008.

12 A. J. Arduengo III, C. J. Carmalt, J. A. C. Clyburne, A. H. Cowley and R. Pyati, Nature of the Bonding in a Carbene-Phosphinidene: a Main Group Analogue of a Fischer Carbene Complex? Isolation and Characterisation of a Bis(borane) Adduct, *Chem. Commun.*, 1997, 981–982.

13 (*a*) R. Breslow, Rapid Deuterium Exchange in Thiazolium, *J. Am. Chem. Soc.*, 1957, **79**, 1762–1763; (*b*) R. Breslow, On the Mechanism of Thiamine Action. IV. Evidence from Studies on Model Systems, *J. Am. Chem. Soc.*, 1958, **80**, 3719–3726; (*c*) V. Dhayalan, S. C. Gadekar, Z. Alassad and A. Milo, Unravelling Mechanistic Features of Organocatalysis with in Situ Modifications at the Secondary Sphere, *Nat. Chem.*, 2019, **11**, 543–551; (*d*) S. C. Gadekar, V. Dhayalan, A. Nandi, I. L. Zak, M. S. Mizrachi, S. Kozuch and A. Milo, Rerouting the Organocatalytic Benzoin Reaction toward Aldehyde Deuteration, *ACS Catal.*, 2021, **11**, 14561–14569.

14 N. Kuhn, H. Bohnen, D. Bläser and R. Boese, $(C_8H_{14}N_2)M(CO)_5$ (M = Mo, W)-Terminale Koordination Eines Olefins in Pentacarbonylmetall-Komplexen, *Chem. Ber.*, 1994, **127**, 1405–1407.

15 K.-M. Wang, S.-J. Yan and J. Lin, Heterocyclic Ketene Aminals: Scaffolds for Heterocycle Molecular Diversity, *Eur. J. Org Chem.*, 2014, **2014**, 1129–1145.

16 N. Kuhn, H. Bohnen, J. Kreutzberg, D. Bläser and R. Boese, 1,3,4,5-Tetramethyl-2-Methyleneimidazoline-an Ylidic Olefin, *J. Chem. Soc., Chem. Commun.*, 1993, 1136–1137.

17 (*a*) B. Maji, M. Horn and H. Mayr, Nucleophilic Reactivities of Deoxy Breslow Intermediates: How does Aromaticity Affect the Catalytic Activities of N-Heterocyclic Carbenes?, *Angew. Chem., Int. Ed.*, 2012, **51**, 6231–6235; (*b*) Z. Li, P. Ji and J.-P. Cheng, Brönsted Basicities and Nucleophilicities of N-Heterocyclic Olefins in Solution: N-Heterocyclic Carbene versus N-Heterocyclic Olefin. Which is More Basic, and Which is More Nucleophilic?, *J. Org. Chem.*, 2021, **86**, 2974–2985.

18 (*a*) S. Naumann, Synthesis, Properties & Applications of N-Heterocyclic Olefins in Catalysis, *Chem. Commun.*, 2019, **55**, 11658–11670; (*b*) Z. Wang, Q.-H. Niu, X.-S. Xue and P. Ji, The Brönsted Basicities of N-Heterocyclic Olefins in DMSO: an Effective Way to Evaluate the Stability of NHO-CO_2 Adducts, *J. Org. Chem.*, 2020, **85**, 13204–13210.

19 (*a*) Y.-B. Huang, J. Liang, X.-S. Wang and R. Cao, Multifunctional Metal–Organic Framework Catalysts: Synergistic Catalysis and Tandem Reactions, *Chem. Soc. Rev.*, 2017, **46**, 126–157; (*b*) Q. Zhang, C. Huang, Y. Tao, Y. Zhang, J. Cui, D. Wang, P. Wang and Y.-Y. Zhang, Flexible Triboelectric Nanogenerators Based on Cadmium Metal-Organic Framework/Eethyl Cellulose Composites as Energy Harvesters for Selective Photoinduced Bromination Reaction, *Small*, 2025, **21**, 2406623; (*c*) S. Liu, H. Yang, Y. Zhang, F. Wang, Q. Qin, D. Wang, C. Huang and Y.-Y. Zhang, Robust Cooperative of Cadmium Sulfide with Highly Ordered Hollow Microstructure Coordination Polymers for Regulating the Photocatalytic Performance, *J. Colloid Interface Sci.*, 2024, **663**, 919–929; (*d*) F. Wang, Y.-Y. Zhang, S. Li, L. Zhang, Y. Tao, J. Cui, D. Wang, M. Jiao and C. Huang, Integration of Cobalt Coordination Polymer-Based Triboelectric Nanogenerators as Sustainable Power Sources for Self-Driven Selective Photocatalytic Reactions, *Chem. Eng. J.*, 2025, **503**, 158194; (*e*) Y. Zhang, C. Huang and L. Mi, Metal-Organic Frameworks as Acid- and/or Base-Functionalized Catalysts for Tandem Reactions, *Dalton Trans.*, 2020, **49**, 14723–14730; (*f*) S. Liu, H. Yang, S. Li, Q. Qin, Y. Tao, J. Cui, D. Wang, C. Huang and Y.-Y. Zhang, Enhancement of Synergistic Photocatalytic Performance by Anchoring Cadmium Sulfide on Nanosphere Structured Coordination Polymers, *Inorg. Chem.*, 2024, **63**, 17116–17126.

20 T. Krachko and J. C. Slootweg, N-Heterocyclic Carbene-Phosphinidene Adducts: Synthesis, Properties, and Applications, *Eur. J. Inorg. Chem.*, 2018, 2734–2754.

21 S. Revathi, P. Raja, S. Saha, M. S. Eisen and T. Ghatak, Recent Developments in Highly Basic N-Heterocyclic Iminato Ligands in Actinide Chemistry, *Chem. Commun.*, 2021, **57**, 5483–5502.

22 M. M. D. Roy and E. Rivard, Pushing Chemical Boundaries with N-Heterocyclic Olefins (NHOs): from Catalysis to Main Group Element Chemistry, *Acc. Chem. Res.*, 2017, **50**, 2017–2025.

23 R. S. Ghadwal, Tuning the Electronic Properties of Main-Group Species by N-Heterocyclic Vinyl (NHV) Scaffolds, *Acc. Chem. Res.*, 2022, **55**, 457–470.

24 K. Schwedtmann, G. Zanoni and J. J. Weigand, Recent Advances in Imidazoliumyl-Substituted Phosphorus Compounds, *Chem.–Asian J.*, 2018, **13**, 1388–1405.

25 A. Doddi, M. Peters and M. Tamm, N-Heterocyclic Carbene Adducts of Main Group Elements and Their Use as Ligands in Transition Metal Chemistry, *Chem. Rev.*, 2019, **119**, 6994–7112.

26 (*a*) D. Franz, E. Irran and S. Inoue, Synthesis, Characterization and Reactivity of an Imidazolin-2-Iminato Aluminium Dihydride, *Dalton Trans.*, 2014, **43**, 4451–4461; (*b*) D. Franz and S. Inoue, Systematic Investigation of the Ring-Expansion Reaction of N-Heterocyclic Carbenes with an Iminoborane Dihydride, *Chem.–Asian J.*, 2014, **9**, 2083–2087; (*c*) D. Franz, E. Irran and S. Inoue, Isolation of a Three-Coordinate Boron Cation with a Boron-Sulfur Double Bond, *Angew. Chem., Int. Ed.*, 2014, **53**, 14264–14268.

27 C. Hering-Junghans, P. Andreiuk, M. J. Ferguson, R. McDonald and E. Rivard, Using N-Heterocyclic Vinyl Ligands to Access Stable Divinylgermylenes and a Germylium Cation, *Angew. Chem., Int. Ed.*, 2017, **56**, 6272–6275.

28 C. Hering-Junghans, I. C. Watson, M. J. Ferguson, R. McDonald and E. Rivard, Organocatalytic Hydroborylation Promoted by N-Heterocyclic Olefins, *Dalton Trans.*, 2017, **46**, 7150–7153.

29 M. Lafage, A. Pujol, N. Saffon-Merceron and N. Mézailles, BH_3 Activation by Phosphorus-Stabilized Geminal Dianions: Synthesis of Ambiphilic Organoborane, DFT Studies, and Catalytic CO_2 Reduction into Methanol Derivatives, *ACS Catal.*, 2016, **6**, 3030–3035.

30 I. C. Watson, M. J. Ferguson, R. McDonald and E. Rivard, Zinc-Mediated Transmetalation as a Route to Anionic N-Heterocyclic Olefin Complexes in the p-Block, *Inorg. Chem.*, 2021, **60**, 18347–18359.

31 F. Zettler, H. D. Hausen and H. Hess, Die Kristall- und Molekülstruktur des Triphenylborans, *J. Organomet. Chem.*, 1974, **72**, 157–162.

32 S. R. Baird, E. Hupf, I. C. Watson, M. J. Ferguson, R. McDonald and E. Rivard, An Indium(I) Tetramer Bound by Anionic N-Heterocyclic Olefins: Ambiphilic Reactivity, Transmetallation and a Rare Indium-Imide, *Chem. Commun.*, 2023, **59**, 2903–2906.

33 H. Dolati, L. Denker, B. Trzaskowski and R. Frank, Superseding β-Diketiminato Ligands: an Amido Imidazoline-2-Imine Ligand Stabilizes the Exhaustive Series of B = X Boranes (X = O, S, Se, Te), *Angew. Chem., Int. Ed.*, 2021, **60**, 4633–4639.

34 M. W. Lui, N. R. Paisley, R. McDonald, M. J. Ferguson and E. Rivard, Metal-Free Dehydrogenation of Amine-Boranes by Tunable N-Heterocyclic Iminoboranes, *Chem.–Eur. J.*, 2016, **22**, 2134–2145.

35 D. Franz, T. Szilvási, A. Pçthig and S. Inoue, Isolation of an N-Heterocyclic Carbene Complex of a Borasilene, *Chem.–Eur. J.*, 2019, **25**, 11036–11041.

36 J. Han, C. Hu, Q. Li, L. L. Liu, C.-H. Tung, P. Cui and L. Kong, Derivatization of an Alkylideneborane with B=C Bond Cleavage, *Inorg. Chem.*, 2023, **62**, 18820–18824.

37 D. Franz, E. Irran and S. Inoue, Synthesis, Characterization and Reactivity of an Imidazolin-2-Iminato Aluminium Dihydride, *Dalton Trans.*, 2014, **43**, 4451–4461.

38 D. Franz and S. Inoue, Activation of Elemental Sulfur by Aluminum Dihydride: Isolationof Mono- and Bis(hydrogensulfide) Complexes of Aluminum, *Chem.–Eur. J.*, 2014, **20**, 10645–10649.

39 D. Franz, L. Sirtl, A. Pöthig and S. Inoue, Aluminum Hydrides Stabilized by N-Heterocyclic Imines as Catalysts for Hydroborations with Pinacolborane, *Z. Anorg. Allg. Chem.*, 2016, **642**, 1245–1250.

40 (*a*) D. Franz, C. Jandl, C. Stark and S. Inoue, Catalytic CO_2 Reduction with Boron- and Aluminum Hydrides, *ChemCatChem*, 2019, **11**, 5275–5281; (*b*) C. Weetman, N. Ito, M. Unno and S. Inoue, NHI- and NHC-Supported Al(III) Hydrides for Amine-Borane Dehydrocoupling Catalysis, *Inorganics*, 2019, **7**, 92.

41 H. Liu, M. Khononov, N. Fridman, M. Tamm and M. S. Eisen, (Benz)Imidazolin-2-iminato Aluminum, Zinc, and Magnesium Complexes and Their Applications in Ring Opening Polymerization of ε-Caprolactone, *Inorg. Chem.*, 2019, **58**, 13426–13439.

42 S. Pahar, G. Kundu, C. P. George, R. G. Gonnade and S. S. Sen, Substitution at a Coordinatively Saturated Aluminum Center Stabilized by Imidazolidin-2-imine, *Organometallics*, 2023, **42**, 276–282.

43 I. C. Watson, Y. Zhou, M. J. Ferguson, M. Kränzlein, B. Rieger and E. Rivard, Trialkylaluminum N-Heterocyclic Olefin (NHO) Adducts as Catalysts for the Polymerization of Michael-Type Monomers, *Z. Anorg. Allg. Chem.*, 2020, **646**, 547–551.

44 A. D. K. Todd, W. L. McClennan and J. D. Masuda, Organoaluminum(III) Complexes of the Bis-N,N'-(2,6-Diisopropylphenyl)Imidazolin-2-Imine Ligand, *RSC Adv.*, 2016, **6**, 69270–69276.

45 J. W. Turley and H. W. Rinn, Crystal Structure of Aluminum Hydride. The Crystal Structure of Aluminum Hydride, *Inorg. Chem.*, 1969, **8**, 18–22.

46 J. Bhattacharjee, M. Peters, D. Bockfeld and M. Tamm, Isoselective Polymerization of *rac*-Lactide by Aluminum Complexes of N-Heterocyclic Carbene-Phosphinidene Adducts, *Chem.–Eur. J.*, 2021, **27**, 5913–5918.

47 O. Lemp, M. Balmer, K. Reiter, F. Weigendb and C. Hänisch, An NHC-Phosphinidenyl as a Synthon for New Group 13/15 Compounds, *Chem. Commun.*, 2017, **53**, 7620–7623.

48 D. H. Mayo, Y. Peng, S. DeCarlo, X. Li, J. Lightstone, P. Zavalij, K. Bowen, H. Schnöckel and B. Eichhorn, $K[Al_4(PPh_2)_7PPh]$: An Al^{II} Phosphanide/Phosphinidene Intermediate on the Path to AlP Formation, *Z. Anorg. Allg. Chem.*, 2013, **639**, 2558–2560.

49 M. Balmer and C. Hänisch, Synthesis of the Cyclic Group 13 Phosphinidenides $[(NHC)PMCl_2]_2$ (NHC = SIMes, SIDipp; M = Al, Ga), *Z. Anorg. Allg. Chem.*, 2020, **646**, 648–652.

50 L. Denker, B. Trzaskowski and R. Frank, "Give Me Five" - an Amino Imidazoline-2-Imine Ligand Stabilises the First Neutral Five-Membered Cyclic Triel(I) Carbenoides, *Chem. Commun.*, 2021, **57**, 2816–2819.

51 B. Wang, W. Chen, J. Yang, L. Lu, J. Liu, L. Shena and D. Wu, N-Heterocyclic Imine-Based Bis-Gallium(I) Carbene Analogs Featuring a Four-Membered Ga_2N_2 ring, *Dalton Trans.*, 2023, **52**, 12454–12460.

52 K. Powers, C. Hering-Junghans, R. McDonald, M. J. Ferguson and E. Rivard, Improved Synthesis of N-Heterocyclic Olefins and Evaluation of Their Donor Strengths, *Polyhedron*, 2016, **108**, 8–14.

53 T. B. Ditri, B. J. Fox, C. E. Moore, A. L. Rheingold and J. S. Figueroa, Effective Control of Ligation and Geometric Isomerism: Direct Comparison of Steric Properties Associated with Bis-Mesityl and Bis-Diisopropylphenyl *m*-Terphenyl Isocyanides, *Inorg. Chem.*, 2009, **48**, 8362–8375.

54 (*a*) N. Kuhn, R. Fawzi, M. Steimann, J. Wiethoff, D. Bläser and R. Boese, Synthese and Structure of 2-Imino-l,3-dimethylimidazolin, *Z. Naturforsch., B:J. Chem. Sci.*, 1995, **50**, 1779–1784; (*b*) N. Kuhn, R. Fawzi, M. Steimann and J. Wiethoff, 2-Iminoimidazolin Derivatives of Magnesium and Aluminium, *Z. Anorg. Allg. Chem.*, 1997, **623**, 554–560.

55 M. M. D. Roy, M. J. Ferguson, R. McDonald, Y. Zhou and E. Rivard, A Vinyl Silylsilylene and Its Activation of Strong Homo- and Heteroatomic Bonds, *Chem. Sci.*, 2019, **10**, 6476–6481.

56 (*a*) A. V. Protchenko, A. D. Schwarz, M. P. Blake, C. Jones, N. Kaltsoyannis, P. Mountford and S. Aldridge, A Generic One-Pot Route to Acyclic Two-Coordinate Silylenes from Silicon(IV) Precursors: Synthesis and Structural Characterization of a Silylsilylene, *Angew. Chem., Int. Ed.*, 2013, **52**, 568–571; (*b*) T. J. Hadlington, J. A. B. Abdalla, R. Tirfoin, S. Aldridge and C. Jones, Stabilization of a Two-Coordinate, Acyclic Diaminosilylene (ADASi): Completion of the Series of Isolable Diaminotetrylenes, $:E(NR_2)_2$ (E = group 14 element), *Chem. Commun.*, 2016, **52**, 1717–1720; (*c*) D. Wendel, A. Porzelt, F. A. D. Herz, D. Sakar, C. Jandl, S. Inoue and B. Rieger, From Si(II) to Si(IV) and Back: Reversible Intramolecular Carbon-Carbon Bond Activation by an Acyclic Iminosilylene, *J. Am. Chem. Soc.*, 2017, **139**, 8134–8137; (*d*) Y. K. Loh, L. Ying, M. Á. Fuentes, D. C. H. Do and S. Aldridge, An N-Heterocyclic Boryloxy Ligand Isoelectronic with N-HeterocyclicImines: Access to an Acyclic Dioxysilylene and Its Heavier Congeners, *Angew. Chem., Int. Ed.*, 2019, **58**, 4847–4851.

57 M. M. D. Roy, S. R. Baird, E. Dornsiepen, L. A. Paul, L. Miao, M. J. Ferguson, Y. Zhou, I. Siewert and E. Rivard, A Stable Homoleptic Divinyl Tetrelene Series, *Chem.–Eur. J.*, 2021, **27**, 8572–8579.

58 D. Wendel, D. Reiter, A. Porzelt, P. J. Altmann, S. Inoue and B. Rieger, Silicon and Oxygen's Bond of Affection: an Acyclic Three-Coordinate Silanone and Its Transformation to an Iminosiloxysilylene, *J. Am. Chem. Soc.*, 2017, **139**, 17193–17198.

59 T. Eisner, A. Kostenko, F. Hanusch and S. Inoue, Room-Temperature-Observable Interconversion between Si(IV)

and Si(II) via Reversible Intramolecular Insertion into an Aromatic C–C Bond, *Chem.–Eur. J.*, 2022, **28**, e202202330.

60 J. Y. Liu, S. Inoue and B. Rieger, Isolation and Reactivity of Silepins with a Sterically Demanding Silyl Ligand, *Eur. J. Inorg. Chem.*, 2024, **27**, e202400045.

61 M. W. Lui, C. Merten, M. J. Ferguson, R. McDonald, Y. Xu and E. Rivard, Contrasting Reactivities of Silicon and Germanium Complexes Supported by an N-Heterocyclic Guanidine Ligand, *Inorg. Chem.*, 2015, **54**, 2040–2049.

62 D. Reiter, P. Frisch, T. Szilvási and S. Inoue, Heavier Carbonyl Olefination: the Sila-Wittig Reaction, *J. Am. Chem. Soc.*, 2019, **141**, 16991–16996.

63 D. Reiter, P. Frisch, D. Wendel, F. M. Hörmann and S. Inoue, Oxidation Reactions of a Versatile, Two-Coordinate, Acyclic Iminosiloxysilylene, *Dalton Trans.*, 2020, **49**, 7060–7068.

64 H. Zhu, A. Kostenko, D. Franz, F. Hanusch and S. Inoue, Room Temperature Intermolecular Dearomatization of Arenes by an Acyclic Iminosilylene, *J. Am. Chem. Soc.*, 2023, **145**, 1011–1021.

65 H. Zhu, F. Hanusch and S. Inoue, Facile Bond Activation of Small Molecules by an Acyclic Imino(silyl)silylene, *Isr. J. Chem.*, 2023, **63**, e202300012.

66 H. Zhu, A. Kostenko, J. A. Kelly and S. Inoue, Substituent Exchange between an Imino(silyl)silylene and Aryl Isocyanides, *Chem*, 2024, **10**, 1213–1224.

67 M. E. Doleschal, A. Kostenko, J. Y. Liu and S. Inoue, Isolation of a NHC-Stabilized Heavier Nitrile and Its Conversion into an Isonitrile Analogue, *Nat. Chem.*, 2024, **16**, 2009–2016.

68 L. Wang, Y. Li, Z. Li and M. Kira, Isolable Silylenes and Their Diverse Reactivity, *Coord. Chem. Rev.*, 2022, **457**, 214413.

69 M. E. Doleschal, A. Kostenko, J. Y. Liu and S. Inoue, Silicon-Aryl Cooperative Activation of Ammonia, *Chem. Commun.*, 2024, **60**, 13020–13023.

70 S. Du, H. Jia, H. Rong, H. Song, C. Cui and Z. Mo, Synthesis and Reactivity of N-Heterocyclic Silylene Stabilized Disilicon(0) Complexes, *Angew. Chem., Int. Ed.*, 2022, **61**, e202115570.

71 S. Du, F. Cao, X. Chen, H. Rong, H. Song and Z. Mo, A Silylene-Stabilized Ditin(0) Complex and Its Conversion to Methylditin Cation and Distannavinylidene, *Nat. Commun.*, 2023, **14**, 7474.

72 F. J. Kiefer, A. Kostenko, R. Holzner and S. Inoue, A Neutral Crystalline Imino-Substituted Silyl Radical, *Chem. Commun.*, 2024, **60**, 8577–8580.

73 (*a*) Y. Li, Y.-C. Chan, B.-X. Leong, Y. Li, E. Richards, I. Purushothaman, S. De, P. Parameswaran and C.-W. So, Trapping a Silicon(I) Radical with Carbenes: a Cationic CAAC–Silicon(I) Radical and an NHC–Parent-Silyliumylidene Cation, *Angew. Chem., Int. Ed.*, 2017, **129**, 7681–7686; (*b*) S.-H. Zhang, E. Carter, H.-W. Xi, Y. Li, K. H. Lim and C.-W. So, Delocalized Hypervalent Silyl Radical Supported by Amidinate and Imino Substituents, *Inorg. Chem.*, 2017, **56**, 701–704.

74 M. Balmer, Y. J. Franzke, F. Weigend and C. Hänisch, Low-Valent Group 14 Phosphinidenide Complexes [({SIDipp}P)$_2$M] Exhibit P–M pπ-pπ Interaction (M = Ge, Sn, Pb), *Chem.–Eur. J.*, 2020, **26**, 192–197.

75 (*a*) K. Izod, P. Evans, P. G. Waddell and M. R. Probert, Remote Substituent Effects on the Structures and Stabilities of P=E π-Stabilized Diphosphatetrylenes $(R_2P)_2E$ (E = Ge, Sn), *Inorg. Chem.*, 2016, **55**, 10510–10522; (*b*) M. Driess, S. Rell, H. Pritzkow and R. Janoschek, [R–PLi$_2$(F–R)]$_2$ [R = SiPr$^i_2$(C$_6$H$_2$Pr$^i_3$-2,4,6)] the First Structural Characterization of a Dilithium Phosphandiide in the Form of a Fluorosilane Complex, *Chem. Commun.*, 1996, **2**, 305–306.

76 M. E. Doleschal, A. E. Ferao, A. Kostenko, F. J. Kiefer and S. Inoue, The Substituent-Effect in NHCP-Plumbylenes with a Phosphaplumbene Character, *Angew. Chem., Int. Ed.*, 2025, e202422186.

77 F. Goerigk, N. Birchall, C. M. Feil, M. Nieger and D. Gudat, Reactions of Imidazolio-Phosphides with Organotin Chlorides: Surprisingly Diverse, *Eur. J. Inorg. Chem.*, 2022, e202101026.

78 V. Nesterov, R. Baierl, F. Hanusch, A. E. Ferao and S. Inoue, N-Heterocyclic Carbene-Stabilized Germanium and Tin Analogues of Heavier Nitriles: Synthesis, Reactivity, and Catalytic Application, *J. Am. Chem. Soc.*, 2019, **141**, 14576–14580.

79 (*a*) M. Usher, A. V. Protchenko, A. Rit, J. Campos, E. L. Kolychev, R. Tirfoin and S. Aldridge, A Systematic Study of Structure and E–H Bond Activation Chemistry by Sterically Encumbered Germylene Complexes, *Chem.–Eur. J.*, 2016, **22**, 11685–11698; (*b*) W. A. Merrill, R. J. Wright, C. S. Stanciu, M. M. Olmstead, J. C. Fettinger and P. P. Power, Synthesis and Structural Characterization of a Series of Dimeric Metal(II) Imido Complexes {M(μ-NAr$^\#$)}$_2$ [M = Ge, Sn, Pb; Ar$^\#$ = C$_6$H$_3$–2,6–(C$_6$H$_2$–2,4,6–Me$_3$)$_2$] and the Related Monomeric Primary Amido Derivatives M{N(H)Ar$^\#$}$_2$ (M = Ge, Sn, Pb): Spectroscopic Manifestations of Secondary Metal-Ligand Interactions, *Inorg. Chem.*, 2010, **49**, 7097–7105.

80 S. Brooker, J.-K. Buijink and F. T. Edelmann, Synthesis, Structure, and Reactivity of the First Stable Diaryllead(II), *Organometallics*, 1991, **10**, 25–26.

81 T. Ochiai and S. Inoue, Synthesis of a Cyclopentadienyl(imino)stannylene and Its Direct Conversion into Halo(imino)stannylenes, *RSC Adv.*, 2017, **7**, 801–804.

82 D. Stalke, M. A. Paver and D. S. Wright, Nucleophilic Substitution of Bis(cyclopentadienyl)-tin(II); Synthesis, Structure, and Solution Dynamicsof Trans-[(η^3-Cp)Sn{μ^2-N=C(NMe$_2$)$_2$}]$_2$, *Angew. Chem., Int. Ed. Engl.*, 1993, **32**, 428–429.

83 X.-X. Zhao, T. Szilvási, F. Hanusch, J. A. Kelly and S. Inoue, Isolation and Reactivity of Tetrylene-Tetrylone-Iron Complexes Supported by Bis(N-Heterocyclic Imine) Ligands, *Angew. Chem., Int. Ed.*, 2022, **61**, e202208930.

84 X.-X. Zhao, T. Szilvási, F. Hanusch and S. Inoue, An Isolable Three-Coordinate Germanone and Its Reactivity, *Chem.–Eur. J.*, 2021, **27**, 15914–15917.

85 D. Sarkar, L. Groll, D. Munz, D. Hanusch and S. Inoue, Ligand Assisted CO_2 Activation and Catalytic Valorization by an NHI-Stabilized Stannylene, *ChemCatChem*, 2022, **14**, e202201048.

86 X.-X. Zhao, S. Fujimori, J. A. Kelly and S. Inoue, Isolation and Reactivity of Stannylenoids Stabilized by Amido/imino Ligands, *Chem.–Eur. J.*, 2023, **29**, e202202712.

87 L. Groll, J. A. Kelly and S. Inoue, Reactivity of NHI-Stabilized Heavier Tetrylenes towards CO_2 and N_2O, *Chem.–Asian J.*, 2024, **19**, e202300941.

88 M. J. S. Gynane, D. H. Harris, M. F. Lappert, P. P. Power, P. Rivière and M. Rivière-Baudet, Subvalent Group 4B Metal Alkyls and Amides. Part 5. the Synthesis and Physical Properties of Thermally Stable Amides of Germanium(II). Tin(II), and Lead(II), *J. Chem. Soc., Dalton Trans.*, 1977, 2004–2009.

89 J. Schreiber, H. Maag, N. Hashimoto and A. Eschenmoser, Dimethyl(methylene)ammonium Iodidei, *Angew. Chem., Int. Ed. Engl.*, 1971, **10**, 330–331.

90 N. R. Paisley, M. W. Lui, R. McDonald, M. J. Ferguson and E. Rivard, Structurally Versatile Phosphine and Amine Donors Constructed from N-Heterocyclic Olefin Units, *Dalton Trans.*, 2016, **45**, 9860–9870.

91 L. Y. M. Eymann, P. Varava, A. M. Shved, B. F. E. Curchod, Y. Liu, O. M. Planes, A. Sienkiewicz, R. Scopelliti, F. F. Tirani and K. Severin, Synthesis of Organic Super-Electron-Donors by Reaction of Nitrous Oxide with N-Heterocyclic Olefins, *J. Am. Chem. Soc.*, 2019, **141**, 17112–17116.

92 P. Varava, Z. Dong, R. Scopelliti, F. Fadaei-Tirani and K. Severin, Isolation and Characterization of Diazoolefins, *Nat. Chem.*, 2021, **13**, 1055–1060.

93 P. Varava, T. Wong, Z. Dong, A. Y. Gitlina, A. Sienkiewicz, W. Feuerstein, R. Scopelliti, F. Fadaei-Tirani and K. Severin, Head-to-Tail Dimerization of N-Heterocyclic Diazoolefins, *Angew. Chem., Int. Ed.*, 2023, **62**, e202303375.

94 T. Eisner, A. Kostenko, F. J. Kiefer and S. Inoue, Synthesis and Isolation of a Cyclic Bis-Vinyl Germylene via a Diazoolefin Adduct of Germylene Dichloride, *Chem. Commun.*, 2024, **60**, 558–561.

95 Y. He, Y. Lyu, D. Tymann, P. W. Antoni and M. M. Hansmann, Cleavage of Carbodicarbenes with N_2O for Accessing Stable Diazoalkenes: Two-Fold Ligand Exchange at a C(0)-Atom, *Angew. Chem., Int. Ed.*, 2025, **64**, e202415228.

96 L. P. Ho, M.-K. Zaretzke, T. Bannenberg and M. Tamm, Heteroleptic Diphosphenes and Arsaphosphenes Bearing Neutral and Anionic N-Heterocyclic Carbenes, *Chem. Commun.*, 2019, **55**, 10709–10712.

97 J. Haberstroh, C. Taube, J. Fidelius, S. Schulz, N. Israel, E. Dmitrieva, R. M. Gomila, A. Frontera, R. Wolf, K. Schwedtmann and J. J. Weigand, A Neutral Diphosphene Radical: Synthesis, Electronic Structure and White Phosphorus Activation, *Chem. Commun.*, 2024, **60**, 8537–8540.

98 M. A. Wünsche, T. Witteler and F. Dielmann, Lewis Base Free Oxophosphonium Ions: Tunable, Trigonal-Planar Lewis Acids, *Angew. Chem., Int. Ed.*, 2018, **57**, 7234–7239.

99 P. Mehlmann, T. Witteler, L. F. B. Wilm and F. Dielmann, Isolation, Characterization and Reactivity of Three Coordinate Phosphorus Dications Isoelectronic to Alanes and Silylium Cations, *Nat. Chem.*, 2019, **11**, 1139–1143.

100 P. Löwe, M. A. Wünsche, F. R. S. Purtscher, J. Gamper, T. S. Hofer, L. F. B. Wilm, M. B. Röthel and F. Dielmann, Terminal Methylene Phosphonium Ions: Precursors for Transient Monosubstituted Phosphinocarbenes, *Chem. Sci.*, 2023, **14**, 7928–7935.

101 F. Buß, M. Das, D. Janssen-Müller, A. Sietmann, A. Das, L. F. B. Wilm, M. Freitag, M. Seidl, F. Glorius and F. Dielmann, Photoswitchable Electron-Rich Phosphines: Using Light to Modulate the Electron-Donating Ability of Phosphines, *Chem. Commun.*, 2023, **59**, 12019–12022.

102 J. L. Lortie, M. Davies, P. D. Boyle, M. Karttunen and P. J. Ragogna, Chemoselective Staudinger Reactivity of Bis(azido)phosphines Supported with a π-Donating Imidazolin-2-iminato Ligand, *Inorg. Chem.*, 2024, **63**, 6335–6345.

103 K. Paul Lüdtke, E. Zander, F. Taube, J.-E. Siewert, B. Corzilius, C. Hering-Junghans, J. Bresien and A. Schulz, Reaction of NHOs with Bisphosphanes-Designing Diradicaloids, Zwitterions and Radicals, *Angew. Chem., Int. Ed.*, 2025, e202423347.

104 (*a*) A. Dumrath, X.-F. Wu, H. Neumann, A. Spannenberg, R. Jackstell and M. Beller, Recyclable Catalysts for Palladium-Catalyzed C–O Coupling Reactions, Buchwald-Hartwig Aminations, and Sonogashira Reactions, *Angew. Chem., Int. Ed.*, 2010, **49**, 8988–8992; (*b*) A. Dumrath, C. Lübbe, H. Neumann, R. Jackstell and M. Beller, Recyclable Catalysts for Palladium-Catalyzed Aminations of Aryl Halides, *Chem.–Eur. J.*, 2011, **17**, 9599–9604.

105 S. J. Berners-Price, L. A. Colquhoun, P. C. Healy, K. A. Byriel and J. V. Hanna, Copper(I) and Gold(I) Complexes with Cis-Bis(diphenyl-phosphino)ethylene. Crystal Structures and ^{31}P Cross-Polarization Magic Angle Spinning Nuclear Magnetic Resonance Studies, *J. Chem. Soc., Dalton Trans.*, 1992, 3357–3363.

106 M. W. Lui, O. Shynkaruk, M. S. Oakley, R. Sinelnikov, R. McDonald, M. J. Ferguson, A. Meldrum, M. Klobukowski and E. Rivard, Engaging Dual Donor Sites within an N-Heterocyclic Olefin Phosphine Ligand, *Dalton Trans.*, 2017, **46**, 5946–5954.

107 A. K. Sahoo, B. Das, S. J. Panda, C. S. Purohit and A. Doddi, N-Heterocyclic Olefin-Phosphines Based Cationic Ruthenium Complexes as Pre-Catalysts for Dual C–H Bond Functionalizations, *Adv. Synth. Catal.*, 2024, **366**, 2468–2476.

108 (*a*) T. Witteler, H. Darmandeh, P. Mehlmann and F. Dielmann, Dialkyl(1,3-diarylimidazolin-2-ylidenamino) phosphines: Strongly Electron-Donating, Buchwald-Type Phosphines, *Organometallics*, 2018, **37**, 3064–3072; (*b*) L. F. B. Wilm, P. Mehlmann, F. Buß and F. Dielmann, Synthesis and Characterization of Strongly Electron-

Donating Bidentate Phosphines Containing Imidazolin-2-Ylidenamino Substituents and Their Electron-Rich Nickel(0), Palladium(II) and Gold(I) Chelate Complexes, *J. Organomet. Chem.*, 2020, **909**, 121097; (*c*) T.-F. Leung, D. Jiang, M.-C. Wu, D. Xiao, W.-M. Ching, G. P. A. Yap, T. Yang, L. Zhao, T.-G. Ong and G. Frenking, Isolable Dicarbon Stabilized by a Single Phosphine Ligand, *Nat. Chem.*, 2021, **12**, 89–93; (*d*) S. Anga, J. Acharya and V. Chandrasekhar, An Unsymmetric Imino-Phosphanamidinate Ligand and its Y(III) Complex: Synthesis, Characterization, and Catalytic Hydroboration of Carbonyl Compounds, *J. Org. Chem.*, 2021, **86**, 2224–2234; (*e*) H. Karmakar, S. Anga, T. K. Panda and V. Chandrasekhar, Aluminium Alkyl Complexes Supported by Imino Phosphanamide Ligand as Precursors for Catalytic Guanylation Reactions of Carbodiimides, *RSC Adv.*, 2022, **12**, 4501–4509.

109 P. Löwe and F. Dielmann, Crystalline Phosphino(silyl) carbenes that Readily Form Transition Metal Complexes, *Chem. Commun.*, 2022, **58**, 11831–11834.

110 M. D. Böhme, T. Eder, M. B. Röthel, P. D. Dutschke, L. F. B. Wilm, F. E. Hahn and F. Dielmann, Synthesis of N-Heterocyclic Carbenes and Their Complexes by Chloronium Ion Abstraction from 2-Chloroazolium Salts Using Electron-Rich Phosphines, *Angew. Chem., Int. Ed.*, 2022, **61**, e202202190.

111 (*a*) E. Despagnet, H. Gornitzka, A. B. Rozhenko, W. W. Schoeller, D. Bourissou and G. Bertrand, Stable Non Push-Pull (phosphino)carbenes: NMR Characterization of a Methylcarbene, *Angew. Chem., Int. Ed.*, 2002, **41**, 2835–2837; (*b*) C. Buron, H. Gornitzka, V. Romanenko and G. Bertrand, Stable Versions of Transient Push-Pull Carbenes: Extending Lifetimes from Nanoseconds to Weeks, *Science*, 2000, **288**, 834–836.

112 S. Wang, C. Zhu, L. Ning, D. Li, X. Feng and S. Dong, Regioselective C–H Alkylation of Anisoles with Olefins by Cationic Imidazolin-2-Iminato Scandium(III) Alkyl Complexes, *Chem. Sci.*, 2023, **14**, 3132–3139.

113 B. Feng, L.-W. Ye, N. Wang, H.-S. Hu, J. Li, M. Tamm and Y. Chen, Endeavoring Cerium(IV)-Alkyl, -Aryl and -Alkynyl Complexes by an Energy-Level Match Strategy, *CCS Chem.*, 2025, **7**, 1043–1053.

114 Y. Guan, K. Chang, Y. Su, X. Xu and X. Xu, Frustrated Lewis Pair-Type Reactivity of Intermolecular Rare-Earth Aryloxide and N-Heterocyclic Carbene/Olefin Combinations, *Chem.–Asian J.*, 2024, **19**, e202400190.

115 B. Wang, X. Wang, R. Zhuang, C. Zhang, H. Liu, T. Tang, M. S. Eisen and X. Zhang, Synthesis of Mono- and Bis-Benzimidazolin-2-Iminato Titanium Complexes and Their Catalytic Performances in Ethylene Homo- and Co-Polymerizations, *Mol. Catal.*, 2021, **516**, 111974.

116 (*a*) I. Haas, C. Hübner, W. P. Kretschmer and R. Kempe, A Highly Efficient Titanium Catalyst for the Synthesis of Ultrahigh-Molecular-Weight Polyethylene (UHMWPE), *Chem.–Eur. J.*, 2013, **19**, 9132–9136; (*b*) M. Rep, J.-W. F. Kaagman, C. J. Elsevier, P. Sedmera, J. Hiller, U. Thewalt, M. Horáček and K. Mach, Reactions of Methyl-Substituted Titanocene-Bis(trimethylsilyl)acetylene Complexes with Acetone Azine: Crystal Structures of $(\eta^5{:}\eta^1\text{-}C_5HMe_3CH_2CMe_2NH)_2Ti$ and $(C_5Me_5)_2Ti(N\ CMe_2)$, *J. Organomet. Chem.*, 2000, **597**, 146–156; (*c*) K. Nomura, J. Yamada, W. Wang and J. Liu, Effect of Ketimide Ligand for Ethylene Polymerization and Ethylene/Norbornene Copolymerization Catalyzed by (Cyclopentadienyl)(Ketimide)Titanium Complexes-MAO Catalyst Systems: Structural Analysis for $Cp^*TiCl_2(N{=}CPh_2)$, *J. Organomet. Chem.*, 2007, **692**, 4675–4682.

117 M. Koneczny, A. B. Erol, M. Mauduit, M. S. Eisen and M. Tamm, Titanium Complexes with Unsymmetrically Substituted Imidazolin-2-Iminato Ligands, *Dalton Trans.*, 2022, **51**, 11448–11456.

118 M. Fischer, M. M. D. Roy, S. Hüller, M. Schmidtmannb and R. Beckhaus, Reaction of a Bis(Pentafulvene)Titanium Complex with an N-Heterocyclic Olefin: C–H activation Leads to Resonance between a Titanium Vinyl and Titanium Alkylidene Complex, *Dalton Trans.*, 2022, **51**, 10690–10696.

119 I. C. Watson, Y. Zhou, M. J. Ferguson and E. Rivard, Group 4 Transition Metal Complexes with Anionic N-Heterocyclic Olefin Ligands, *Z. Anorg. Allg. Chem.*, 2022, **648**, e202200082.

120 M. Khononov, H. Liu, N. Fridman, M. Tamm and M. S. Eisen, Mono(imidazolin-2-iminato) Hafnium Complexes: Synthesis and Application in the Ring-Opening Polymerization of ε-Caprolactone and *rac*-Lactide, *Catalysts*, 2022, **12**, 1201.

121 M. Peters, D. Baabe, M. Maekawa, D. Bockfeld, M.-K. Zaretzke, M. Tamm and M. D. Walter, Pogo-Stick Iron and Cobalt Complexes: Synthesis, Structures, and Magnetic Properties, *Inorg. Chem.*, 2019, **58**, 16475–16486.

122 (*a*) M. D. Walter and P. S. White, $\{Cp'Fe(\mu\text{-}OH)\}_3$: The Synthesis of a Unique Organometallic Iron Hydroxide, *Dalton Trans.*, 2012, **41**, 8506–8508; (*b*) M. D. Walter and P. S. White, Reactivity Studies on $Cp'FeI_2$: Monomeric Amido, Phenoxo, and Alkyl Complexes, *Inorg. Chem.*, 2012, **51**, 11860–11872; (*c*) M. Reiners, D. Baabe, K. Harms, M. Maekawa, C. G. Daniliuc, M. Freytag, P. G. Jones and M. D. Walter, N-Heterocyclic Carbene Adducts to $[Cp'FeI]_2$: Synthesis and Molecular and Electronic Structure, *Inorg. Chem. Front.*, 2016, **3**, 250–262; (*d*) U. Siemeling, U. Vorfeld, B. Neumann and H.-G. Stammler, [Bis(trimethylsilyl)amido](η^5-pentamethylcyclopentadienyl)-iron-(II): A Diamagnetic 14-Electron Complex with a "Pogo-Stick" Structure, *Organometallics*, 1998, **17**, 483–484; (*e*) O. A. Groß, S. Lauk, C. Muller, W. Gidt, Y. Sun, S. Demeshko, F. Meyer and H. Sitzmann, Iron(II) High-Spin and Low-Spin Complexes from Pentaisopropylcyclopentadienyliron(II) Bis- (trimethylsilyl) amide, *Eur. J. Inorg. Chem.*, 2017, 3635–3643; (*f*) M. Wallasch, G. Wolmershauser and H. Sitzmann, Phenolate Complexes of Iron(II) in Different Spin States, *Angew. Chem., Int. Ed.*, 2005, **44**, 2597–2599.

123 R. Weller, A. Gonzalez, H. Gottschling, C. Hänisch and C. G. Werncke, NHC-stabilized Parent Phosphinidene Adducts of Metal(II) Hexamethyldisilazanides of Manganese - Cobalt and Their Lability in Solution, *Z. Anorg. Allg. Chem.*, 2022, **648**, e202100338.

124 L. L. Liu, D. A. Ruiz, F. Dahcheh and G. Bertrand, Isolation of a Lewis Base Stabilized Parent Phosphenium (PH_2^+) and Related Species, *Chem. Commun.*, 2015, **51**, 12732–12735.

125 (*a*) D. Bockfeld, A. Doddi, P. G. Jones and M. Tamm, Transition-Metal Carbonyl Complexes and Electron-Donating Properties of N-Heterocyclic-Carbene-Phosphinidene Adducts, *Eur. J. Inorg. Chem.*, 2016, 3704–3712; (*b*) A. Doddi, D. Bockfeld, A. Nasr, T. Bannenberg, P. G. Jones and M. Tamm, N-Heterocyclic Carbene–Phosphinidene Complexes of the Coinage Metals, *Chem.–Eur. J.*, 2015, **21**, 16178–16189; (*c*) T. G. Larocque and G. G. Lavoie, Reactivity Study of Low-Coordinate Phosphaalkene IMes=PPh with Grubbs First-Generation Ruthenium Benzylidene Complexes, *New J. Chem.*, 2014, **38**, 499–502; (*d*) M. Peters, A. Doddi, T. Bannenberg, M. Freytag, P. G. Jones and M. Tamm, N-Heterocyclic Carbene-Phosphinidene and Carbene-Phosphinidenide Transition Metal Complexes, *Inorg. Chem.*, 2017, **56**, 10785–10793.

126 A. Doddi, D. Bockfeld and M. Tamm, Synthesis and Structures of Rh^I and Ir^I Complexes Supported by N-Heterocyclic Carbene-Phosphinidene Adducts, *Z. Anorg. Allg. Chem.*, 2019, **645**, 44–49.

127 G.-W. Chen, Y.-H. Chen, H.-K. Liu and C.-Y. Lin, Three-Coordinate Halide and Methyl Complexes of Chromium, Manganese, Iron, Cobalt, and Nickel Enabled by an Imidazolin-2-iminato Ligand, *Organometallics*, 2023, **42**, 2395–2404.

128 D. Becker, D. Bockfeld and M. Tamm, An Update on Phosphine-Imidazolin-2-Imine Iridium(I) Catalysts for Hydrogen Isotope Exchange, *Adv. Synth. Catal.*, 2023, **365**, 367–372.

129 I. C. Watson, A. Schumann, H. Yu, E. C. Davy, R. McDonald, M. J. Ferguson, C. Hering-Junghans and E. Rivard, N-Heterocyclic Olefin-Ligated Palladium(II) Complexes as Pre-Catalysts for Buchwald-Hartwig Aminations, *Chem.–Eur. J.*, 2019, **25**, 9678–9690.

130 I. Antsiburov, J. Stephan, R. J. Weininger, C. Gemel and R. A. Fischer, Copper Imidazolin-Imine Coordination Compounds as Precursors for a Cu/Al Complex, *Inorg. Chem.*, 2024, **63**, 17331–17339.

131 A. Doddi, M. Peters, D. Bockfeld and M. Tamm, Copper and Silver Complexes of N-Heterocyclic Carbene-Parent Phosphinidene Adducts, *Z. Anorg. Allg. Chem.*, 2023, **649**, e202200364.

132 H. Deka, N. Fridman, M. Koneczny, M. Tamm and M. S. Eisen, Base-Free Transfer Hydrogenation of Aldehydes and Ketones Catalyzed by Imidazolin-2-Iminato Actinide Complexes, *Catal. Sci. Technol.*, 2023, **13**, 352–361.

133 (*a*) O. Bienemann, A. Hoffmann and S. Herres-Pawlis, (Guanidine)Copper Complexes: Structural Variety and Application in Bioinorganic Chemistry and Catalysis, *Rev. Inorg. Chem.*, 2011, **31**, 83–108; (*b*) I. dos Santos Vieira and S. Herres-Pawlis, Lactide Polymerisation with Complexes of Neutral N-Donors-New Strategies for Robust Catalysts, *Eur. J. Inorg. Chem.*, 2012, 765–774; (*c*) H.-J. Himmel, Guanidinyl-Functionalized Aromatic Compounds (GFAs)-Charge and Spin Density Studies as Starting Points for the Development of a New Class of Redox-Active Ligands, *Z. Anorg. Allg. Chem.*, 2013, **639**, 1940–1952; (*d*) H.-J. Himmel, Valence Tautomerism in Copper Coordination Chemistry, *Inorg. Chim. Acta*, 2018, **481**, 56–68.

134 (*a*) A. Maronna, E. Bindewald, E. Kaifer, H. Wadepohl and H.-J. Himmel, Synthesis and Characterization of Novel Guanidine Ligands Featuring Biphenylor Binaphthyl Backbones, *Eur. J. Inorg. Chem.*, 2011, 1302–1314; (*b*) P. Roquette, A. Maronna, M. Reinmuth, E. Kaifer, M. Enders and H.-J. Himmel, Combining NMR of Dynamic and Paramagnetic Molecules: Fluxional High-Spin Nickel(II) Complexes Bearing Bisguanidine Ligands, *Inorg. Chem.*, 2011, **50**, 1942–1955; (*c*) P. Roquette, A. Maronna, A. Peters, E. Kaifer, H.-J. Himmel, C. Hauf, V. Herz, E.-W. Scheidt and W. Scherer, On the Electronic Structure of Ni^{II} Complexes that Feature Chelating Bisguanidine Ligands, *Chem.–Eur. J.*, 2010, **16**, 1336–1350; (*d*) P. Roquette, C. Konig, O. Hubner, A. Wagner, E. Kaifer, M. Enders and H.-J. Himmel, *Eur. J. Inorg. Chem.*, 2010, 4770–4782; (*e*) M. Reinmuth, U. Wild, D. Rudolf, E. Kaifer, M. Enders, H. Wadepohl and H.-J. Himmel, Stabilization and Activation: New Alkyl Complexes of Zinc, Magnesium and Cationic Aluminium Featuring Chelating Bisguanidine Ligands, *Eur. J. Inorg. Chem.*, 2009, 4795–4808; (*f*) U. Wild, O. Hubner, A. Maronna, M. Enders, E. Kaifer, H. Wadepohl and H.-J. Himmel, The First Metal Complexes of the Proton Sponge 1,8-Bis(N,N,N′,N′-Tetramethylguanidino) naphthalene: Syntheses and Properties, *Eur. J. Inorg. Chem.*, 2008, 4440–4447; (*g*) V. Raab, K. Harms, J. Sundermeyer, B. Kovacevic and Z. B. Maksic, 1,8-Bis(dimethylethyleneguanidino)naphthalene: Tailoring the Basicity of Bisguanidine "Proton Sponges" by Experiment and Theory, *J. Org. Chem.*, 2003, **68**, 8790–8797; (*h*) V. Raab, J. Kipke, R. M. Gschwind and J. Sundermeyer, 1,8-Bis(tetramethylguanidino) naphthalene (TMGN): a New, Superbasic and Kinetically Active "Proton Sponge", *Chem.–Eur. J.*, 2002, **8**, 1682–1693.

135 D. Franz, T. Szilvási, A. Pçthig, F. Deiser and S. Inoue, Three-Coordinate Boron (III) and Diboron (II) Dications, *Chem.–Eur. J.*, 2018, **24**, 4283–4288.

136 F. Hanusch, D. Munz, J. Sutter, K. Meyer and S. Inoue, A Zwitterionic Heterobimetallic Gold–Iron Complex Supported by Bis(N-Heterocyclic Imine)Silyliumylidene, *Angew. Chem., Int. Ed.*, 2021, **60**, 23274–23280.

137 F. S. Tschernuth, F. Hanusch, T. Szilvási and S. Inoue, Isolation and Reactivity of Chlorotetryliumylidenes Using a Bidentate Bis(N-Heterocyclic Imine) Ligand, *Organometallics*, 2020, **39**, 4265–4272.

138 S. V. Hirmer, F. S. Tschernuth, F. Hanusch, R. Baierl, M. Muhrb and S. Inoue, S. Modification of Bidentate Bis(N-Heterocyclic Imine) Ligands for Low-Valent Main Group Complexes, *Mendeleev Commun.*, 2022, **32**, 16–18.

139 M. Park, C. Schmidt, S. Türck, F. Hanusch, S. V. Hirmer, I. Ott, A. Casini and S. Inoue, Potent Anticancer Activity of a Dinuclear Gold(I) Bis-N-Heterocyclic Imine Complex Related to Thioredoxin Reductase Inhibition in Vitro, *ChemPlusChem*, 2024, **89**, e202300557.

140 T. Glöge, D. Petrovic, C. G. Hrib, C. Daniliuc, E. Herdtweck, P. G. Jones and M. Tamm, Synthesis and Structural Characterisation of an Isomorphous Series of Bis(imidazolin-2-imine) Metal Dichlorides Containing the First Row Transition Metals Mn, Fe, Co, Ni, Cu and Zn, *Z. Anorg. Allg. Chem.*, 2010, **636**, 2303–2308.

141 K. Jess, D. Baabe, T. Bannenberg, K. Brandhorst, M. Freytag, P. G. Jones and M. Tamm, Ni–Fe and Pd–Fe Interactions in Nickel(II) and Palladium(II) Complexes of a Ferrocene-Bridged Bis(imidazolin-2-imine) Ligand, *Inorg. Chem.*, 2015, **54**, 12032–12045.

142 K. Jess, D. Baabe, M. Freytag, P. G. Jones and M. Tamm, Transition-Metal Complexes with Ferrocene-Bridged Bis(imidazolin-2-imine) and Bis(diaminocyclopropenimine) Ligands, *Eur. J. Inorg. Chem.*, 2017, 412–423.

143 (*a*) C. Metallinos, D. Tremblay, F. B. Barrett and N. J. Taylor, 1,1'-Bis(phosphoranylidenamino)ferrocene Palladium(II) Complexes: an Unusual Case of Dative Fe → Pd Bonding, *J. Organomet. Chem.*, 2006, **691**, 2044–2047; (*b*) L. R. R. Klapp, C. Bruhn, M. Leibold and U. Siemeling, Ferrocene-Based Bis(guanidines): Superbases for Tridentate N, Fe, N-Coordination, *Organometallics*, 2013, **32**, 5862–5872.

144 T. J. Hadlington, A. Kostenko and M. Driess, Synthesis and Coordination Ability of a Donor-Stabilised Bis-Phosphinidene, *Chem.–Eur. J.*, 2021, **27**, 2476–2482.

145 R. Baierl, A. Kostenko, F. Hanusch and S. Inoue, Application of Ferrocene-Bridged N-Heterocyclic Carbene Stabilised Bis-Phosphinidenes in Sn(II) Complexation, *Dalton Trans.*, 2021, **50**, 14842–14848.

146 J.-K. Siewert, B. M. P. Lombardi, N. Jannsen, R. Roesler and C. Hering-Junghans, Synthesis and Ligand Properties of Chelating Bis(N-Heterocyclic Carbene)-Stabilized Bis(phosphinidenes), *Inorg. Chem.*, 2023, **62**, 16832–16841.

147 J.-K. Siewert, A. Schumann, T. Wellnitz, F. Dankert and C. Hering-Junghans, Triphosphiranes as Phosphinidene-Transfer Agents - Synthesis of Regular and Chelating NHC Phosphinidene Adducts, *Dalton Trans.*, 2023, **52**, 15747–15756.

148 R. Baierl, A. Kostenko, F. Hanusch, A. D. Beck and S. Inoue, Synthesis and Reactivity of Bidentate N-Heterocyclic Carbene-Phosphinidene Supported Si(IV) Dicationic Complexes, *Eur. J. Org Chem.*, 2022, e202201072.

149 C. C. Chong, B. Rao, R. Ganguly, Y. Li and R. Kinjo, Bis(N-heterocyclic olefin) Derivative: an Efficient Precursor for Isophosphindolylium Species, *Inorg. Chem.*, 2017, **56**, 8608–8614.

150 R. Guthardt, J. Mellin, C. Bruhn and U. Siemeling, 1,1'-Ferrocenylene-Bridged Bis(N-Heterocyclic Olefin) Derivatives, *Eur. J. Inorg. Chem.*, 2022, e202100903.

151 J. Raynaud, W. N. Ottou, Y. Gnanou and D. Taton, Metal-Free and Solvent-Free Access to α,ω-Heterodifunctionalized Poly(propylene oxide)s by N-Heterocyclic Carbene-Induced Ring Opening Polymerization, *Chem. Commun.*, 2010, **46**, 3203–3205.

152 S. Naumann, A. W. Thomas and A. P. Dove, N-Heterocyclic Olefins as Organocatalysts for Polymerization: Preparation of Well-Defined Poly(propylene oxide), *Angew. Chem., Int. Ed.*, 2015, **54**, 9550–9554.

153 E. Kersten, O. Linker, J. Blankenburg, M. Wagner, P. Walther, S. Naumann and H. Frey, Revealing the Monomer Gradient of Polyether Copolymers Prepared Using N-Heterocyclic Olefins: Metal-Free Anionic versus Zwitterionic Lewis Pair Polymerization, Macromol, *Chem. Phys.*, 2023, **224**, 2300097.

154 S. Wang, C. Zhang, D. Li, Y. Zhou, Z. Su, X. Feng and S. Dong, New Chiral N-Heterocyclic Olefin Bifunctional Organocatalysis in α-Functionalization of β-Ketoesters, *Sci. China:Chem.*, 2023, **66**, 147–154.

155 S. Wang, J. Yang, H. Zeng, Y. Zhou, F. Wang, X. Feng and S. Dong, Asymmetric Formal Coupling of β-Ketoesters with Quinones Promoted by a Chiral Bifunctional N-Heterocyclic Olefin, *Org. Lett.*, 2023, **25**, 7247–7251.

156 P. Sreejyothi, K. Bhattacharyya, S. Kumar, P. K. Hota, A. Datta and S. K. Mandal, An NHC-Stabilised Phosphinidene for Catalytic Formylation: A DFT-Guided Approach, *Chem.–Eur. J.*, 2021, **27**, 11656–11662.

157 S. P, N. Gautam, S. Maji, K. Bhattacharyya and S. K. Mandal, Transition Metal-Mimicking Relay Catalysis by a Low-Valent Phosphorus Compound, *J. Am. Chem. Soc.*, 2024, **146**, 16743–16752.

158 D. Li, L. Ning, Q. Luo, S. Wang, X. Feng and S. Dong, C-H Alkylation of Pyridines with Olefins Catalyzed by Imidazolin-2-Iminato-Ligated Rare-Earth Alkyl Complexes, *Sci. China:Chem.*, 2023, **66**, 1804–1813.

159 D. Li, Y. Wang, S. Wang and S. Dong, The Effect of Basic Ligands and Alkenes on the Regioselectivity of C-H Additions of Tertiary Amines to Alkenes, *Chem.–Eur. J.*, 2024, **30**, e202401014.

160 S. Wang, L. Ning, T. Mao, Y. Zhou, M. Pu, X. Feng and S. Dong, Anti-Markovnikov hydroallylation reaction of alkenes via scandium-catalyzed allylic C-H activation, *Nat. Commun.*, 2025, **16**, 1423.